COMPARATIVE IMAGING OF THE CANINE ACUTE ABDOMEN: SURVEY RADIOGRAPHY, CONTRAST-ENHANCED ULTRASOUND AND CONTRAST-ENHANCED MULTI-DETECTOR HELICAL COMPUTED TOMOGRAPHY

BY

MIRIAM MAGGIE SHANAMAN

THESIS

Submitted in partial fulfillment of the requirements
for the degree of Master of Science in VMS - Veterinary Clinical Medicine
in the Graduate College of the
University of Illinois at Urbana-Champaign, 2013

Urbana, Illinois

Master's Committee:

Professor Robert T. O'Brien
Associate Professor Timothy A. Fan
Professor Mark A. Mitchell

ABSTRACT

Canine patients with acute abdominal signs are often clinically unstable and need a rapid and accurate diagnosis. Contrast-enhanced multi-detector computed tomography (CE-MDCT) is the current modality of choice for evaluating acute abdominal pain in people. In phase one of this study we hypothesized that CE-MDCT would be a feasible and safe technique for use in awake and lightly sedated dogs with acute abdominal signs. Eighteen client-owned dogs were enrolled, all presenting with acute abdominal signs. Dogs were scanned using a dual-phase protocol that included pre-contrast, arterial and portal venous phases. Eight dogs were scanned awake and 10 were given light sedation as chosen by the primary care clinician. Two observers who were unaware of clinical findings and sedation status scored image quality for each scan by consensus opinion. Mean serum creatinine in the sedated group was significantly higher than in the awake group but was within the normal reference range for dogs. Other laboratory and physiologic measures did not differ between awake and sedated groups. No intravenous contrast-related adverse reactions were seen in any of the dogs. Median scan time for all patients was less than 10 minutes. Sixteen of 18 CE-MDCT scans were scored fair to excellent in diagnostic quality, with no statistical difference in diagnostic quality for awake versus sedated patients. The two poor quality diagnostic scans were attributed to severe beam hardening from previously administered barium contrast agent and severe motion artifacts. The results of this study suggest that dual-phase CE-MDCT is a feasible and safe technique for evaluating awake and minimally sedated dogs presenting with acute abdominal signs.

Unlike CE-MDCT, contrast-enhanced ultrasound (CEUS) continues to be in its infancy as it relates to evaluation of the acute abdomen. The primary purpose of phase two of this study, therefore, was to determine the level of agreement between survey radiography, combined B-Mode/CEUS, and CE-MDCT in the same population of canine patients; particularly the ability of these modalities to differentiate surgical from non-surgical conditions. Nineteen dogs (18 from phase 1 plus one additional case) with acute abdominal signs were prospectively enrolled. Inclusion required the cytologic, radiographic or sonographic detection of an underlying surgical condition or alternatively a source of acute abdominal disease that would necessitate medical management. Agreement for the majority of imaging features assessed was at least moderate. There was poor agreement in the identification of pneumoperitoneum and in the comparison of pancreatic lesion dimensions on B-mode vs. CEUS. The CT feature of fat stranding was noted in a variety of disease processes including gastric neoplasia with perforation, pancreatitis, and small intestinal foreign body. Ultrasound underestimated both the size and number of specific lesions when compared with CE-MDCT. CEUS was successful in the detection of bowel and pancreatic perfusion deficits that CE-MDCT failed to identify. Accuracy for the differentiation of surgical from non-surgical conditions was high for all modalities; 100%, 94% and 94% for CE-MDCT, US and survey radiography, respectively. CE-MDCT is an effective screening test of choice in the differentiation of surgical vs. non-surgical acute abdominal conditions. Focused CEUS may be beneficial following preliminary CE-MDCT or B-mode US given the potential for identifying clinically significant hypoperfused lesions.

TABLE OF CONTENTS

CHAPTER 1

REVIEW OF THE LITERATURE

Brief Review of Digital Radiography: Physics

Production of X-Rays: X-rays are produced by the conversion of electron kinetic energy into electromagnetic radiation. A large voltage is applied across two electrodes (the cathode-negatively charged and is the electron source via thermionic emission, and the anode-positively charged and is electron target) in an evacuated envelope. As the electrons travel from the cathode to the anode, they are accelerated by the electrical potential difference (voltage) between these electrodes, and in doing so attain kinetic energy.

Upon impact with the target, the kinetic energy of the electrons is converted into other forms of energy (predominantly heat). This intense heating limits the number of x-ray photons that can be produced in a given time. About 0.5% of the time, an electron comes into close proximity of a positively charged nucleus at the target cathode. Coulombic forces attract and decelerate the electron, causing a significant loss of kinetic energy and change in electron trajectory. An x-ray photon with energy equal to the kinetic energy lost by the electron is produced; this is termed *bremsstrahlung* or "breaking radiation." At relatively closer interaction distances, the force acting on the electron increases, causing a more dramatic change in the electron's trajectory and a larger loss of energy, producing higher x-ray energies. The highest x-ray energy is determined by the peak voltage (kVP) applied across the x-ray tube.

Common x-ray tube target materials include Tungsten, Molybdenum and Rhodium. When the energy of an electron incident on the target exceeds the binding energy of an electron of a target atom (varies with target material), it is energetically possible for a collisional interaction to eject the electron and ionize the atom. The vacated shell is energetically unstable so is filled with an outer shell electron with less binding energy. This electron transition to a lower energy state releases the excess energy in the form of a *characteristic* x-ray photon, with an energy equal to the difference between the binding energies of the electron shells [1].

Interaction of X-Rays with Tissue: X-rays produce ionization in tissue (most tissue is 70% water) with ionization of water resulting in the formation of chemically active free radicals; accounting for the majority of radiation damage to DNA. Interaction of photons with matter can occur by five possible mechanisms: Coherent scattering, photoelectric effect, Compton scattering, pair production, and photodisintegration (the latter two of which will not be discussed further due to lack of diagnostic significance). In *Coherent* scattering, a photon interacts with an object and changes its direction, but the subject does not absorb the photon and a change in photon energy *does not* occur. This accounts for approximately 5% of interactions and is not useful in the production of a radiograph; this actually may result in degradation of image quality or increased personnel radiation exposure. The *photoelectric effect* is responsible for image formation, whereby the x-ray striking the patient is completely absorbed (i.e., no scatter). The absorbed x-ray photon ejects an electron (called photoelectron) from an inner shell of a tissue atom. When this vacancy is filled by a peripheral shell electron, a characteristic x-ray is produced. Within the body the

energy of the characteristic x-ray is so low such that it is locally absorbed. The probability of a photoelectric interaction is directly proportional to the cube of the atomic number and inversely proportion to the cube of the photon energy; this is ultimately responsible for the tissue contrast we recognize radiographically. Finally, *Compton scattering* accounts for the majority of scattered radiation in diagnostic radiology. In the Compton reaction, an incoming x-ray photon interacts with a peripheral shell electron. This electron is ejected and the photon is scattered at a different angle; this scattered photon also has a lower energy than the original photon. The probability of such a reaction depends on the total number of electrons in the patient, which in turn depends on the patient's physical density and number of electrons per gram. As photon energy increases, so does the probability of a Compton interaction. Compton interaction, unlike photoelectric absorption, is independent of atomic number; ultimately resulting in worsening of image contrast [2].

The Basics of Image Capture: In the past decade, digital radiography has rapidly replaced film-based radiographic image capture in both human and veterinary medicine due to ease and rapidity of image acquisition along with markedly improved image quality. The term *digital radiography* refers to both computed radiography (CR) and direct digital radiography (DDR) systems.

CR and DDR systems differ from film-screen systems only in the method by which the radiation is detected after the x-rays are transmitted through the patient.

CR was developed by Fuji (Tokyo, Japan) and has been in use since the 1980's. The basic components of a CR system include a detector or image plate for acquiring the image, a device to read the imaging plate, an analog to digital converter, and computer and software to process the digitized image [3]. In CR, the radiographic system differs only in the use of a specialized cassette with an imaging plate rather than a cassette containing intensifying screens and film. This plate is coated with photostimulable phosphors (crystals). As x-rays strike the imaging plate, electrons in the crystals are energized to a higher energy state and stored in electron traps thus forming the latent image. This exposed cassette is placed in a plate reader that scans the plate with a laser light in a series of horizontal lines. Through this process, previously trapped electrons are released into a lower energy state, thereby stimulating phosphorescence. The light that is produced is then coupled to an optical system ultimately amplifying the light energy and converting it to an electrical signal that is proportional to the released light intensity; hence the analog signal (to be described shortly) [4].

In DDR, the image is formed after x-rays expose a detector. This eliminates the need for an image/plate reader (as with CR) and results in faster image acquisition [3]. Two main detector types exist; flat panel and charge coupled device (CCD) detectors. Flat panel detectors use thin-film transistor (TFT) technology; the arrays of which are composed of many small detector elements. When the TFT is exposed to x-rays, energy is converted to an electrical charge; this can be direct (conversion to electrical pulse via a photoconductive layer such as amorphous selenium) or indirect (conversion into light via a scintillator-commonly cesium iodide crystals). CCD systems are considered a type of indirect

conversion because a scintillator is used to convert x-ray energy to light that is ultimately converted to an electrical signal [4].

Analog to Digital Conversion and Spatial Resolution: Digital image acquisition relies on an initial conversion of an analog voltage waveform to digital information (binary and decimal numbers) by an analog to digital converter (ADC). ADC's can vary in their sampling rates; these are typically very high in medical imaging, rendering sampling error negligible. It is important to note that while the analog signal described is continuous, digital data has a finite limit of possibilities resulting in a phenomenon known as quantization. The digital data, therefore, represents a "rounded off" form of the initial analog signal. When digital data is then converted back to an analog form for display on a video monitor (via a digital to analog converter-DAC), the original analog signal cannot be restored due to both sampling and quantization data loss [2].

The digital image that is ultimately viewed on the computer monitor is a composite of pixels or picture elements to which a shade of grey is assigned pending the numeric value of the pixel in question. The number of values available to each pixel (or number of shades of grey) is dependent upon the bit depth of the computer. N bits will allow for 2^N possibilities for data representation. For example the standard 8 bit system will result in a range of 256 shades of grey [2].

Spatial resolution in digital radiography is largely dependent on pixel size, with smaller pixel size within the same field of view (actual physical area included/captured) resulting

in improved spatial resolution. Pixel size is determined by dividing the size of the field of view by the matrix size. The matrix size represents the number of pixels across the image. For digital radiography a 2048 x 2048 (2K) matrix or higher is generally preferred [2].

Interestingly, digital imaging systems still do not have the degree of spatial resolution possible with older film-screen technologies. For example, CR systems have a spatial resolution of approximately 2.5 line pairs/mm, whereas film-screen systems range from 6-10 line pairs/mm. Ultimately, however, this is of little clinical consequence and is overcome by its many advantages [2]. These include but are not limited to the following: Ease and rapidity of acquisition and storage, rapid access for future reference, lower film cost, fewer repeat exposures, remote image interpretation, post acquisition window/level capabilities, computed image enhancement, greater image latitude (range of exposures that results in a useable or diagnostic image), improved contrast, and elimination of manual processing errors.

Clinical Applications: Human Medicine

Development of the 3-view Abdominal series: More than a decade ago, plain abdominal radiography was the mainstay in the evaluation of the human emergency patient with acute abdominal pain; especially as it relates to the identification of free peritoneal gas consistent with underlying rupture of a hollow viscus. In fact, the value of a chest radiograph in the visualization of intraperitoneal free gas was first suggested in 1915 by Popper, who detected subphrenic collections of gas in the diagnosis of peptic ulcer [5]. It has

been proposed that as small a quantity of gas as 1 cc can be recognized in erect chest and left lateral decubitus abdominal films [6].

The identification of thoracic lesions (such as pleural free fluid) in addition to possible pneumoperitoneum in patients presenting for abdominal signs prompted the routine use of a three-view radiographic series in preliminary imaging evaluation. This 3-film series included an erect and supine abdominal view with the addition of an erect thoracic study. The clinical necessity of each view was ultimately evaluated in a study reviewing 252 consecutive emergency-room patients presenting with abdominal pain or acute abdomen. Each of the three standard radiographic views was evaluated independently for their relative diagnostic value and ultimately the supine abdominal view and erect chest study were most beneficial; diagnosing normality or abnormality in 98% of these patients [7]. In a recent retrospective review of survey radiographs obtained on 250 cases with surgically confirmed hollow organ perforation, the positive rate for identification of free air was 85.1% on erect chest radiographs and 98% on left decubitus abdominal radiographs, supporting the previous study's finding [8].

Clinical Utility and Indications in the Acute Abdominal Emergency Patient: With the increasing reliance and availability of survey radiographs for patients presenting with abdominal symptoms, clinicians started to question both the clinical utility and appropriate indications for this modality in an attempt to reduce hospital costs and patient/staff radiation exposure [9], [10]. In the latter study, the authors recommended survey abdominal radiography in patients with moderate to severe tenderness who have a high clinical

suspicion of bowel obstruction, renal-ureteral calculi, trauma, ischemia or gallstones (if ultrasound is unavailable). Had those referral criteria been adopted, 53.7% of the 1780 examinations that were evaluated would have been avoided, with only 33 radiographic abnormalities missed (almost all localized or generalized ileus). Furthermore, they proposed that no radiographic findings that would reflect a serious pathologic process would have been missed [10].

In a pilot study evaluating the effect of chest and abdominal radiographs on the initial management of 100 consecutive acute abdominal patients, abdominal radiography was associated with a change in the stated management of 10 patients (in eight from surgical to conservative management and vice versa in two). Abdominal radiographic findings were consistent with a final diagnosis of intestinal obstruction in five of eight patients with this condition. Abdominal radiography was not associated with the change in management of 15 patients with cholecystitis; in only four did the findings support the final diagnosis. In 13 patients with non-specific abdominal pain, no abnormal radiographic findings were reported [11].

In addition to the acute abdominal conditions described above, the evaluation of the role of plain films in the diagnosis and management of acute pancreatitis was also being pursued [12], [13]. Both studies agreed that duodenal abnormalities are the most reliable sign of acute pancreatitis. An air-fluid level, usually associated with dilatation, was found in 42% of acute pancreatitis cases evaluated in the latter study, compared with 21% of controls. The same study identified left pleural effusion as the most common abnormality in severe

pancreatitis (43%) and was seen significantly more often than in mild pancreatitis [13]. This highlights the importance of evaluating the periphery of abdominal radiographs, paying particular attention to the pleural space, as such factors may reflect a particular clinical course or worsened prognosis.

In a recent study, 54% of prospectively evaluated patients presenting for acute abdominal conditions had plain abdominal radiographs that showed positive diagnostic features; the greatest sensitivity of which was achieved in the identification of intestinal obstruction (100%) and perforated peptic ulcer (90%). Sensitivity was reduced in patients with perforated typhoid, acute appendicitis, blunt abdominal trauma and generalized peritonitis [14]. Similar results were reported in a second prospective evaluation of 168 patients presenting for acute abdominal pain in which plain abdominal radiographs were most sensitive in cases of intestinal obstruction (90.9 % had positive plain abdominal radiographic findings). Positive plain radiographic findings were noted in 44.4% (4 cases) of perforated viscus, 47.8% (11 cases) of urinary tract disease, and 38.1 % (8 cases) of hepatobiliary and pancreatic diseases. 61.3% of patients (total of 103) were found to have inappropriate survey radiographic findings that did not correlate with the clinical diagnosis [15].

Acute abdominal pain of the right lower quadrant, particularly in the evaluation of patients with suspected acute appendicitis, remains a diagnostic challenge. The utility of abdominal radiographs under these circumstances has been evaluated both prospectively and retrospectively [16], [17]. In a prospective study, 104 patients admitted to the emergency room

for acute pain of the right lower quadrant underwent clinical examination, white blood cell count and plain abdominal radiographs. A total of 76 ultimately underwent surgery, with a negative laparotomy rate of 22%. Plain abdominal radiographs changed the suspected diagnosis and management of 6 patients, leading in one case to a negative laparotomy. Of the remaining 5, 3 were operated (2 for acute appendicitis and one for small bowel obstruction) and 2 treated conservatively for ureteral calculi. It was the opinion of the authors, that the indiscriminate use of plain abdominal radiographs is not helpful for most patients with acute pain of the right lower quadrant, however, may be performed in select patients with clinically suspected small bowel obstruction or urinary tract symptoms [16]. In a retrospective evaluation of 821 patients hospitalized for suspect appendicitis radiographic findings were noted in 51% of patients with, and 47% of patients without appendicitis, with no individual finding reported as either sensitive or specific. Radiological impressions were normal in 50% of patients with appendicitis [17].

The limitations of abdominal radiography continue to be highlighted in a later retrospective study evaluating the non-traumatic emergency patient. 874 patients were included in the study. Interpretation was normal in 34% (n=300), nonspecific in 46% (n=406), and abnormal in 19% (n=168) of patients. 50% of patients underwent additional abdominal imaging (including upper gastrointestinal imaging, and computed tomography with or without concurrent ultrasound). Of patients whose abdominal radiography results were normal, 72% (90 of 125) were found to have abnormal findings at follow-up imaging, including major abnormalities (78%,70 of 90 cases) [18]. A multicenter prospective trial evaluating patients presenting to the emergency department with abdominal pain revealed

similar limitations. A total of 1021 patients were included in the study. In 117 patients, the diagnosis changed after plain radiographs (and this change was accurate) in 39 patients (22% of changed diagnoses and 4% of total study population). Overall, the primary clinical diagnosis corresponded with the final diagnosis in 49% of patients. The diagnosis following radiographic evaluation was correct in 50% (n=514) of the patients. This improvement in accuracy was not statistically significant (p=0.14). The authors concluded that plain radiography in patients with acute abdominal pain has limited additional value [19].

Role of Reviewer Experience: Given that the majority of abdominal radiographs are obtained and initially reviewed on an emergency basis, one must pose the question of the role of the attending clinician's experience as it relates to the diagnostic limitations previously described. The accuracy of abdominal radiography in acute small bowel obstruction was evaluated retrospectively among three groups of radiologists: senior staff, junior staff and second-year radiology residents. A total of 90 patients met inclusion criteria. Sensitivity for detection of small bowel obstruction ranged from 59% to 93%. When comparing the three groups of radiologists, senior staff had a statistically significantly higher rate of detection of small bowel obstruction than either junior staff ($p<0.001$) or residents ($p<0.004$). Interestingly, residents had statistically significantly better sensitivity than junior staff ($p<0.02$). For the combination of sensitivity and specificity (which is a measure of accuracy), senior staff were significantly more accurate than either of the other two groups. The results of this study suggest that radiologists with a greater degree of experience are likely to be more accurate in the evaluation of acute

abdominal radiographs [20]. A second study prospectively evaluated the ability of doctors of different skill level and specialty to interpret plain abdominal radiographs. A total of 76 doctors participated, each evaluating a predetermined set of 14 plain abdominal radiographs (5 normal and 9 abnormal). A positive correlation was drawn between seniority and score ($p=0.028$), similar to the previous study [21].

Clinical Applications: Veterinary Medicine

Unlike human medicine, for which survey radiography has largely been replaced by advanced imaging techniques (computed tomography in particular), the reduced financial burden and accessible nature of survey radiography in veterinary medicine are responsible for its continued widespread and frequently exclusive use in evaluation of the acute abdominal patient.

Brief History: Articles in veterinary radiology started to appear in print as early as 1896, one year following Karl Wilhelm Roentgen's discovery of the x-ray. The first several decades after Roentgen's discovery placed particular emphasis on therapeutic radiology (x-radiation therapy) rather than diagnostic imaging. The risks placed upon the radiographer's assistant outweighed the potential patient benefit at the time. The first text on veterinary radiology was published in 1926 in Berlin, written by Dr. Paul Henkel. Barium enema and normal upper gastrointestinal visualization were characterized at the time. It was not until 1962 that the Journal of the American Veterinary Radiology Society was formally established. The so-called "radiation explosion" after World War II ultimately

set the stage for the rapid development of the science of radiology in veterinary medicine [22].

Disease of the Peritoneal Cavity: Under normal conditions in the adult dog, the serosal surfaces of the small intestines are adequately visualized due to the presence of peritoneal fat. Reduced serosal detail can be caused by peritoneal effusion, hemorrhage, emaciation, or lack of fat [23]. One of the earliest descriptive survey radiographic studies in veterinary medicine characterizes the imaging appearance of peritonitis in the dog and cat. The author describes early radiologic signs of peritonitis including a "flaky or mottled appearance of the abdominal organs," further stating that "the borders between the bowel loops and the abdominal organs, which normally are well delineated" as being blurred. In more advanced cases the author describes a "ground glass" appearance of the abdomen due to an increase in abdominal fluid. Additional findings include corrugation of the intestinal wall (especially large bowel) [24].

The identification of pneumoperitoneum is of significant importance as this warrants immediately surgical intervention. Pneumoperitoneum in the absence of recent laparotomy is consistent with rupture of a hollow viscus, as previously described. In veterinary medicine, the most sensitive projection for detecting small volumes of gas is a lateral view, made with a horizontally directed x-ray beam, with the patient in dorsal recumbency and with the cranial portion of the abdomen slightly elevated [25]. An alternate projection is a ventrodorsal view obtained with the patient in left recumbency with the use of a horizontally directed x-ray beam. Right lateral recumbency is not recommended

because the gas bubble rises to the left side and may be confused with gas within the gastric fundus [2].

Intestinal Obstructive Disease: Radiographic signs of intestinal disease were described shortly thereafter and included the following: Ileus (classified as localized, generalized, mechanical or adynamic/non-obstructive), irregular mucosal pattern, stricture (apple core or ring stricture), filling defects (foreign body, neoplasia, instussusception, feces), displacement, and perforation (peritoneal gas, loss of abdominal detail) [26].

In a case series describing diagnostic and clinical outcome in 9 dogs with intestinal volvulus, the following radiographic findings were reported: Distension of the stomach and majority of small intestine with gas and fluid and loss of serosal detail [27]. Similar findings were reported in 2 cases of cecal-colic volvulus [28], and in a third study of canine intestinal volvulus [29].

Linear foreign bodies (routinely encountered in small animal patients) result in plication of the small intestine. Because of peristalsis, the intestines gather around the foreign object, which is fixed more proximally in the gastrointestinal tract. The presence of small, eccentrically located luminal gas bubbles in the small intestines also supports the presence of a linear foreign object. This may be the only radiographic sign if there is decreased serosal detail due to concurrent peritonitis [30], [31]. These findings can be nonspecific as additional differentials with similar radiographic findings include intestinal

hyperperistalsis (e.g., secondary to infectious disease), peritoneal adhesions from prior laparotomy, and intestinal parasites [30].

Small intestinal obstruction secondary to intramural or extramural masses, intussusception and other foreign objects are also possible, resulting in small intestinal dilation orad to the obstruction. Affected bowel typically contains both fluid and gas [2]. A value of 1.6 representing the ratio of the maximal small intestinal diameter relative to the height of the body of the 5th lumbar vertebra at its narrowest point is recommended as the upper limit of normal intestinal diameter in the dog, with values greater than 2 having a very high probability of obstruction [32].

"The obstructive bowel pattern," remains a current diagnostic dilemma, as such a pattern in the absence of follow-up imaging (such as abdominal ultrasound) typically results in a recommendation for surgical intervention. Widespread, marked, fluid-distension of the intestine, for example, can be compatible with mechanical obstruction (as described above); however, it may also be observed with infectious or inflammatory bowel diseases. Furthermore, reduction in serosal detail can be secondary to peritoneal free fluid in such cases, or alternatively "pseudofluid" produced by many, closely approximated, large, fluid-filled bowel segments [33].

Gastric Dilatation and Volvulus: Gastric torsion is a common cause of gastric obstruction in the large breed dog. Radiographically the important features in patients with rotation greater than 90 degrees (typically clockwise when viewing the patient from the caudal

direction) include: large distended stomach, pylorus being located near or to the left of midline and dorsally, tissue-dense line across the distended stomach (resulting in compartmentalization), splenomegaly with variable location of the body of the spleen, possible gastric pneumatosis, compression of the liver with small posterior vena cava and cardiac silhouette, and ileus secondary to pain and esophageal dilation [34]. Lateral abdominal views are usually of greatest value; both of which may be necessary, starting always with the right lateral view. With the patient in right lateral recumbency, gas fills the pyloric portion of the stomach, and fluid shifts to the fundus or body of the stomach. This gas distribution is opposite to what is normally expected [2], and is therefore diagnostic for volvulus unless there is a 360 degree volvulus for which the pylorus and fundus will be positioned normally.

Gastric Ulceration: While gastric ulceration is a possible cause of acute abdominal pain, in the absence of perforation (and subsequent pneumoperitoneum), plain abdominal radiographs are of little to no diagnostic benefit. Double-contrast gastrograms are of potential diagnostic benefit, however, contrast radiography is not the subject of this paper and will not be discussed further.

Note on 3-View Radiographic Series for Evaluation of Gastrointestinal Disease: In the standard 2-view abdominal series (ventrodorsal and medio-lateral views), the lateral view of choice is typically based on personal preference with the exception of cases with suspect gastric dilatation and volvulus as previously described. It has been proposed that the same principle employed for evaluation of the stomach, whereby gas is used as a negative

contrast agent, can be of benefit for both small and large intestinal disorders. A review of 7 cases for which both lateral projections were obtained was done to determine the clinical utility of these methods. In one case, the left lateral view revealed a soft tissue tubular structure suggestive of intussusception (later confirmed in surgery), while the right lateral view revealed segmental small intestinal dilation for which the underlying cause remained unknown. A second case revealed moderate distension of multiple small bowel loops in the craniodorsal abdomen on the right lateral view, while the left lateral view resulted in a shift of fundic gas to the pylorus (highlighting linear foreign material in the pylorus that was noted to extend into the duodenum); this was surgically confirmed as a pyloric foreign body with attached linear foreign body extending to the level of the proximal jejunum [35]. The University of Illinois College of Veterinary Medicine routinely employs the 3-view radiographic series and clinicians have routinely identified a clinical benefit (identification of additional clinically significant information); this data, however, has not been officially reported.

Pancreatitis: Under normal circumstances the pancreas is not radiographically visible in the dog. In a radiographic study evaluating 182 dogs with pancreatitis, the most common findings included increased opacity, decreased abdominal detail, and granularity in the right cranial abdomen on ventrodorsal radiographs. Additional findings included displacement of the pyloric antrum toward the left, a mass medial to the proximal descending duodenum, displacement of the duodenum toward the right, a static gas pattern in the descending duodenum or thickening of the wall of the descending duodenum, a static gas pattern in the transverse colon, and caudal displacement of the

transverse colon [36]. As with the human cases, pancreatitis can also result in pleural effusion [37]. In a retrospective review of 70 dogs with fatal acute pancreatitis, abdominal radiographs from 41 dogs were available for evaluation. Only 10 (24%) had radiographic abnormalities suggestive of acute pancreatitis; 8 had increased radiopacity and loss of detail in the right cranial quadrant, and 2 had a gas-filled, displaced duodenums. Only 5 had gas in the colon. For 6 of the 10 dogs for which results of abdominal radiography were suggestive of acute pancreatitis, results of abdominal ultrasonography were also suggestive of acute pancreatitis. For 9 of 31 dogs for which results of abdominal radiography were not suggestive of acute pancreatitis, results of abdominal ultrasonography were suggestive of acute pancreatitis [38]. The frequency of radiographic abnormalities in more common, less severe cases of acute pancreatitis is likely to be even lower than this study group. These results suggest that the negative predictive value, or the ability of negative findings on plain radiography to exclude the presence of acute pancreatitis is low [39].

Splenic Torsion: Limitations of plain abdominal radiographs also exist in the diagnosis of other ischemic acute abdominal conditions such as splenic torsion (which can occur as an isolated condition or can be associated with concurrent gastric dilatation and volvulus); as radiographic findings are non-specific; these can mimic other etiologies of generalized splenomegaly such as splenic neoplasia. Reported radiographic features of splenic torsion include abnormal location or shape of the spleen, loss of abdominal detail, and intrasplenic gas [40]. In a second retrospective analysis of 19 cases of isolated splenic torsion in dogs, abdominal radiographs were obtained in 16 dogs and similarly revealed splenomegaly in all cases and reduced abdominal serosal detail in 6 [41]. Complimentary imaging techniques,

most commonly abdominal ultrasound, are typically pursued to help confirm the diagnosis prior to surgical intervention.

Abdominal Ultrasound (US)

B-Mode US; Basic Physical Principles: Sound is a form of mechanical energy that propagates through a continuous, elastic medium by the compression and rarefaction (with associated distance between compression and rarefaction representing the wavelength) of "particles" that compose it. The frequency of the sound wave is the number of times the wave oscillates through a cycle each second. Ultrasound represents the frequency range above 20 kHz. Medical ultrasound uses frequencies in the range of 2-10 MHz. The product of the wavelength (λ) and frequency (f) is equal to the speed of sound of the ultrasound in a given medium (c); hence the relationship $c=\lambda f$. The speed of sound through a medium depends on the following relationship: $c=\sqrt{(B/\rho)}$, where B represents the bulk modulus (a measure of the stiffness of a medium and its resistance to being compressed) and ρ represents the density of the medium. A highly compressible medium (air) has a low speed of sound (330 m/sec), while a less compressible medium (bone) has a higher speed of sound (skull bone, 4080 m/sec). *Medical ultrasound machines assume a speed of sound of 1540 m/sec (the speed of sound in soft tissue).* Ultrasound frequency is unaffected by changes in sound speed as the acoustic beam propagates through matter; ultrasound wavelength is therefore dependent on the medium. Resolution of the ultrasound image and attenuation of the ultrasound beam energy depend on both wavelength and frequency. Wavelength determines the spatial resolution along the direction of the beam, with higher frequencies

(small wavelength) providing superior resolution with a trade-off in reduction of beam penetration depth [1].

Interaction of US with Matter: Types of interactions include reflection, refraction, scattering and absorption. *Reflection* occurs at tissue interfaces where there is a difference in acoustic impedance (Z); for a particular material this is defined as $Z=\rho c$. A large acoustic impedance mismatch results in a relatively greater reflection of energy, while minor differences allow the continued propagation of energy with little ultrasound reflection. *Refraction* describes the change in direction of the transmitted ultrasound energy with nonperpendicular incidence, the angle of which is determined by the change in speed of sound that occurs at a tissue interface. When $c_2>c_1$, the angle of transmission is greater than the angle of incidence; the opposite is true when $c_2>c_1$. The concept of *scatter* becomes clinically relevant as the echo signal amplitude from the insonated tissues depends on the number of scatterers per unit volume, the acoustic impedance differences at the scatterer interfaces, the sizes of the scatterers, and the ultrasonic frequency; with hyperechoic referring to higher scatter amplitude and hypoechoic referring to lower scatter amplitude relative to the average background signal. *Attenuation* (the loss of acoustic energy with distance traveled) is caused by both scattering and tissue absorption of the incident beam. This is symbolized by the attenuation coefficient μ, expressed in dB/cm. Attenuation occurs exponentially with penetration depth, and increases with increased frequency [1].

Transducer Selection: The ultrasound transducer is composed of one or more ceramic elements (piezoelectric material) with electromechanical properties that convert electrical

energy into mechanical energy (to produce ultrasound) and mechanical into electrical energy (for ultrasound detection). Ultrasound transducers for medical applications employ a synthetic piezoelectric ceramic, most often lead-zirconate-titanate (PZT). The operating frequency of the probe is determined from the speed of sound in, and the thickness of, the piezoelectric material. Higher frequencies are achieved with thinner elements and vice versa. The damping block, layered on the back of the piezoelectric element, absorbs the backward directed ultrasound energy and attenuates stray ultrasound signals from the housing. This component also dampens the transducer vibration to create an ultrasound pulse with a short spatial pulse length (necessary to preserve axial resolution). Finally, the matching layer provides the interface between the transducer element and the skin surface, minimizing differences in acoustic impedance [1].

Resolution: Axial resolution refers to the ability to discern two closely spaced objects in the direction of the ultrasound beam. The minimal required separation distance between two reflectors is one-half the spatial pulse length (SPL=number of cycles emitted per pulse by the transducer multiplied by the wavelength); this avoids overlap of returning echoes. Objects spaced closer than ½ SPL cannot be resolved. Shorter pulses produce better axial resolution and can be achieved by greater damping of the transducer element or with a higher frequency transducer. For example, a 5 MHz transducer has an SPL of approximately 0.93 mm, providing an axial resolution of 0.47 mm. *Lateral* resolution refers to the ability to discern two separate closely spaced objects perpendicular to the direction of the sound beam. For both single and multi-element array transducers, the beam diameter determines the lateral resolution. Lateral resolution, unlike axial resolution, is

therefore depth dependent. The typical lateral resolution for an unfocused transducer is approximately 2-5 mm. Finally, *elevational* resolution describes the slice-thickness dimension of the ultrasound beam. This is dependent upon the transducer element height (similar to the dependence of lateral resolution on element width) [1].

Display Modes: A-mode (for amplitude) is the display of processed information (digital signal proportional to echo amplitude) from the receiver as a function of time. A-mode display is seldomly used in diagnostic imaging, with the exception of certain ophthalmology applications. *B-mode* (for brightness), is the electronic conversion of the A-mode information into brightness-modulated dots on a display screen. Generally speaking, the brightness of each dot is proportional to the echo signal amplitude [1]. The B-mode display is used for both M-mode and 2D gray-scale imaging (the latter of which is the subject of this paper).

Clinical Applications: Human Medicine

The diagnostic benefit of conventional B-mode ultrasound in the characterization of intra-abdominal conditions was described as early as 1970 in a case series where detection, diagnosis, and delineation of specific pancreatic conditions (including edema, pseudocysts and carcinomas) were reported [42]. It was shortly thereafter that the added benefit of sonography in addition to survey radiography in the acute abdominal patient continued to be recognized. For example, in patients with complicated peptic ulcer, upper abdominal sonography detected multiple lesions that were not visible on plain films; these included perihepatic fluid collections, inflammatory paraduodenal masses, and a sinus tract [43].

Similarly, sonography allowed the identification of hepatic, renal and other sources of right upper quadrant pain, when plain radiography was unable to do so [44].

In a prospective evaluation of 95 patients with acute abdominal pain, real-time sonography was performed in conjunction with plain films of the abdomen in order to detect what, if any, added information was provided by the sonographic examination. Not unexpectedly, in 21% of patients, the sonogram contributed important diagnostic information not provided by the plain films. In this subgroup of patients, pathology was referable to the biliary tract (9), gallbladder (4), liver (2), ovary (2), pancreas (1), kidney (1), and abdominal wall (1). Lesions identified sonographically (but not radiographically) included but were not limited to the following: duct dilation, choledocholithiasis, cholelithiasis, metastatic liver disease, and pancreatic pseudocyst. In only 5% of cases did the plain film provide more information than the sonogram. Two such cases suffered from underlying small bowel obstruction secondary to metastatic carcinoma that were simply described as being "gassy" on sonographic evaluation. Ultimately, the authors proposed that when plain films reveal gallstones in a patient with right upper quadrant pain, presence of free air, or a bowel obstruction, that no further imaging is necessary. However, when plain films are negative in the presence of acute abdominal pain, sonography can be used as an immediate imaging technique and can be expected to add useful diagnostic information in approximately 20% of patients [45].

While only representing a limited number of cases in the study described above, ultrasound of acute GI tract conditions was described extensively over the following

decade. A technique termed "graded compression" sonography was routinely employed such that it would provide a technique comparable to gentle abdominal palpation. Compression was considered essential for 3 primary reasons: To displace and compress bowel loops in order to eliminate influence of bowel contents, to decrease transducer to bowel distance (permitting the use of high-frequency transducers), and finally to assess if a lesion is rigid or not (of special importance in differentiating normal soft intra-abdominal fat from inflamed non-compressible fat) [46].

In cases of intestinal perforation, while sonography is considered inferior to survey radiography for the identification of free peritoneal gas, it may still be beneficial in the identification of findings that indirectly imply potential perforation such as reduced bowel peristalsis and presence of free fluid between intestinal loops. In 146 cases of perforated bowel, free air was not identified in 12 and in 66% of the cases intraperitoneal free fluid was the only sign of perforation [47]. The same group retrospectively evaluated the sonographic findings in 184 cases of confirmed small bowel obstruction and found: dilation of small bowel loops, bowel wall thickness, evidence of peristalsis and presence/echogenecity of extraluminal fluid. They ultimately concluded that worsening free peritoneal fluid between dilated small bowel loops is suggestive of worsening mechanical ileus and requires immediate surgical intervention [48].

The use of ultrasound as the primary imaging diagnostic tool in the work-up of acute right upper quadrant pain due to acute cholecystitis has also been evaluated. The differentiation of acute cholecystitis from chronic cholecystitis or cholelithiasis is of urgent importance;

especially as it relates to therapeutic intervention. It was proposed that ultrasound may be particularly efficacious in the jaundiced patient where the distinction between obstructive and nonobstructive disease needs to be made; as the cause of obstruction (if present) can often be identified [49].

With the improvement of sonographic techniques, continued ultrasonographic characterization of acute abdominal conditions became possible and were pursued with increased frequency. Acute edematous pancreatitis sonographically was described as revealing an enlargement of the organ with fewer echoes in the parenchyma than normally expected. Ultrasound was also proposed to identify gastrointestinal ileus before all other methods; fluid-filled bowel with pendular peristalsis or no peristalsis were reported as typical signs. Ultimately, beyond visualization of a pathologically altered organ, sonography permits for visualization of normal organs (thus decreasing the spectrum of differential diagnoses) and aids in the identification of intra-abdominal fluid collection(permitting ultrasound-guided puncture) [50].

Beyond the identification of intra-abdominal free fluid, the sonographic identification of pneumoperitoneum has also been described. In a study comparing the identification of free peritoneal air in perforated peptic ulcer with plain radiography versus abdominal ultrasound, intraperitoneal free air was diagnosed in 90% (9/10) of patients with ultrasound in comparison with 80% (8/10) by abdominal and chest radiographs. The characteristic sonographic finding was described as the presence of an interference echo with shifting phenomenon. The interference echo pattern is defined as an interruption of

echo transmission when the space between the parietal peritoneum and surface of the liver is filled with air. As this free air can be shifted easily by changing the patient's position, detection of a shift in the interference echo pattern is strong sonographic evidence of pneumoperitoneum [51].

Sonography (both B-Mode and color Doppler) of infants and children with acute abdominal symptoms has also been characterized in conditions such as trauma (with duodenal hematoma considered the most frequent visceral injury in children suffering from abuse), intussusception ("bowel within bowel" appearance), necrotizing enterocolitis, appendicitis (non-perforated vs. perforated), acute cholecystitis, and intestinal obstructive disease. [52], [53]. Given the relative inability of young children to accurately describe their clinical symptoms, the importance of diagnostic imaging cannot be underestimated. In a prospective evaluation of 101 patients who presented to a large urban children's hospital and underwent lower abdominal and pelvic sonographic examinations for urgent evaluation of acute abdominal/pelvic pain, sonographic evaluation resulted in a change in initial treatment plans for 43 patients (46%) [54].

In the case of necrotizing enterocolitis, retrospective analysis of B-Mode and color Doppler ultrasound findings in neonates presenting to a neonatal intensive care unit over a 3-year period revealed specific criteria that were responsible for a negative outcome. These included the identification of free gas, focal fluid collection or three or more of the following: increased bowel wall echogenicity, bowel wall thinning/thickening, absent bowel perfusion, portal venous gas, free fluid with echoes and intramural gas. Free gas and

focal fluid collection were only identified in the group of neonates who required surgery or who passed away. In fact, in two cases ultrasound detected free gas when survey radiography was unable to do so. Bowel wall perfusion and the presence of anechoic peritoneal free fluid were considered unhelpful in predicting adverse outcome [55].

While sonographer training/expertise is a possible limitation of the modality as it relates to the evaluation after-hours emergency acute abdominal cases, the technique has proven to be beneficial with minimal training among a group of surgeons who prospectively performed 205 emergency scans; the information acquired of which contributed to the establishment or alteration of a diagnosis in 67.3% of cases. Confirming or excluding hepatobiliary disease, tubo-ovarian pathology, aortic aneurysm and evidence of blunt trauma were the primary goals [56]. This is of paramount clinical importance in surgical emergencies where a prompt diagnosis is needed. In a separate study prospectively evaluating 1671 patients presenting to the emergency room for blunt abdominal trauma, radiologists who performed a sonographic evaluation within minutes of arrival correctly identified all patients requiring emergency laparotomy. 470 patients with negative sonographic findings were discharged approximately 12 hr after admission; two of which (0.4%) were mistakenly discharged. Sonographic examination was considered positive if free intraperitoneal fluid or visceral injury was identified. 3 of the reportedly false-positive results concerned small amounts of free fluid identified sonographically but not on subsequent CT; however, sonography is possibly more sensitive than CT in this respect rendering these cases possible “true positives” [57]. In a second prospective study evaluating sonographic assessment of blunt abdominal trauma, the sensitivity of sonographic

identification of fluid and/or parenchymal abnormalities in diagnosing intra-abdominal injury was 67% [58]. Upon evaluation of outcome in patients with negative screening sonographic scans post-blunt trauma, among 3,679 patients, 99.9% were true negatives. Of the 38 false-negative studies, 24 of the cases were non- surgical and 14 were surgical. The combination of negative ultrasound findings and negative clinical observation virtually excluded abdominal injury in patients admitted and observed for 12-24 hours [59].

Focused abdominal sonography for trauma (FAST; described again later in the text) has been used effectively in the triage of hypotensive patients presenting with blunt abdominal trauma; a large proportion (79%) of which were taken directly to therapeutic laparotomy following positive findings without the need for CT. In predicting the need for therapeutic laparotomy in hypotensive patients, sensitivity of FAST was 85%, specificity 60%, and accuracy 77%. Ultimately, in hypotensive patients with moderate to large fluid collections, immediate triage to the operating room may be required. In hypotensive patients, bowel or mesenteric injuries may not be associated with a significant amount of free fluid and therefore may lead to false-negative findings on FAST; further evaluation with CT may be indicated in these cases [60].

As diaphragmatic rupture is a possible sequela to severe blunt abdominal trauma, sonographic characterization of this condition has also been reported. Consideration for this condition upon FAST examination may be beneficial as a result and would only minimally extent examination length. M-mode evaluation of diaphragmatic motion may reveal absence of deflection in these cases [61].

The role of sonography in penetrating abdominal trauma is also of clinical interest given early reports of a nontherapeutic laparotomy rate of approximately 30% using mandatory exploration in these cases. Focused assessment with sonography for trauma (FAST) was therefore assessed prospectively for its utility in detecting penetrating abdominal injury at a level I trauma center; performed within 20 minutes of admission. Perihepatic, perisplenic, pelvic and pericardial imaging was performed according to prior recommendations; results were positive if free intraperitoneal fluid was discernible (excluding pericardial evaluation). Parenchymal injuries were not recorded. FAST was positive in 21 patients (19 of which were true positives). The 2 false-positive studies included a gunshot wound to the right upper quadrant where free fluid was noted sonographically but not on follow-up CT. The second was a stab wound case where CT demonstrated mild pleural free fluid rather than peritoneal free fluid. 54 patients had a negative FAST, 32 of which were true-negatives. The 22 false-negative cases had intra-abdominal injury at laparotomy; of these cases 13 had significant free peritoneal blood (volumes ranging from 150-2000ml). The authors reported that additional free fluid accumulation may have occurred between sonographic evaluation and surgical intervention. Ultimately, FAST in penetrating trauma was deemed not as reliable as in blunt trauma cases [62].

Ultrasonography of the acute abdomen: Lost art or future stethoscope? With the increased availability of advanced imaging techniques that are capable of providing a definitive diagnosis (CT especially), the benefits of abdominal ultrasound are in question. Ultrasound

does not require ionizing radiation which is of benefit to younger patients and pregnant women. Secondly, spatial resolution of high frequency ultrasound is greater than that of a CT image (pending ability to image the organ in question). Furthermore, the dynamic nature of ultrasound is unique (bowel peristalsis for example, direct visualization of blood flow, etc.). Mobility and flexibility of the modality in combination with ultrasound guided puncture are additional benefits [63]. Abdominal ultrasound also remains the current modality of choice in the evaluation of suspect acute cholecystitis.

Clinical Applications: Veterinary Medicine

One of the earliest reports describing the use of B-Mode ultrasound in evaluation of the small animal abdomen was published in 1976 by James et al. At the time, structures including the pancreas and adrenal glands were not readily visualized unless enlarged. While the safety and potential clinical utility of ultrasound was immediately recognized, technological limitations in probe frequency and penetration in addition to the need for pharmacological restraint rendered routine ultrasound of limited utility in small animal patients at the time [64].

By 1981, multiple clinical cases were described in the literature highlighting the utility of B-Mode ultrasound in the characterization of hepatobiliary, urinary tract and prostatic disease. The ability to assess both the size and optimal site for percutaneous ultrasound-guided biopsy was also noted [65]. Principles of ultrasound physics (including commonly recognized artifacts) and ultrasound interpretation were published simultaneously [66], [67].

Pancreas: Both the normal and abnormal sonographic characteristics of the small animal pancreas are well recognized and have been reported in a review paper [68]. One of the earliest reports of sonographic evaluation of the abnormal pancreas described B-Mode ultrasonography in experimentally induced canine acute pancreatitis. Following induction of pancreatitis, identification of ill-defined masses with nonhomogeneous echodensity accompanying an overall decrease in echogenecity could be detected in the right and left pancreatic lobes; consistent with similar findings in humans with evidence of pancreatic edema, hemorrhage and inflammatory exudate [69]. Beyond the identification of pancreatitis (even as an incidental finding), routine sonography also permits assessment of the severity of disease, distribution of disease, identification of secondary duodenal inflammation/ileus and finally to evaluate for the presence of additional possible complications including extrahepatic biliary obstruction and abscess/pseudocyst formation [70]. A retrospective review of fatal acute pancreatitis in 70 dogs highlights the possibility of negative sonographic findings as was the case in 2 dogs where plain radiography was more informative. Sonographic evaluation was, however, consistent with the final diagnosis in 68% of patients while survey radiography was consistent in only 24% of dogs [38]. The importance of color/power Doppler evaluation in cases of acute pancreatitis as it relates to a relatively high incidence of thromboembolic disease is highlighted in a later study [71].

Gastrointestinal (GI) Tract: The normal sonographic appearance of the canine GI tract was first described in 1989 and highlighted the ability of routine ultrasound to characterize bowel peristalsis, the histological layers and corresponding wall thickness of the GI (not detectable radiographically)[72]. Shortly thereafter, the sonographic characterization of GI

disease in small animals was described. In a clinical case series of 22 animals with GI disease, neoplasia, intussusception ("target pattern"), ileus, inflammation secondary to pancreatitis, enteritis, and gastrointestinal foreign objects were described. Wall thickening was the most commonly reported abnormality; this was either localized and symmetric/asymmetric or generalized. Localized, asymmetric thickening, was characteristic of most neoplasms included in the study. Gastric ulceration was identified in both benign (gastritis) and malignant conditions and was characterized by a hyperechoic appearance presumptively due to trapped gas. Foreign objects had a variable appearance depending on their physical properties [73].

Given the relatively high frequency of foreign body ingestion in small animals, these were characterized in further detail by multiple groups [74], [75], [76]. In a case series including 10 dogs, 3 cats and 1 harbor seal suffering from foreign body ingestion, the sonographic characteristics were recorded and compared with survey radiography. Distension of the stomach and/or intestine consistent with mechanical ileus was noted in 6 patients, hyperperistalsis in 7, and plication associated with linear foreign bodies in 4. Curvilinear shadowing within the lumen of the stomach was considered highly suggestive of a ball. In fact, strong acoustic shadowing proved to be a useful indicator of foreign material when seen in association with the lumen of the GI tract; the majority of which also demonstrated a strong, echogenic border. Plication of bowel was considered diagnostic for a linear foreign body even when the object itself was not visualized [74]. In a study comparing the clinical utility of ultrasound and survey radiography in the investigation of GI foreign bodies, ultrasound was able to detect a foreign body in all cases while only 9/16 were

radiographically identifiable [77]. In a second study comparing radiography and ultrasound in the diagnosis of small intestinal mechanical obstruction in vomiting dogs, ultrasound produced a definitive result in 97% of cases while radiography produced a definitive result in 70% of cases. Survey radiographs were more frequently equivocal (n=24 versus n=2 for abdominal ultrasound). Sonographic identification of jejunal dilation of exceeding 1.5 cm was also found to be a useful discriminatory finding [78].

Ultrasound features of canine intestinal intussusception was further characterized in retrospective case series of 10 dogs. Ultrasound revealed a concentric ring sign in all cases, 2 showed an associated intestinal mass (both neoplastic), another patient had multiple mesenteric cysts, and a single case had an associated luminal foreign body. Peritoneal free fluid and regional lymphadenopathy was also identified in 2 additional cases, respectively. Eight dogs in this same case series underwent survey radiography prior to ultrasound; only one of which was definitively diagnostic for intussusception due to the presence of a meniscus sign [79]; again highlighting the increased sensitivity of routine ultrasound in the assessment of acute intestinal conditions when compared with survey radiography.

Sonographic findings in canine gastric neoplasia have also been reported and are of great clinical relevance, especially when survey radiographic findings are equivocal [80], [81], [82], [83]. In a canine case series including 13 patients, carcinoma was the most commonly reported neoplasm; the majority of cases of which were middle-aged to old medium to large breed dogs. Thickening of the gastric wall accompanied by loss of layering and enlarged regional lymph nodes were likely sonographic findings. Lesion echogenicity was variable [80]. A

retrospective case series in 16 dogs with confirmed gastric epithelial neoplasia revealed similar findings, however, it also described a feature termed “pseudolayering”, which is characterized as a poorly echogenic lining often noted on the innermost and/or outermost portions of the gastric wall and separated by a more echogenic central zone [82].

Gastric ulceration is of particular clinical interest due to the risk for perforation, and has also been described sonographically in clinical case series including 7 dogs. Ultrasound features include local thickening of the gastric wall, loss of layering, presence of a wall defect or “crater,” gastric fluid accumulation, and reduced motility. The “crater” was often centrally located and appeared as a mucosal defect associated with persistent accumulation of small echoes (most likely representing microbubbles as described above). Benign and malignant ulcers could not be differentiated. In 3 dogs, administration of a small amount of water per os was necessary to facilitate mural evaluation [84]. Gastric ulceration can only be identified radiographically via specialized (double-contrast) procedures.

Spleen: Characterization of splenic hypoperfusive conditions via routine abdominal ultrasound has also shown to be beneficial as an adjunct to survey radiography; both in man and in small animal patients. The diffuse, heteroechoic or hypoechoic, course/”lacy” parenchymal pattern without deformation of the splenic margins was first described in dogs in 1988 by Schelling at al. as a sign of splenic infarction and necrosis [85]. Splenic torsion is of particular interest as it relates to surgical acute abdominal conditions. In a retrospective review of 19 canine clinical cases, abdominal ultrasound proved beneficial in

identifying the need for surgical intervention. A hypoechoic pattern in the splenic parenchyma was noted in 9 patients, reduced color Doppler flow in 11 and visible intravascular thrombi in 6 [41].

Peritoneal Space: Conditions of the peritoneal cavity, especially as it relates to the identification of small volumes of peritoneal free fluid, have relied primarily on routine B-Mode ultrasound. Following the administration of incremental doses of intraperitoneal fluid into 5 healthy dogs (at 1ml/lb body weight), ultrasound was able to detect free fluid at a dose of 2ml/lb while radiography could detect free fluid with a high degree of accuracy at 4ml/lb [86]. Acute abdominal conditions are often accompanied by peritoneal free fluid; highlighting the clinical relevance of this finding. Both the identification of and volume of peritoneal free fluid identified are clinically relevant and highlighted further in a study evaluating an abdominal fluid scoring (AFS) system using an abdominal focused assessment with sonography for trauma (AFAST) protocol. An AFS system used in conjunction with initial and serial AFAST examinations in trauma patients consistently provided a semiquantitative measure of free abdominal fluid that reliably estimated the degree of intra-abdominal hemorrhage and was related to actual decreases in PCV and need for transfusion. Clinical decision making and selection of therapy in the initial 4 hours following presentation were also improved [87]. Rapidity (usually 3 minutes or less) and ease of the scan are additional advantages and involve imaging 4 quadrants: diaphragmatico-hepatic, spleno-renal, cysto-colic and hepato-renal. Additional clinical applications of this and similar procedures are reviewed by the same author [88].

The sonographic characteristics of GI perforation have also been described in a retrospective study including both dogs and cat (14 and 5, respectively). Sonographic findings included regional bright mesenteric fat (19), peritoneal effusion (16), fluid-filled stomach or intestines (12), GI wall thickening (11), free air (9), loss of GI wall layering (9), lymphadenopathy (8), presence of a foreign body (3) and gastric wall mineralization (1). In 14 patients, "perforation" was listed as a differential by the sonographer. Radiographs were performed in 14 patients, 8 of which showed free air. In one case where free air was identified sonographically, free air was not detected radiographically at initial presentation. In fact, 42.9% of patients in this study had no radiographic evidence of pneumoperitoneum. Abdominal ultrasound can also help identify the source of perforation and correctly identified the responsible segment of GI in 94,7% (18/19) of cases [89].

Pneumoperitoneum may be the result of ruptured hollow viscus, however, additional differentials including penetrating wounds, presence of gas-producing organisms and recent abdominal surgery are other possibilities. Small volumes of gas produce an artifact known as reverberation; this occurs with repeated reflection of the ultrasound pulse between the strong reflective surface of the gas and the transducer. Small gas bubbles result in a distinct form of reverberation termed the comet-tail artifact. Comet-tail artifacts are distinguished as a closely spaced series of discrete hyperechoic echoes which are located at a distance equal to that of the width of the gas bubble. This artifact permits identification of small volume pneumoperitoneum using routine ultrasound with a reasonably high sensitivity [90].

Ultrasound has also shown to be beneficial in conditions that disrupt the normal peritoneal cavity (i.e. diaphragmatic rupture). Clinical signs may varybut can be rapidly progressive and life-threatening; these cases require prompt and efficient diagnosis. In some cases survey radiographic evaluation can be complicated by concurrent pleural free fluid in which case positive contrast gastrography or peritoneography may be beneficial. In a prospective study, the correct diagnosis was achieved sonographically in 92.6% (25/27) animals. Findings reported included an irregular or asymmetric cranial hepatic border and visualization of abdominal viscera lateral to the heart (93.7%, 15/16 patients with diaphragmatic rupture) [91].

Contrast-Enhanced US

Review of Contrast Agent Including Safety Considerations; Physical Properties: Contrast agents developed for ultrasound consist of microbubbles comprised of small spheres of gas with low solubility in blood (such as perfluorocarbon) stabilized by a thin shell layer of a flexible, biocompatible material (typically a lipid, though protein and polymer shells are also available). The resulting encapsulated bubble measures approximately 3-5μm; slightly small than a red blood cell. Given their size, these bubbles are unable to pass through the vascular endothelium; thus they serve purely as an intravascular contrast agent. These bubbles are commercially available as a suspension in water that is ultimately injected into a peripheral vein at very small volumes (typically 0.2-2ml), with each injection containing a few tens of million bubbles. The effect of the bolus injection, therefore, is to increase the echo from the blood by a factor of 500-1000 times. This is especially important within

organ parenchyma where blood flow is often too slow to be discriminated from tissue motion; and therefore is difficult to assess with Doppler alone [92].

Blood-borne bubbles provide a distinct acoustic "label" that is independent of flow velocity; this is characterized by the presence of harmonics in the echo which are a consequence of nonlinear oscillation from the bubbles. Due to the specific bubble size, the bubble is capable of natural resonance between 3-5 MHz, which is fortuitously within the diagnostic ultrasound frequency range. The incident ultrasound beam excites the bubbles into nonlinear oscillation that can last seconds or even minutes; permitting a steady stream of harmonic echoes and real-time imaging. This nonlinear bubble oscillation is in contrast to tissue structures which give rise to echoes that simply mirror the incident pulse. *Pulse inversion* imaging exploits this property [92]. Pulse inversion imaging is described in Figure 1 below [93].

If the ultrasound amplitude is increased by the operator (to the level used in normal unenhanced imaging), the result is that the oscillations of the bubbles become large enough to disrupt the shell and cause immediate loss of its gas. This can happen as rapidly as 1/1000 of a second [92].

Safety Considerations: In a multi-center, randomized, placebo-controlled, double blind trial, the efficacy and safety of the contrast agent Perflutren (Definity™) was evaluated in 211 patients with suspected cardiac disease and suboptimal baseline left ventricular echocardiographic images. No clinically significant change in physical examination, vital

signs, electrocardiographic tracings or chemistry/hematology laboratory values was noted. The adverse event rates were similar across treatment groups; occurring in 30 of 169 patients (18%) in the combined perflutren-treated group and in 6 of 42 (14%) of the placebo-treated group. Headache was the most frequently reported adverse even, reported in 5% of patients who received perflutren and in 7% of patients who received placebo. Most importantly, 77 of the 211 patients had chronic obstructive pulmonary disease or congestive heart failure; conditions thought to be at increased risk of adverse events. The adverse event profiles in these groups were similar to the overall study population, were not clinically significant and were not different from placebo. The authors concluded, therefore, that the administration of perflutren to patients with suboptimal baseline images is well tolerated and additionally provided substantial left ventricular cavity opacification and improvement in endocardial border delineation [94].

As the frequency of use of ultrasound contrast agents continued to increase, additional safety studies were performed. In 2005, the contrast media safety committee of the European society of urogenital radiology decided to review the safety of ultrasound contrast agents in humans and develop a set of guidelines. The cavitation phenomenon was referenced, describing the formation, growth and collapse by implosion of microbubbles. In so doing, large changes in pressure and temperature occur in the close vicinity, which raises a safety concern. This is thought to be responsible for potential hemolysis and platelet aggregation that has been demonstrated in previous in vitro studies [95].

Pulmonary effects have also been evaluated and reviewed by the same group, noting that there seems to be a species difference in terms of how the lungs may react to contrast media as well as contrast tolerability [95]. Specifically, a prior study demonstrated that two of 26 anesthetized dogs given the cardiac echo-enhancing agent Optison®, showed anaphylactoid responses though to be related to the human albumin component of the agent [96]. A second canine study evaluated the effects of Optison® on pulmonary gas exchange and hemodynamics. Twelve dogs with experimentally induced pulmonary hypertension were compared with twelve normal dogs (all previously healthy, with each group of twelve divided evenly into control and treatment groups). The study ultimately showed that Optison may produce a small, dose-related increase in pulmonary arterial pressure without change in cardiac output in normal dogs; a reaction that peaks about 3-4 minutes after injection, and essentially disappears within 8 minutes. There was no associated effect on pulmonary gas exchange. When given to dogs with pulmonary hypertension (mean pulmonary arterial pressure of 33 mmHg), there was no measurable effect on pulmonary arterial pressure nor gas exchange [97].

The contrast media safety committee ultimately concluded that ultrasound contrast agents approved for clinical use are well tolerated and serious adverse reactions are rare. Adverse events are usually minor as previously described (including headache, nausea, altered taste) and self-resolving. As these have been reported in placebo-control groups, the cause and effect relationship is ill-defined. The authors ultimately recommended that scanning

time and acoustic output be minimized to a level consistent with obtaining diagnostic information and that adverse reactions be treated symptomatically [95].

In 2006, the safety of SonoVue® in abdominal applications was retrospectively evaluated in a study including 23, 188 investigations. This study followed a brief hold on SonoVue® clinical studies that was placed in 2004 by the United States Food and Drug Administration due primarily to three reported serious events with fatal outcomes in patients with coronary artery disease; later considered idiosyncratic hypersensitivity events not unusual for injectables. The overall reporting rate of serious adverse events in the current safety study was 0.0086%, with only 4 adverse events requiring treatment. No fatalities were reported [98].

Finally, a recent study evaluated acute mortality in hospitalized patients undergoing echocardiography both with and without the use of an ultrasound contrast agent (specifically Definity). A total of 18, 671 patients were retrospectively reviewed, 6, 196 of whom received the contrast agent. There was no statistical difference in percentage acute mortality in the patients that underwent unenhanced echocardiogram versus enhanced echocardiogram ($p=0.60$) [99].

Clinical Applications (limited to acute abdominal conditions): Human Medicine

In the last 15 years contrast-enhanced ultrasound has been used with increasing frequency in evaluation of acute abdominal conditions. Reported applications include, but are not limited to, the following: vascular imaging, pancreatic imaging, active hemorrhage and small bowel ischemia/infarction.

GI: Vascular compromise of the gut is responsible for approximately 0.1% of all hospital admissions and 1.0% of admissions for acute abdomen. The relative incidence of intestinal ischemic disorders are as follows: colonic ischemia (75%), acute mesenteric ischemia (25%), focal mesenteric ischemia (5%), and chronic mesenteric ischemia (5%) [100].

The utility of CEUS (Levovist) in the depiction of bowel ischemia in patients with radiographic evidence of small-bowel dilation has been evaluated prospectively. Twenty patients had bowel ischemia; 5 secondary to thromboembolism of the superior mesenteric artery and 15 secondary to bowel strangulation. Definitive diagnosis was obtained at the time of surgery (18) or autopsy (2). Color signals were absent in 5 patients with superior mesenteric arterial thromboembolism and in 7 with strangulation, were diminished in 5 with strangulation, and were normal in 3 patients with strangulation and 31 with simple obstruction. By pooling absent and diminished color signals together as an indicator of bowel ischemia, the sensitivity was 85%, specificity 100%, PPV 100% and NPV 91.2% [101].
In a second study, 50 patients admitted for bowel obstruction were evaluated prospectively with CEUS (Levovist) for evidence of bowel ischemia. Seventeen patients had

intestinal ischemia (bowel strangulation in 9, superior mesenteric artery thromboembolism in 4 and non-occlusive mesenteric ischemia in 4). Definitive diagnosis was established at the time of surgery. Following administration of IV contrast, the least peristaltic and/or the most dilated segments were imaged. Color signal was categorized as absent, diminished or normal. Assuming that absent or diminished color signal is indicative of intestinal ischemia, the sensitivity, specificity, positive and negative predictive values were 94.1%, 100%, 100% and 97.1%, respectively [102].

Pancreas: Dynamic imaging of pancreatic diseases by contrast enhanced coded phase inversion harmonic ultrasonography has been reported with the use of Levovist (galactose/palmitic acid shell containing air). Sixty-five patients suspected of having a pancreatic mass (based on prior imaging screening tests) were enrolled in a prospective study. Figure 2 demonstrates the classification of vascular patterns in pancreatic lesions evaluated in the study. Note that normal pancreatic tissue showed several vessels distributed homogenously on the vessel image and a homogeneous stain on the perfusion image. Fourteen of 15 tumors classified as type I were ductal carcinomas; one was an endocrine tumor. All 29 type II lesions were ductal carcinomas. Seven inflammatory pseudotumors caused by chronic pancreatitis showed a type III pattern; one case of ductal carcinoma also showed a type III pattern. Seven of 10 tumors classified as type IV were endocrine in origin; the three remaining cases were pancreatic carcinomas. It was shown that the vascular patterns of tumors on contrast enhanced US correlated well with those on contrast enhanced CT; suggesting that these modalities are similarly reliable in the

diagnosis of pancreatic neoplasia. CEUS depicted 6 tumors that contrast enhanced CT failed to detect [103].

In a second study, 60 patients for whom it was not possible to differentiate between an inflammatory focal lesion of the pancreas and a pancreatic carcinoma underwent quantitative perfusion analysis CEUS with a second-generation contrast agent. Time intensity curves were obtained in all exams in 2 regions of interest; within the lesion and within normal pancreatic tissue. Forty-five malignant masses and 15 inflammatory lesions were confirmed histologically. Arrival time and time to peak enhancement in cancerous lesions was significantly longer than in healthy pancreata and in focal inflammatory lesions. Peak intensity, however, did not significantly differ and were significantly lower than in healthy volunteers [104].

In a prospective study evaluating CEUS in the characterization of pancreatic lesions with a cystic appearance, the ability to visualize microvascularization (even in small nodules) associated with cystic lesions was shown to be an indicator for cystic pancreatic neoplasia (as opposed to pancreatic benign pseudocyst formation). CEUS showed improved specificity, as a result, when compared with B-Mode ultrasound for the differentiation of benign vs. malignant cystic lesions (76.6% vs. 43.8%, respectively) [105].

The use of CEUS in the staging of acute pancreatitis has also been reported [106] [107]. In a prospective study comparing CEUS and contrast-enhanced CT in 50 patients with acute pancreatitis, CEUS was comparable to CT in identifying pancreatic necrosis as well as

predicting its clinical course. Grade of necrosis was similar across modalities in all patients with the exception of 3 cases where grade was underestimated by CEUS. Furthermore, CEUS missed 3 cases with mild necrosis (86% sensitivity). Ultimately the authors advocated the use of CEUS in the assessment of acute pancreatitis when CT may be contraindicated [106]. In a separate quantitative prospective CEUS study also evaluating the severity of acute pancreatitis, 62.5% concordance was identified in the assessment of degree of necrosis when comparing CEUS and CECT. Real-time vascular assessment with improved temporal resolution remain benefits of CEUS [107].

Trauma: The clinical utility of a second-generation contrast agent (SonoVue) in the detection of solid organ injuries (of the liver, spleen, kidneys or adrenal glands) as it relates to blunt abdominal trauma was evaluated prospectively in 210 hemodynamically stable trauma patients. All enrolled patients underwent abdominal contrast-enhanced CT, surgery or both. In spite of a satisfactory quality examination, 18% of solid organ injuries shown on CT were false-negative results on contrast-enhanced US. Four of these were considered major injuries. CEUS did show a statistically significant improvement in the detection rate of solid organ injury relative to routine B-Mode ultrasound. With respect to the potential of CEUS to identify intraparenchymal vascular injuries, all 5 pseudoaneurysms that were identified on CT were also clearly depicted on CEUS. Ultimately, CEUS could not be recommended to replace CT in the triage of hemodynamically stable trauma patients due to the possibility of missing major solid organ injuries. There may be clinical benefit, however, in the use of CEUS as an alternative to control CT for the depiction of delayed splenic pseudoaneurysm from trauma [108]. In a

separate study, the sensitivity for detection of solid organ injuries with CEUS relative to routine B-Mode ultrasound improved from 45.7% to 91.4%. Moreover, CEUS could detect contrast extravasation (consistent with hemorrhage; to be discussed further in the following paragraphs). Contrary to the study by Poletti et al. referenced above, no major lesions identified on CT were missed with CEUS; possibly due to the improvement of sonographic technologies. The authors suggest that CEUS can be a useful screening tool in the trauma patient and CT potentially reserved for patients with negative sonographic findings [109]. In a prospective multi-center study evaluating CEUS in abdominal trauma cases (utilizing CT and/or surgery as the gold standard), CEUS only missed minor traumatic injuries, none of which required surgery or died as a consequence of the missed lesion. Sensitivity of CEUS was better than plain US (consistent with previous studies) and approached that of CT [110]. Findings were also similar in a prospective study evaluating children presenting for blunt abdominal trauma [111].

The use of CEUS specifically in the detection of active hemorrhage has also been evaluated [112,113]. In a 2 year period, 153 emergent CEUS studies (SonoVue) were performed and reviewed retrospectively. Contrast extravasation was found in 13% of cases and included splenic injury, liver injury, renal injury, abdominal aortic aneurysm rupture, splenic angiosarcoma rupture and post-surgical bleeding. Nine of these cases had undergone a contrast-enhanced CT scan which confirmed the CEUS findings in all cases. Active extravasation appeared as a round, hyperechoic pool or as a fountain-like hyperechoic jet [113].

Clinical Applications: Veterinary Medicine

The veterinary literature as it relates to the use of contrast-enhanced ultrasound is limited predominantly to the past decade and excludes evaluation of the acute abdomen,which is the subject of this thesis. The following paragraphs summarize the reported normal CEUS appearance of specific viscera followed by a discussion of reported characterization of clinical disease.

Normal CEUS findings in the Dog: The normal CEUS appearance of the canine adrenal gland, medial ilial lymph node, prostate, jejunum, duodenum, pancreas, liver, spleen and kidney have all been reported [114-121].

Adrenal Gland: In human patients, contrast-enhanced ultrasonography is reportedly useful in differentiating adrenal adenomas from nonadenomatous tissue, prompting evaluation of the normal adrenal gland in the dog. Six healthy dogs were enrolled in a prospective study utilizing the contrast agent SonoVue. Aortic enhancement was immediately followed by the renal artery and finally the adrenal gland (10-15 sec post injection). Adrenal enhancement was uniform, centrifugal and rapid from medulla to cortex. Following peak enhancement, a gradual homogenous decrease in echogenecity of the gland began and simultaneous enhancement of the phrenicoabdominal vessels was observed [119]. Feasibility and pattern of enhancement were therefore established for the canine adrenal gland; however, clinical studies remain necessary to ascertain if CEUS is useful in disease conditions.

Medial Iliac Lymph Node: Fourteen healthy dogs were evaluated prospectively with contrast-enhanced harmonic ultrasound using Definity contrast media. Power and color Doppler evaluation of the lymph nodes was also performed for comparison. Normal lymph nodes showed a mean contrast wash-in phase beginning at 6.3 seconds from the time of injection, with mean peak pixel intensity at 12.1 seconds. Angioarchitecture was best visualized with CEUS as compared to power and color Doppler in which the regularly spaced intranodal branches were not visible in any of the dogs. Normal lymph nodes showed a central artery with centrifugal and uniform branching pattern [116].

Prostate: Ten healthy dogs were prospectively evaluated prior to and following injection of Levovist contrast media. The mean time from contrast injection to enhancement of the Doppler signal in the prostatic and capsular arteries was 10.4 seconds, whereas the time from initial enhancement to the arrival of contrast in the parenchymal vessels and periurethral veins was shorter (3-7 seconds). Contrast administration improved assessment of the vascular architecture in all dogs, and this was statistically significant. Prostatic cancer has been associated with an increase in glandular blood flow in people and therefore may similarly be of clinical benefit in small animal patients; however, this has not been established in clinical canine cases to date [115].

Pancreas and Small Intestines: The normal CEUS appearance of the canine duodenum, pancreas and jejunum have been characterized in two separate studies both utilizing Definity contrast media [117,118]. The pancreas and proximal duodenum of 8 healthy dogs were imaged prospectively via a right intercostal approach; subjective and quantitative

perfusion data was recorded. Following contrast administration, microbubbles were first seen arriving within the cranial pancreaticoduodenal (CrPDA) artery of the pancreas. Contrast inflow and concentration within the capillary beds of the pancreatic parenchyma from the CrPDA ultimately produced a sharply marginated and uniformly contrast-enhanced pancreas at peak intensity. The anechoic non-contrast enhancing cranial pancreaticoduodenal vein (CrPDV) was immediately adjacent to (and typically dorsal to) the CrPDA. During pancreatic outflow, continual decline in parenchymal intensity occurred via contrast drainage into the CrPDV. Enhancement of the serosal and mucosal layers of the duodenum was seen concurrently with the parenchymal phase of the pancreas followed by homogeneous enhancement of all duodenal layers at peak intensity. Peak intensity and washout of the duodenal wall and pancreas occurred subjectively at the same time. Time to peak intensity was rapid for both the pancreas and duodenum (13.16 +/- 6.27 sec and 13.08 +/- 6.16 sec, respectively) [118].

CEUS evaluation of the normal canine jejunum was performed prospectively in 9 healthy client-owned dogs undergoing planned elective surgery. Three serial doses of Definity (0.007 ml/kg, 0.015 ml/kg, 0.03 ml/kg) were administered in an escalating dose protocol. Mean time to peak values were 14.1, 19.6 and 21.9 seconds for low, medium and high doses, respectively. Peak intensity mean values were 38.3, 58 and 79.2 mean pixel value for low, medium and high doses, respectively. No association between time to initial arrival, baseline, inflow or outflow slope with dose was identified. Subjective evaluation with the high dose revealed clear delineation of jejunal arteries and enhancement of the

jejunal wall in a serosal to luminal direction. Contrast enhancement was unsatisfactory in 77% (7/9) of dogs with low dosing [117].

Liver and Spleen: One of the first reports describing the use of CEUS in veterinary patients described the normal appearance of the liver, spleen and kidney using Imagent contrast media (perflexane lipid microspheres). Six healthy dogs were enrolled in this study. Initial peak enhancement following Imagent injection occurred by 30-40 seconds in the region of interest at 3 cm of depth in the liver. Findings in the spleen were similar to those in the liver [114]. In a second study evaluating Definity contrast media imaging of the normal canine liver, bolus injection and CRI were compared; the former yielding more consistent results with a subjectively less cumbersome protocol. In the same study, time to peak (from injection) was determined to be 22.88 +/- 6.79 seconds. The majority of patients enrolled were imaged under general anesthesia (6) and only 2 with manual restraint while the difference between these groups was not assessed statistically [122]. A separate study evaluating the liver of 11 healthy dogs via SonoVue CEUS was later published. In addition to evaluating transit time indices in the normal liver, additional goals included examining the effect of anesthesia (Propofol) on these parameters and evaluating the safety of this contrast agent in dogs. The mean relative peak enhancement with and without anesthesia was 14.3%. Time to peak enhancement was significantly prolonged in awake dogs (46.3 seconds) when compared with anesthetized dogs (34.6 seconds). This difference can likely be explained by the effect of Propofol on the vascular system; that is the proposed increase in hepatic arterial blood flow and reduction of systemic arterial pressure while not having

an effect on cardiac output or portal venous flow. Mean upslope was identical in both groups. No adverse reactions to the contrast agent were observed [121].

Quantitative contrast-enhanced ultrasound of the normal canine spleen has also been reported with a second-generation contrast agent (Sonazoid-perfluorobutane microspheres). Sonazoid is of particular interest given its utility in both real-time contrast imaging along with parenchymal imaging. Six healthy adult beagle dogs were evaluated prospectively. Time to initial upslope from injection of the splenic arteries was 5.2 +/- 0.4 sec and time to peak enhancement from initial upslope 2.7 +/- 1.0 sec. Beyond 23 sec, no significant difference was noted between the grey-scale of arteries and that of the parenchyma. Time to initial upslope from injection of the parenchyma was 7.0 +/- 1.6 sec and time to peak enhancement from initial upslope 20.8 +/- 2.1 sec. A high grey-scale value was maintained in the parenchyma for up to 30 min [123]. CEUS of the accessory spleen (via SonoVue) revealed similar type and timing of enhancement to the parent spleen in 4 healthy dogs [124].

Kidney: Quantitative contrast ultrasound of normal renal perfusion has been evaluated. Eight healthy dogs were evaluated prospectively with Definity contrast agent. This study demonstrated maximal renal cortical enhancement at approximately 15 seconds followed by maximal medullary enhancement at approximately 30 seconds. Initial medullary enhancement was always found to occur (subjectively) later and slower than in the cortex; the medulla also usually remained mildly hypoechoic compared with the cortex throughout contrast medium inflow and outflow. The dual capillary bed system of the kidney provides

an explanation for the difference between cortical and medullary enhancement patterns; with fast early cortical inflow as a reflection of blood flow to the glomeruli and the delayed peak possibly representing tubular perfusion in the second capillary bed concurrent with more gradual inflow of the medulla [120].

Abnormal CEUS Findings in the Dog: The veterinary literature as it relates to the use of CEUS in the canine clinical patient is extremely limited; including descriptions of the modality in the characterization of lymphomatous lymph nodes, porto-systemic shunt, and hepatic, splenic and renal lesions only [125-132].

Liver: In two separate studies a variety of contrast agents (Definity, SonoVue and Sonazoid) were used to characterize focal liver nodules in dogs; both studies of which agree that there is a statistically significant association with malignancy when a nodule appears hypoechoic compared to surrounding normal liver at peak liver/parenchymal enhancement. Decreased conspicuity of benign nodules following contrast enhancement is also reported [126,129]. Improved detectability of hepatic hamangiosarcoma metastases (where lesions were not identified on conventional gray-scale ultrasound) is also reported in a separate case series with Definity contrast media [130]. In an unrelated study evaluating congenital extra-hepatic portosystemic shunts in 3 dogs, CEUS with Definity contrast media was able to demonstrate that mean peak perfusion times of dogs with PSS were significantly shorter than in reported normal dogs. The contrast inflow slope was also significantly larger than reported normal dogs. The explanation for this finding is that of

increased arterial flow to the liver in this disease as a possible protective hemodynamic function to ensure normal levels of overall hepatic blood flow [131].

Spleen: Multiple veterinary studies describe the appearance of focal splenic lesions on CEUS utilizing SonoVue and Sonazoid contrast media. These studies consistently report that malignancy is associated with hypoechogenecity in the late-vascular or wash-out phases [125,127,128]. Given the small numbers of individual malignancy types across these studies, accurate characterization of specific diseases is difficult.

Kidney: A single study describes the contrast harmonic sonographic appearance of focal space-occupying renal lesions in 15 dogs and 1 cat using SonoVue contrast media. Final diagnoses included 11 malignant lesions (including the cat) and 5 benign lesions (hematoma, abscess, and hemorrhagic and necrotic nodular lesion). B-mode sonographic examination of the renal masses revealed non-specific findings as it relates to the differentiation of benign vs. malignant disease. With the exception of metastatic lesions, all malignancies in this study were vascularized and had large (renal cell carcinoma) or smaller vessels (histiocytic sarcoma, lymphoma) during the arterial phase and became gradually hypoechoic during the late corticomedullary phase of enhancement; washout was early (histiocytic sarcoma, lymphoma) or late (renal cell carcinoma). All hemangiosarcoma metastases appeared as nonenhancing nodules during the early arterial and late corticomedullary phases of enhancement and additional lesions were detected. Benign lesions were better defined following administration of contrast agent [133].

Lymph Nodes: Eleven client-owned dogs with multicentric malignant lymphoma were enrolled in a prospective study and peripheral lymph nodes scanned prior to administration of chemotherapy. The angioarchitecture of lymphomatous nodes in this study were similar to those reported in human patients with almost ½ showing displacement of the central hilar vessel and aberrant vessels, 63.6% showing pericapsular vessels, 36.4% showing subcapsular vessels, and 81.8% showing loss of the central hyperechoic band in fundamental sonography. Vessels were 2.1 times more likely to be seen following administration of contrast media [132].

Computed Tomography (CT)

Basic Physical Principles of Multislice Helical CT

The purpose of multislice technology is to improve volume coverage speed performance; scanning at higher speeds with higher pitch ratios to cover larger volumes with equivalent image quality (when compared with single-slice volume CT). These scanners were introduced at the 1998 meeting of the Radiological Society of North America in Chicago and are based on spiral/helical scanning using multiple detector rows (ranging between 8, 16, 32, 40, 64, 256 and 320 depending on the manufacturer) [134].

The third generation geometry (which is the subject of this paper) is based on a tube-detector array that rotates around the scan plane. The fan-shaped beam is collimated and exposes one or, in the case of multidetector CT, multiple parallel detector arrays that are arranged in a circular segment opposite to the x-ray tube. The slip-ring technique

(developed in the late '80's) is responsible for the continuous one-way rotation of the tube-detector system; enabling continuous data acquisition. During a helical CT acquisition, the patient is moved through the gantry while the tube-detector system rotates continuously. From this volumetric acquisition, CT images are reconstructed in the standard transverse x-y plane. The collimation of the x-ray beam determines slice thickness. Images can then be reconstructed at any location within the scan volume along the longitudinal direction z; allowing the reconstruction interval to be chosen independently from the slice thickness. From 16-slice scanners onwards, substantial anatomic volumes can be acquired with isotropic sub-millimeter spatial resolution and short scan times; allowing reconstruction of images in any arbitrary plane without loss of image quality. With the most recent technologies, rotation time can range from 0.27-0.5 seconds, and table speeds can exceed 20cm/sec [135].

The benefits of multi-detector helical CT as it relates to clinical applications in both human and veterinary medicine (especially in comparison to plain radiography) is the subject of the sections to follow.

Contrast-Enhanced CT

Brief Review of Non-Ionic Iodinated Contrast Agents and Safety Considerations: To date there are no reports describing adverse effects of non-ionic iodinated contrast in veterinary clinical patients; the following discussion, therefore, is limited to several recent human publications.

Iohexol (Omnipaque), a non-ionic, monomeric, triiodinated water-soluble x-ray contrast medium is used exclusively as the intravenous CT contrast agent in the institutional study described in the chapters to follow. Close to 100% of the IV injected iohexol is excreted unchanged through the kidneys within 24 hours in patients with normal renal function. No metabolites have been detected and protein binding is very low (less than 2%) [136].

Pending the patient sub-population in question, the rate of adverse reactions/events related to the administration of non-ionic iodinated contrast medium is variable and may range from hypersensitivity-type reactions to acute nephrotoxicity; the latter of which will be the primary focus of the following paragraphs given the potential immediate life-threatening nature of this condition.

There are several proposed mechanisms of the pathogenesis of contrast-induced nephropathy. Two major theories include renal vasoconstriction resulting in medullary hypoxemia (mediated by alterations in nitric oxide, endothelin, or adenosine) and the direct cytotoxic effects of contrast media [137].

While there are clearly conflicting reports regarding the benefits of different preventative measures, data consistently support the routine use of prehydration. Intravenous normal saline volume supplementation reduces the hazards of contrast-induced nephropathy, is relatively cost-effecting and safe, and should be considered in all patients undergoing procedures with intravascular contrast [137]. Using the lowest possible effective dose of

contrast in addition to the potential use of iso-osmolar contrast media in high-risk patients are additional recommendations [138].

Contrast-induced nephropathy in people is considered the third leading cause of hospital-acquired acute renal insufficiency and is associated with an increased mortality. The potential risk for contrast-induced nephropathy has potentially even increased in recent years given the more frequent use of contrast-enhanced CT in the emergency department; which is of particular interest as it relates to evaluation of the acute abdomen in canine clinical patients. In a retrospective review of 750 patients who underwent emergency CECT, nephropathy was observed in 34 (4.5%). Old age, diabetes mellitus, low mean blood pressure and higher basal serum creatinine were all associated with nephropathy. Ten of these patients died, 1 required permanent renal replacement therapy, and 23 showed complete recovery of their baseline renal function. A limitation of this study was the patient selection criteria as only patients with baseline and follow-up serum creatinine levels were included. All patients received a low osmolar non-ionic contrast agent [139].

While complications related to non-ionic iodinated contrast medium have yet to be reported in the veterinary literature, a need for increased implementation of evidence-based protocols to improve prevention of contrast-induced nephropathy ,including routine identification of at-risk patients, withdrawal of nephrotoxic drugs, use of volume repletion regimens, lowest possible dose of contrast medium, and appropriate contrast medium, has been recognized in the human radiology field [140]. These techniques are feasible and cost-effective for veterinary diagnostic imaging professionals and should routinely be

considered in patient screening/management as the frequency of contrast-enhanced veterinary imaging studies continue to rise.

CECT: Clinical Applications in Human Medicine

In the last 2 decades, there has been a gradual emergence in the use of multi-detector helical CT in the evaluation of patients presenting to the emergency room with acute abdominal signs. The acute abdomen is generally recognized as a clinical syndrome causing acute abdominal pain of sufficient severity and duration to require hospitalization or immediate surgical intervention. The following discussion will be limited to the recent and pertinent CT literature as it relates to evaluation of the non-specific "Acute Abdomen," acute pancreatitis and ischemic/obstructive disease of the bowel.

Acute Abdomen: In an early review paper, the role of CT as it relates to the workup of acute abdominal disease was characterized in light of 3 potential clinical entities: abdominal pain with fever, abdominal pain that is associated with contracture or hypotension, and obstructive disease. The first category recognizes conditions including but not limited to cholecystitis, cholangitis, pyelonephritis, acute appendicitis, pancreatitis and hepatic/splenic abscess; the former three of which are better evaluated with ultrasound and/or initial clinical evaluation. In acute abdominal conditions causing intense abdominal pain or abdominal pain coexisting with contracture or hypotension, peritonitis secondary to GI perforation is a possibility; CT is especially beneficial in cases with small volume pneumoperitoneum or walled-off perforated lesions. Finally in the case of obstruction, CT

is superior to plain films at all stages of diagnosis and permits assessment of bowel wall ischemia [141].

In a retrospective evaluation of 91 patients admitted to an emergency department for acute abdominal pain that was initially medically managed, axial contrast-enhanced CT evaluation revealed the correct diagnosis in 78 patients (sensitivity of 90%) versus a correct clinical diagnosis in 55 patients (sensitivity 76%). In 25 patients, CT permitted modification of patient management [142]. Similar benefits of CT relative to clinical examination performance were also highlighted in an earlier prospective study where CT allowed appropriate therapeutic decisions in 95% of acute abdominal cases, while clinical examination was successful in only 60%. Pre-CT therapeutic decisions included the evaluation of plain abdominal radiographs in all patients [143].

Prior to the routine use of helical CT technology (studies described thus far deal with axial technology), careful consideration for the CT technique was necessary due to the time-consuming nature of the scan. The decision to administer contrast, for example, was not necessarily routine and was instead patient-dependent. The benefits of contrast administration (oral, rectal and IV) were, however, recognized early on, including visualization of vasculature, bowel lumen characterization, identification of enhancement patterns, and extravasation of contrast [144]. Targeted helical CT of the acute abdomen was described concurrently/shortly thereafter [145-147]. The latter publication proposes the following protocols for non-localizable acute abdominal pain (Table 1) and CT evaluation of acute abdominal patients with a working clinical diagnosis (Table 2) [146].

With the development of multidetector row helical CT (MDCT), high-resolution axial sections (0.65-2.5 mm) through the entire abdomen and pelvis can be performed in a single breath-hold. Furthermore, thin collimation enables sub-millimeter isotropic imaging, permitting reconstructions in any arbitrary plane with a spatial resolution similar to that of the axial plane. Exploratory laparotomy, therefore, has become somewhat of a historical artifact in the human emergency room setting and CT the recognized first-line imaging modality of choice in patients with acute abdominal pain (with the exception of cholecystitis) [148], [149]. In a retrospective review of 2,222 patients with acute abdominal pain who underwent contrast-enhanced CT within 24 hours of admission, the suggested diagnoses were correct in 96.8% of cases. Incorrect diagnoses are, however, possible and were reported in 16 cases, resulting in 7 unnecessary laparotomies; 5 of which were wrongly diagnosed with acute appendicitis, and 2 suspect GI tract perforations [150]. Note that even unenhanced helical CT has even been proven to yield superior results to a three-view abdominal radiographic series with a sensitivity, specificity and accuracy of 96%, 95.1% and 95.6%, respectively; compared with radiographic sensitivity, specificity and accuracy of 30%, 87.8% and 56%, respectively [151]. A second study evaluating non-contrast enhanced MDCT revealed similarly promising results indicating a sensitivity, specificity and PPV of 100%, 98.5% and 91.7%, respectively, for the detection of free gas, stones and intestinal obstruction [152]. A separate group showed that no statistically significant difference was noted between unenhanced and contrast enhanced CT in the ability to diagnose a suspected acute abdominal process[153]. A recognized concern and possible limitation of routine CT use in the emergency setting is the relatively increased overall

patient radiation dose; it has been noted, however, that the use of CT ultimately reduces the total number of additional radiographs needed when compared with plain radiography. Furthermore, a low CT dose approach (50mAs) does not appear to significantly affect diagnostic quality [154].

Acute Pancreatitis: Severe pancreatitis occurs in 20-30% of human patients with acute pancreatitis and is characterized by a protracted clinical course, multiorgan failure, and pancreatic necrosis. Early staging relies on the presence and degree of systemic failure and on the presence and extent of pancreatic necrosis. Clinical evaluation is limited and often non-specific with reported prediction rates of severe pancreatitis in only 34-39% at the time of admission [155]. Various scoring systems have been developed over the years to help identify patients suffering from severe pancreatitis. The Ranson system is still the most widely used; the clinical and laboratory parameters of which are summarized in Table 3 [156]. With an increased number of risk factors, morbidity and mortality are likewise increased.

CT has become integral in the evaluation of acute pancreatitis and helps overcome certain limitations of abdominal ultrasound such as limited visualization of the pancreas due to overlying bowel gas. CT grading systems (Table 4) have been reported and show reasonable correlation with clinical outcome. Most patients with severe pancreatitis were shown to exhibit one or several pancreatic fluid collections (grades D and E) on initial CT evaluation. Patients with grade D or E had a mortality rate of 14% and morbidity rate of 54% compared with no mortality and morbidity rate of only 4% in patients with grade A, B or C [155].

With the addition of intravenous contrast, parenchymal necrosis could be better characterized (a major limitation of the scoring system established above). The following CT severity index has been proposed (Table 5); a severity index of 7-10 yielded a 17% mortality rate and 92% complication rate while a severity index of 0-1 exhibited a 0% mortality rate with no morbidity [155].

When the CT grading system (A-E) was evaluated retrospectively in patients undergoing helical CT evaluation for acute pancreatitis within 72 hours of admission, it was found that all complications and deaths occurred in patients with a CT grade of severe disease. CT grade had a sensitivity and specificity of 100% and 61.6%, respectively, for predicting morbidity, and 100% and 56.9%, respectively, for predicting mortality [157]. A modified CT severity index was later proposed, now including extrapancreatic complications and thought to more closely correlate with patient outcome [158]; with mild acute pancreatitis 0-2 points, moderate 4-6 points and severe 7-10 points.

Ultimately, the major indications for CT-CT (which remains the gold-standard for evaluation of acute pancreatitis to date) are the following: 1) To establish or confirm the diagnosis when clinical signs and laboratory investigations are indeterminate (CECT can also sometimes demonstrate the underlying cause or may reveal an alternate diagnosis); 2) To determine the severity of acute pancreatitis and to detect pancreatic and peri-pancreatic complications; 3) To guide percutaneous interventions such as catheter drainage of fluid collections [159].

Bowel Obstruction and Ischemic Bowel Disease: Just as early diagnosis and staging of acute pancreatitis is of great clinical relevance, so is the early diagnosis of small bowel obstructive disease. Small bowel obstruction is though to account for 20% of surgical acute abdominal conditions [160]. Limitations of plain radiography have long been recognized. Even with axial CT technology, a sensitivity of 100% (versus 46% for plain radiography) was reported in the diagnosis of complete bowel obstruction [161]. CT was similarly superior to survey radiography in distinguishing mechanical from functional ileus in the post-operative patient revealing a sensitivity and specificity of 100% versus a sensitivity of only 19% for combined clinical and plain film findings [162]. In a retrospective study, CT importantly modified patient management from conservative to surgical management in 10 cases (prior to CT evaluation 26 patients in the study population were determined to require only conservative management) [163].

Helical multi-detector CT permits reformatting of images in multiple planes and therefore helps confirm and complement information obtained on axial images as demonstrated in a pictorial essay [160]. Tailored helical CT techniques specific to small bowel obstruction have been proposed; a zone of transition from distended to decompressed bowel is critical to the diagnosis with a small bowel diameter greater than 2.5 cm considered distended by CT criteria [147]:

Additional reported reliable features of small bowel obstruction on CT include the string-of-pearls sign and small bowel feces sign. The latter is a result of stasis and mixing of small bowel contents and is present in 82% of cases [164].

Beyond the identification of small bowel obstruction, there remains a diagnostic dilemma in determining if there is a need for surgical intervention as a subset of cases may be managed conservatively. A CT scoring system was attempted with the goal of predicting the need for surgical intervention and was successful in doing so 75% of the time with a score of 8 or higher (Table 7)[165].

Bowel ischemia, which is a possible life-threatening sequela to obstructive bowel disease, has also been well characterized by abdominal CT. The benefits of CT in the diagnosis of intestinal perforation were recognized early. CT findings considered diagnostic for bowel perforation are GI contrast extravasation and extraluminal air[166]. Using these criteria, a sensitivity of approximately 85.5% was demonstrated in a later study [167]. CT has been shown to detect extraluminal air in more cases than upright plain films (in one study a difference of 69% vs. 19%)[168].

The accuracy of MDCT in predicting site of GI perforation was assessed prospectively in a separate study with successful prediction in 86% of cases. Concentration of extraluminal air bubbles, segmental bowel wall thickening and focal defect of the bowel wall were all strong predictors of the site of perforation [169]. Direct and indirect findings, however, remain important in correctly diagnosing the site of perforation [170,171]. The periportal free air sign has been specifically evaluated retrospectively, and is thought to be strongly suggestive of upper GI perforation (and is discussed further below as it relates to bowel ischemia) [172].

CT detection of intestinal ischemia (specifically in patients with obstruction secondary to adhesions or hernia) has also been characterized, and demonstrated a sensitivity of 100%. Bowel wall thickening and high attenuation of the bowel were important signs on unenhanced CT whereas abnormal bowel wall enhancement and mesenteric fluid correlated best on enhanced CT evaluation [173]. In a case series describing the CECT diagnosis of acute bowel infarction, the following findings reportedly demonstrate a specificity of >95%: superior mesenteric artery or vein thrombosis (SMA, SMV), intramural bowel gas, portal vein gas, focal lack of bowel enhancement, and ischemia of other organs [174]. Arterial versus venous obstruction is of important clinical consequence as it relates to outcome; in one CT study arterial forms of the disease resulted in an 89% mortality rate while venous forms only 11% [175]. Biphasic MDCT (arterial and portal venous phases respectively) has been assessed in the evaluation of acute mesenteric ischemia revealing similar results. A finding of any one of pneumatosis intestinalis, venous gas, SMA occlusion, celiac and inferior mesenteric artery occlusion with distal SMA disease or arterial embolism was 100% specific but only 73% sensitive. A finding of bowel wall thickening in addition to focal lack of bowel wall enhancement, solid organ infarction or venous thrombosis was 50% sensitive and 94% specific [176]. When a separate group performed a biphasic mesenteric angiography CT protocol for acute mesenteric ischemia, a sensitivity of 93%, specificity of 100% and PPV/NPV of 100%/94% were achieved for CT findings of visceral arterial occlusion, intestinal pneumatosis, portomesenteric venous gas or bowel wall thickening in combination with either portomesenteric thrombosis or solid organ

infarction [177]. A correlation between specific types of pathological damage and associated CT findings can be found in Table 8 [178]:

In a prospective study evaluating 291 consecutive patients who underwent single, portal-venous phase contrast-enhanced MDCT for an acute/subacute abdomen, 24 (8.2%) were diagnosed with acute bowel ischemia. Imaging findings included wall thickening (21), mesenteric stranding and/or little mesenteric fluid (21), pneumatosis (8), mesenteric arterial occlusion (11), and portal venous gas (2) [179]. When results of 11 separate studies were evaluated retrospectively in an attempt to assess the diagnostic performance of CT in assessing bowel ischemia, a sensitivity of 83% (range 63-100%), specificity of 92% (range 61-100%), PPV of 79% (range 69-100%) and NPV of 93% (range 33.3-100%) was identified. These same statistical analyses were performed on 7 studies evaluating the CT classification of complete obstruction, revealing >90% sensitivity, specificity, PPV and NPV [180].

CECT: Clinical Applications in Veterinary Medicine

There are a limited number of publications in the veterinary literature, predominantly emerging within the past decade, that characterized the use of CT in evaluation of intra-abdominal disease. Evaluation of conditions of the upper and lower urinary tract [181-187], spleen [188,189], hepatic/portal venous abnormalities [190-202], pancreas [71,203,204], mesenteric/intrapelvic neoplasia [205,206], adrenal gland [207-209], and GI [210]. The following discussion will be limited to those publications utilizing helical, contrast-enhanced CT.

Urinary Tract: A triphasic helical CT protocol has been described in evaluation of the normal canine kidney. The 3 phases represent an unenhanced phase, corticomedullary phase and nephrographic phase. The renal cortex enhanced immediately following aortic enhancement with a lower HU value than the aorta (scanned with a delayed less than or equal to 10 seconds). The medulla showed gradual enhancement following cortical enhancement [187]. CT characterization of renal mass lesions in small animals are limited to two studies utilizing single-slice CT technology [181,182].

CT evaluation of the lower urinary tract is essentially limited to normal expected findings and the characterization of ureteral anomalies. When helical CT was compared with digital fluoroscopic excretory urography and digital fluoroscopic urethrography, the CT results more closely agreed with both cystoscopy and surgical/postmortem examination findings with regard to status of ureteral ectopia. Furthermore, CT results more closely agreed with both cystoscopy and surgery/postmortem examination in determining the site of ureteral ectopia when compared with the other listed imaging modalities. Sensitivity and specificity of CT were 91% and 100%, respectively [184].

Hepatic and Portal Venous Abnormalities: Hepatic and portal venous anomalies constitute the majority of the veterinary literature as it relates to abdominal CT imaging. The first CT portography protocol described the use of a dynamic study at the level of the portal vein to determine time to peak enhancement; this was later utilized to calculate an appropriate scan delay time for helical scanning. Delay times for normal dogs ranged from 34.5-66 seconds. For patients with confirmed portosystemic shunt, the delay times were 16.5-70.5

seconds. Adequate visualization of the aorta, caudal vena cava, portal vein, shunt vessels and their respective branches were achieved on CT [190]. Shortly thereafter, a dual phase CT angiography protocol for evaluating the normal canine portal and hepatic vasculature was proposed; now including an arterial phase in addition to the portal venous phase which was characterized by median time to peak of the aorta at 12 seconds [191]. When the latter protocol was utilized in a separate study evaluating clinical cases, this was shown to provide improved vascular anatomic detail when compared with a single-phase protocol; all scans were, however, diagnostic [194]. A transplenic CT portography protocol has also been assessed in normal dogs, revealing inconsistent intrahepatic portal branch and parenchymal opacification due to streamlining and streak artifacts with an overall lower total contrast dose when compared with dual phase CT [196]. With the arrival of multi-slice multi-detector helical CT in the veterinary field, maximum intensity projections (MIP) and volume rendering (VR) reconstructions are now feasible and have been proven to be beneficial in the case of portosystemic shunt characterization [201].

Pancreas: Two cases of acute necrotizing pancreatitis in the dog were reported and imaging findings of contrast-enhanced CT and abdominal ultrasonography described. Post-contrast helical acquisition was obtained immediately following injection for the CT portion of the study; both cases revealing non-enhancing portions of the pancreatic parenchyma interpreted as pancreatic necrosis. Subjective reduction in color Doppler flow to the pancreas was noted sonographically in both cases. CECT revealed additional lesions not identified sonographically in one case; these included renal hemorrhage, renal infarction and splenic infarction [71]. A specific CECT protocol was later proposed based on

imaging of the normal canine pancreas. Pancreatic parenchyma showed heterogeneous arterial and homogeneous venous enhancement which was slightly hypoattenuating to the normal liver. Similar to previously described CT angiography protocols for portal venous anomalies, a dynamic study preceded dual-phase CT angiography in the evaluation of the pancreas and associated vasculature so that appropriate timing could be determined. The arterial phase was initiated at the calculated aortic time to arrival with a caudo-cranial scan direction and venous phase initiated shortly before peak venous enhancement or immediately following the minimum reset time between the two phases with a cranio-caudal scan direction [204].

Miscellaneous: Adrenal-CECT has been used in the preoperative evaluation of adrenal masses in dogs in an attempt to determine the extent of associated vascular invasion. CT correctly identified the presence of vascular invasion in 91.6% (11/12) of dogs. Invasion of the phrenicoabdominal vein in one dog was missed on CT. Six of 8 masses with evidence of vascular invasion on CT (for which a histologic diagnosis was available) were malignant. All pheochromocytomas invaded adjacent vasculature. Vascular invasion in this study occurred by way of luminal invasion of the phrenicoabdominal vein with subsequent intraluminal extension into other veins rather than via mural erosion. Specific protocols were variable across patients that were enrolled; all scans, however, included a post-contrast scan obtained immediately following manual IV bolus administration of ionic or non-ionic contrast media [209].

GI: There are a limited number of publications regarding CT evaluation of the GI tract in small animals including a study describing the use of virtual endoscopy in healthy beagle dogs. Virtual endoscopy via MDCT was attempted in 10 healthy beagle dogs and compared with conventional endoscopy. Orogastric administration of air was performed prior to CT image acquisition. No IV contrast was administered. 3-D volume rendering was performed post-acquisition in DICOM format using a dedicated image processing workstation. Lesions requiring recognition of color change on mucosal surfaces (ex. Hemorrhage and bile) could not be seen on virtual endoscopic images. Respiration and gastric peristalsis sometimes resulted in step-like mucosal artifacts in virtual images. Virtual images were, however, comparable in the area of the angular incisure and pylorus. Ultimately, however, in the authors' impression conventional endoscopy remained superior overall [210].

CHAPTER 2

FEASIBILITY FOR USING DUAL-PHASE CONTRAST-ENHANCED MULTI-DETECTOR HELICAL CT TO EVALUATE AWAKE AND SEDATED DOGS WITH ACUTE ABDOMINAL SIGNS

Vet Radiol Ultrasound. 2012; 53(6): 605-612. (Hooray!)

Miriam M. Shanaman, Susan K. Hartman, Robert T. O'Brien

Introduction

Acute abdominal pain in the small animal patient may be minor and transient or the result of an immediately life-threatening process. Specific injury or disease of the peritoneal or retroperitoneal structures, diaphragm, or body wall constituents constitute the majority of underlying etiologies, although referred pain from other sites (especially the spine) may also be mistaken for abdominal pain.[211] Survey radiography and routine B-Mode abdominal ultrasound (US) are the conventional imaging techniques used in the small animal emergency setting, and are characterized by multiple limitations. With the exception of the identification of spontaneous pneumoperitoneum, survey radiographic findings are often non-specific. As a result, routine abdominal US is often performed in conjunction with the added advantage of elimination of visceral superimposition and ability to evaluate parenchymal detail. Limitations of abdominal US in small animal patients with acute abdominal pain include interference by bowel gas, patient discomfort, inter-operator variability and long scan times.

Targeted helical computed tomography (CT) of the abdomen has been described as the modality of choice in people with acute abdominal pain.[145-147] Multi-detector helical CT

advantages include relative rapidity of image acquisition and high spatial resolution. In cases with non-localizable abdominal pain a contrast-enhanced single portal venous phase protocol has been proposed and a dual phase acquisition has been recommended for patients with suspected acute pancreatitis.[146]

Reports describing CT evaluation of the canine abdomen have increased during the past decade. Applications include suspected disease of the upper and lower urinary tract,[181-187] spleen, [188,189] hepatic/portal venous system, [190-202] pancreas, [71,203,204] mesenteric/intrapelvic regions, [205,206] adrenal gland, [207-209] and gastrointestinal tract. [210,212] These reports primarily describe the use of anesthesia or heavy sedation during scan procedures in order to minimize motion artifacts that could result in non-diagnostic scans. Given the recent success of awake imaging protocols for evaluating small animal upper airway and intrathoracic diseases,[213-215] we hypothesized that dual-phase contrast-enhanced MDCT would be feasible and safe for use in awake and lightly sedated canine patients with acute abdominal signs.

Materials and Methods

All protocols were approved by the institutional animal care and use committee of the University of Illinois. Eighteen client-owned dogs presented to the University of Illinois Veterinary Teaching Hospital between February 2011 and January 2012 for acute abdominal signs were enrolled. Study inclusion criteria were cytologic, survey radiographic and/or sonographic detection of a condition requiring immediate surgical intervention (visceral abscess, spontaneous pneumoperitoneum, or small intestinal mechanical obstruction); or a sonographic abnormality consistent with acute pancreatitis,[38,68-71,216,217] or gastrointestinal neoplasia.[73,80-83] Study inclusion was based on the opinion of a board-certified veterinary radiologist and/or radiology resident under the supervision of a board-certified veterinary radiologist. An attempt was made to scan patients awake first; however, minimal intravenous sedation was used when there was poor patient cooperation or evidence of discomfort. Sedation protocols consisted of an opioid with or without addition of a benzodiazepine administered intravenously as a bolus or continuous rate infusion. Specific drug and dosage combinations were selected by the primary care clinician and are summarized in Table 9.

All patients underwent dual-phase contrast-enhanced abdominal CT using a 16-slice helical CT scanner* and the following technique settings: kV 120, mA ranging from 200-325, slice width 2.5 mm with 1.25 mm overlap, pitch 0.9:1 or 1.3:1, and rotation time 0.5 seconds. A dose of 2 ml/kg (600 mg I/kg) of nonionic iodinated contrast medium† was administered intravenously in all patients with the exception of two of the large breed dogs (Boxer and Bloodhound) that received a maximum of 60 ml (1.6 ml/kg and 1 ml/kg, respectively). The contrast agent was administered as a hand injected fast bolus in patients weighing ≤ 20 lbs.

In patients weighing ≥ 20 lbs, the contrast agent was administered via power injector at a rate of 3 ml/sec followed by a 10 ml 0.9% saline flush.

Pre-contrast abdominal CT was first performed, extending from the cranial margin of the diaphragm to the coxo-femoral joints. An initial post-contrast series was initiated immediately at the termination of contrast medium injection (arterial phase). A second post-contrast series was initiated at 40 seconds following initiation of contrast agent administration (portal venous phase). When arterial phase scan time and associated scan delay exceeded 40 seconds, the portal venous phase was initiated immediately; with a 1 second delay necessary for table movement. A third post-contrast series was obtained 52-120 seconds following termination of the portal venous phase in 16 cases to evaluate renal excretion. The timing protocol was selected based on results of angiographic CT studies performed in healthy staff-owned dogs of variable breeds and ages. Scan time was calculated in minutes from the initiation of the pre-contrast series to termination of the intended portal venous phase.

Transverse CT images (pre-contrast, arterial and portal venous phases) were reviewed by the primary author (MMS) and a board-certified radiologist (RTO) on a dedicated DICOM workstation‡. Reviewers were unaware of patient signalment, date of admission, and sedation status. Images were displayed in a soft tissue window (with ability to window/level as needed) and a consensus opinion was recorded for the following image quality factors: motion artifact, anatomic exclusion, presence of non-anatomic beam hardening, vascular phase achieved and presence of contrast agent within the urinary

bladder. Objective criteria used for image quality factors are summarized in Table 10. Vascular phase achieved was based on a selected region of interest (ROI) and Hounsfield unit (HU) measurement within the aorta and portal vein at the level of the porta hepatis; with successful arterial phase imaging defined as an aortic threshold of greater than 250 HU. Overall diagnostic quality was ranked based on a consensus opinion and criteria listed in Table 11.

A commercial software§ was used for all statistical analyses and a p-value < 0.05 was considered statistically significant. Continuous data was assessed for normality using a Shapiro-Wilk test on a per group basis (awake vs. sedated).[218] For continuous data that met the assumption of normality, a Levene's test was performed to assess for homogeneity of variance.[219] Following verification of homogeneity of variances, an independent samples t-test was performed to compare the dependent continuous variables in awake vs. sedated patients. For comparison of ordinal data or non-normally distributed continuous data between groups (sedated vs. awake), the Mann-Whitney U test was used.[220] Mean, minimum-maximum (min-max) and standard deviation (SD) were reported for normally distributed data while median and min-max were reported for non-normally distributed data. Dependent (continuous and ordinal) variables evaluated were: mentation status, age, weight, duration of clinical signs preceding CT (days), hydration status, degree of abdominal pain, systolic blood pressure (17/18 patients), serum lactate (16/18 cases), serum creatinine (16/18 cases), urine specific gravity (12/18 cases), scan time from first pre-contrast image to termination of portal venous phase, motion artifact pre- and post-contrast, anatomic exclusion pre- and post-contrast, measured aortic and portal venous HU

measurements during intended phase respectively at the level of the porta hepatis and overall diagnostic quality.

A Fisher's exact test was used for comparing categorical variables between groups (sedated vs. non-sedated) a.[221] Categorical variables included patient sex, surgical vs. medical underlying condition, and achievement of the arterial post-contrast phase. In cases where specific dependent variables failed to show a statistically significant difference between groups, data was pooled for further evaluation.

Results

Eighteen client-owned dogs met the inclusion criteria. Ten dogs underwent contrast-enhanced MDCT evaluation of the abdomen under sedation and 8 dogs were scanned awake. Eight of the 10 sedated patients had intravenous sedation at the time of the CT scan and 2 patients had recent pharmacological intervention that included sedatives (Table 9). Breeds represented in this group included one each of the following: Golden Retriever, Bloodhound, Australian Shepherd, Labrador Retriever, Tibetan Spaniel, Norwich Terrier and Shetland Sheepdog. Three mixed breed dogs were also included in this group. Six dogs in this group were male (3 intact, 3 neutered) and 4 were female (all spayed). The mean age was 8.68 years (range=4-15.2 years, SD=3.6). Median body weight was 20.75 kg (min-max=6.3-58 kg). Three patients were scanned in sternal recumbency with the aid of the VetMouseTrap™¶ device (head facing away from the CT gantry) and 7 in dorsal recumbency (head facing into the CT gantry). Within the VetMouseTrap™ device, patients were maintained in place with a variable number of foam wedges placed along the lateral chest and abdominal walls and over the neck. Two wide Velcro straps that were fitted to the CT table were then wrapped around the VetMouseTrap™ or patient's dorsum (if the lid was not used). Patients scanned in dorsal recumbency were placed within a cushioned trough fitted with Velcro straps to secure both the forelimbs and hindlimbs individually. Wide Velcro straps were wrapped around the patient and trough for further security.

Eight patients underwent awake abdominal CT. Breeds represented in this group included one each of the following: Scottish Terrier, Basenji, Shih Tzu, Yorkshire Terrier, American Pit Bull Terrier, Boxer, Pug, and Pomeranian. Five were male (1 intact, 4 neutered) and 3

were female (all spayed). The mean age was 6.79 years (min-max=4-9.1 years, SD=1.87). The median weight was 8.4 kg (min-max=5.3-37.5 kg). Mentation status recorded at the time of imaging was quiet, alert and responsive in five patients, bright, alert and responsive in two (American Pit Bull Terrier and Pug) and dull-quiet, alert and responsive in one (Pomeranian). Two patients were scanned in dorsal recumbency within a cushioned trough (American Pit Bull Terrier and Boxer) while the remainder were scanned in sternal recumbency with the aid of the VetMouseTrap™ device (positioned as previously described).

The following continuous dependent variables were normally distributed: age, systolic blood pressure, serum lactate, serum creatinine and urine specific gravity. Following confirmation of homogeneity of variances, independent samples t-testing revealed that serum creatinine was the only variable for which the null hypothesis was rejected (p-=0.041). Mean serum creatinine in the awake group was 0.71 mg/dL, while in the sedated group was 0.99 mg/dL. While a statistically significant difference was detected, these values remain within the acceptable normal canine reference range. All remaining normally distributed-dependent variables did not differ between awake and sedated groups.

Total scan time was less in awake versus sedated groups ($p = 0.05$). Median scan time in the awake group was 6.56 minutes while in the sedated group was 9.79 minutes.

For all dependent categorical variables (patient sex, surgical vs. medical treatment, and achievement of the arterial phase), no differences were identified between awake and sedated groups (p = 1.0, 1.0, and 0.275, respectively). Based on the lack of statistically significant differences in categorical variables between groups, data for all 18 dogs were pooled for analyses described below.

Duration of clinical signs preceding CT scan showed a median of 5 days (min-max=1-10 days). Reported clinical signs included, but were not limited to, the following: Vomiting (14 cases), lethargy (5), inappetance (12), and respiratory distress (1). Results of laboratory testing obtained in the same visit revealed a mean lactate of 3 (min-max=0.70-8, sd=1.98), mean creatinine of 0.87 min-max=0.50-1.50, SD=0.27) and mean urine specific gravity of 1.03 (min-max=1.01-1.05, SD= 0.02). No patients were azotemic prior to diagnostic imaging. For the 16 patients, scanned using a delayed venous phase, all scans confirmed renal excretion bilaterally. Mild dehydration was reported in the majority of patients (10) on the basis of physical examination findings. Three patients were considered moderately dehydrated and 2 severely dehydrated. Intravenous fluid therapy was administered as deemed necessary by the attending clinical either prior to or during CT evaluation. Abdominal pain as assessed by physical examination was reportedly absent (4 cases), mild (8), mild to moderate (1), moderate (4) and moderate to severe (1). Systolic blood pressure (obtained in 17/18 patients) showed a mean of 153.2 mmHg (min-max=70-200 mm Hg, SD=30.56). Eight cases would require medical management while 10 were considered to suffer from conditions requiring surgical intervention.

Total scan time ranged from 3.47-31.6 minutes with a median scan time of 7.95 minutes. Seventeen scans were performed in less than 19 minutes and 11 scans in less than 10 minutes. The arterial phase was successfully achieved in 14/18 cases (78%), based on an aortic HU criteria of >250 at the level of the porta hepatis. In the 4 cases that failed this criterion, aortic HU measurements ranged from 187.6-244. In the portal venous phase, portal vein attenuation values at the level of the porta hepatis ranged from 139.6-280 (median 168.7). A successful portal venous phase was not achieved in 1 patient due to motion artifact.

Across all scans (pre-contrast, arterial and initial portal venous phase; N=54), 15/54 (28%) were rated as having no motion artifact, 30/54 (56%) mild motion artifact, 4/54 (7%) moderate motion artifact and 5/54 (9%) severe motion artifact. The majority of scans were rated as having no beam hardening artifact (48/54, 89%), with mild artifact in 3/54 (5.5%) scans and severe artifact in 3/54 (5.5%). Anatomic exclusion did not occur in the majority of scans 48/54 (89%), with anatomic exclusion of <20% of the peritoneal cavity observed in 6/54 (11%) scans. In scans with anatomic exclusion, this was limited to the cranial abdomen and ranged from a single slice of the cranial-most liver to an estimated 2/3 of the liver parenchyma. Overall diagnostic quality (based on criteria summarized in Table 3) was excellent in 9/18 (50%) cases, good in 4/18 (22%), fair in 3/18 (17%), and poor in 2/18 (11%). Of the two poor quality diagnostic scans, one was the result of severe beam hardening secondary to prior GI barium administration (FIG 3A) and the second was due to failure to capture a true arterial phase (aortic HU 187.6; less than the pre-assigned aortic threshold) and severe motion artifact in both initial post-contrast scans (FIG 3B). In

the latter case, a delayed venous scan was obtained 52 seconds following termination of the intended portal venous phase and was characterized by moderate motion in the cranial abdomen and persistent visceral parenchymal enhancement. This scan was considered to be of sufficient diagnostic quality for clinical decision-making when all available images were interpreted. For two of the excellent diagnostic quality scans, sub-millimeter jejunal arteries were visible (FIG 4).

Discussion

Targeted helical CT protocols for non-localizable abdominal pain and for patients with a working clinical diagnosis have been established and are used routinely in the human clinical setting.[145-147] In an attempt to maximize our ability to evaluate a wide spectrum of potential acute abdominal diseases in dogs, a dual-phase protocol was adopted (pre-contrast, arterial and portal venous phases). An optional delayed scan was added to the protocol for some dogs to ensure renal excretion (Table 12). With the exception of 2 poor diagnostic quality scans, all remaining scans were rated as fair to excellent diagnostic quality with no statistically significant difference in diagnostic quality scores between awake and sedated groups.

Image quality was sufficient to permit the creation of maximum intensity projection (MIP) and three-dimensional (3D) volume-rendered (VR) reconstructions of mesenteric arteries for some of the awake and sedated dogs in our study (Figure 4). This observation warrants further investigation, as evaluation of mesenteric vasculature is an important prognostic indicator in human patients with acute pancreatitis or ischemic bowel disease. In a case series describing the contrast-enhanced CT diagnosis of acute bowel infarction in people, the following findings reportedly demonstrate a specificity of >95%: superior mesenteric artery or vein thrombosis, intramural bowel gas, portal vein gas, focal lack of bowel enhancement and ischemia of other organs.[174] In one CT study, arterial obstruction resulted in an 89% mortality rate while venous obstruction only resulted in 11%.[175]

No statistically significant differences were identified between awake and sedated groups for signalment, clinical signs, or physical examination findings. There were no statistically

significant differences between groups in laboratory parameters with the exception of serum creatinine, although all serum creatinine values were within the normal range in all cases. Behavioral assessment performed on an individual basis at the time of hospital admission and primary clinician preference were the main criteria used for awake versus sedated group assignments in our dogs.

A statistically significant difference in overall scan time was detected between groups. The sedated group unexpectedly had a median scan time that was greater than in the awake group, with a difference of 3.23 minutes. We theorize that this small increase in scan time may have been related to the fact that these patients often required additional monitoring between pre- and post-contrast phases. Overall, median scan time across all patients was rapid and less than 10 minutes. While scan timing for our study did not include patient positioning, preparation of contrast medium and scout planning, we would anticipate that these factors should play a minimal role if the imaging staff is well-trained and adopts an organized team approach. Scan protocols for our study were pre-set according to patient weight. Use of the power-injector in larger patients also permitted consistency in timing of injection and post-contrast scans. However, administration of a flush at the termination of injection likely contributed to failure of arterial capture in at least one of our cases. We therefore would recommend priming an extension set with additional contrast medium and disconnecting the extension set for catheter flushing only at the termination of the exam.

Obtaining a delayed venous scan not only provided additional data in patients that had motion artifacts in the prior scans, but also helped document the absence of acute anuric or oliguric renal failure that could theoretically result from administration of non-ionic iodinated contrast material in dehydrated patients. However, we acknowledge that major contrast-related adverse events for dogs receiving non-ionic iodinated contrast media have not yet been reported in the veterinary literature and only a limited number of adverse reactions have been reported following administration of ionic contrast media. [222-224] Evaluation of patient laboratory findings (most importantly blood urea nitrogen/creatinine when available) was performed in all our cases prior to diagnostic imaging and intravenous fluid therapy was recommended as needed. Based on human studies, intravenous normal saline volume supplementation reduces the risks of contrast-induced nephropathy, is relatively cost-effective, safe, and should be considered in all patients undergoing procedures with intravascular contrast.[137] Using the lowest possible effective dose of contrast media in addition to the potential use of iso-osmolar contrast media in high-risk patients are additional reported recommendations in the human literature.[138] The dose and rate of administration of intravenous contrast agent in this study was found to be safe and effective. Future studies of the efficacy of lower contrast medium doses may be beneficial; especially for assessing perfusion of the gastrointestinal tract and pancreas which are commonly implicated in canine acute abdominal conditions.

The value of non-contrast enhanced helical CT has also been reported for people with acute abdomen signs. In one study, unenhanced helical CT yielded superior results to a three-view abdominal radiographic series with a sensitivity, specificity and accuracy of 96%,

95.1% and 95.6%, respectively; compared with radiographic sensitivity, specificity and accuracy of 30%, 87.8% and 56%, respectively.[151] A second study evaluating non-contrast enhanced MDCT identified a sensitivity, specificity and positive predictive value of 100%, 98.5% and 91.7%, respectively for the detection of free gas, stones and intestinal obstruction.[152] A third study found no statistically significant difference between unenhanced and contrast enhanced CT in the ability to diagnose a suspected acute abdominal process.[153]

Primary limitations of our study included small sample size, unequal group numbers, and non-randomized group assignments. Patient enrollment and client consent were challenging, given that contrast-enhanced MDCT of the acute abdomen is not the current standard of care. It is our hope that results of this study will reduce challenges for future studies and encourage more primary care clinicians to choose MDCT for evaluating their canine patients with acute abdominal conditions.

In conclusion, findings from our study supported the hypothesis that dual-phase contrast-enhanced MDCT protocol is feasible and safe for use in awake or minimally sedated dogs with acute abdominal signs. We also developed and described a standardized protocol for use in future studies. A controlled clinical study comparing this protocol with current standard imaging techniques would be needed in order to determine whether dual-phase MDCT should be the modality of choice for dogs with acute abdominal disease.

Footnotes

*GE Lightspeed 16 Slice CT Milwaukee, WI, USA
†Omnipaque 300™ Iohexol injection, GE Healthcare, Princeton, NJ
‡PACS workstation Carestream Health, Rochester, NY
§SPSS IBM Company, Chicago, IL
¶VetMouseTrap™ University of Illinois, Urbana, IL

CHAPTER 3

COMPARATIVE IMAGING OF THE CANINE ACUTE ABDOMEN: SURVEY RADIOGRAPHY, CONTRAST-ENHANCED ULTRASOUND AND CONTRAST-ENHANCED MULTI-DETECTOR HELICAL CT

Miriam M. Shanaman, Tobias Schwarz, Arnon Gal, Robert T. O'Brien

Introduction

Diagnostic imaging plays a pivotal role in the initial assessment of dogs with acute abdominal signs. The ability to obtain both a rapid and accurate diagnosis is paramount in guiding appropriate medical and/or surgical intervention. Traditionally, survey radiography and abdominal ultrasound are the imaging modalities of choice for evaluating dogs with acute abdominal signs. Ultrasonographic characterization of canine pancreatitis[38,68-71,216,217], in addition to neoplastic and non-neoplastic disease of the gastrointestinal (GI) tract,[73-76,80-84] are well-characterized in the veterinary literature, as these conditions compose a large majority of canine acute abdominal diseases. The benefits of ultrasound (US) in identification of GI tract perforation and characterization of pneumoperitoneum have also been described.[89,90] Multiple veterinary studies have shown that abdominal US improves detection of GI foreign bodies and has improved accuracy for the diagnosis of mechanical ileus when survey radiographic results are equivocal.[77,78] Furthermore, while routine ultrasound is inferior in the detection of pneumoperitoneum when compared with radiography and computed tomography (CT) in people, the improved detection of small volumes of peritoneal free fluid is considered beneficial.[47,48] Abdominal ultrasound, however, is characterized by additional unique limitations including inter-operator variability, possible patient discomfort, duration of study acquisition, limited field

of view, and possible interference/lack of visibility of organs of interest due to overlying bowel or free peritoneal gas.

With the development and increased availability of multi-detector helical CT (MDCT), survey radiography has largely fallen out of favor in the human emergency room due to its relatively poor sensitivity and specificity. The survey radiographic detection of pneumoperitoneum remains potentially advantageous, however, with reported sensitivities as high as 98% in human patients.[8]

CT evaluation of the canine abdomen is limited to a small number of studies including characterization of conditions of the upper and lower urinary tract,[181-187] spleen,[188,189] hepatic/portal venous abnormalities,[190-202] pancreas,[71,203,204] mesenteric/intrapelvic neoplasia,[205,206] adrenal gland,[207-209] and GI tract.[210,212] A recent study describes a sedated contrast-enhanced CT protocol in clinical canine patients.[225] In a separate study by the same group, this same protocol successfully detected a greater number of lesions than routine abdominal ultrasound in patients weighing greater than 25 kg.[226] Our group has recently demonstrated that dual-phase CE-MDCT is feasible and safe in both awake and minimally sedated canine patients with acute abdominal signs.[227]

The goals of this study were multi-fold. Our primary goal was to assess agreement of survey radiography, combined B-mode and contrast-enhanced ultrasound (CEUS), and CE-MDCT in the detection of specific intra-abdominal lesions, and ultimately to differentiate medical from surgical acute abdominal conditions. Accuracy in the differentiation of

surgical from non-surgical conditions was also assessed. We hypothesized that accuracy for the differentiation of surgical from medical conditions would be greatest for CT. For lesions that were evaluated with both CE-MDCT and CEUS, lesion characteristics including maximum size and total number were recorded. We hypothesized that CE-MDCT would detect larger and an overall greater number of lesions relative to CEUS. Furthermore, a specific CT lesion termed mesenteric fat stranding will be introduced and is defined as an abnormal increased attenuation in fat[228]; this is described routinely in the human acute abdominal patient as an imaging feature associated with severe inflammatory and ischemic conditions of the pancreas and bowel.[169,179,229-231]

Materials and Methods

All protocols were approved by the Institutional Animal Care and Use Committee of the University of Illinois. Nineteen client-owned dogs that were presented to the University of Illinois Veterinary Teaching Hospital between December 2010 and January 2012 for acute abdominal signs were enrolled following owner consent. Study enrollment required the cytologic, survey radiographic and/or sonographic detection of a condition requiring immediate surgical intervention (visceral abscess, traumatic diaphragmatic hernia, spontaneous pneumoperitoneum, or small intestinal mechanical obstruction) or alternatively sonographic changes consistent with acute pancreatitis[38,68-71,216,217,232] or gastrointestinal (GI) neoplasia.[73,80-83]

Confirmation of a presumptive surgical diagnosis was made by exploratory laparotomy or alternatively by gross necropsy in patients that were humanely euthanized. Surgically

excised and gross pathological lesions were evaluated histologically by a single pathologist (AG). Sample sections were selected following CT evaluation in an attempt to provide a precise histologic correlation.

Patients who were considered to have a non-surgical underlying condition based on the criteria listed above underwent gross necropsy with histopathology of identified lesion(s) if the owner elected humane euthanasia prior to discharge. For patients that survived to discharge, total survival time (days) was recorded. In patients with sonographic evidence of acute pancreatitis, results of cPLI and ultrasound-guided fine needle aspiration of the pancreas were also required for study inclusion.

Clinical patient data recorded included breed, age (years), sex (male vs. female), spay/neuter status, duration and type of clinical signs (days), select physical examination findings (rectal temperature, heart rate, blood pressure, hydration status, presence and severity of abdominal pain), and select laboratory findings when available (serum lactate, serum creatinine and urine specific gravity).

All patients enrolled were required to undergo routine abdominal radiography, B-mode and CEUS, and CE-MDCT. Thirteen of 19 (68%) cases had all imaging studies performed consecutively the same day (radiographs followed by CT/US), 4/19 (21%) had all imaging studies performed within a 24 hour period, 1/19 (5%) had all studies performed within a 48 hour period, and 1/19 (5%) had US and CT evaluation within 24 hours, however, radiographs were obtained 6 days prior.

A three-view abdominal series (right lateral, left lateral and ventrodorsal view) was obtained in 17/19 (89%) cases, while a 2-view series (right or left lateral and ventrodorsal view) was obtained in 2/19 (11%) cases. Eighteen of 19 radiographic series' were acquired digitally, while a single case had analog films obtained by the referring veterinarian that were later scanned into our PACS system. All radiographic images were reviewed by two board-certified radiologists (TS, RTO) and the primary author (MMS) on dedicated DICOM workstations with calibrated monitors. Radiographic studies were randomized and the reviewers blinded to patient signalment, clinical signs and final diagnosis. To prevent reviewer bias, eight additional digitally acquired 3-view abdominal radiographic studies of normal or non-acute abdominal conditions were incorporated randomly into the study population for interpretation but not statistical analysis. A consensus was achieved for all variables evaluated. Categorical variables evaluated included the following: presence/absence of specific lesions (pneumoperitoneum, small intestinal plication, visible small intestinal foreign material); presence of small bowel distension as previously described[32] (duodenum only, portion of jejunum, duodenum and portion of jejunum, all small bowel); and surgical vs. medical diagnosis (based on imaging findings alone). Peritoneal serosal detail was considered as an ordinal variable (normal detail, focal loss of detail, multifocal loss of detail and generalized loss of detail).

All 19 patients underwent routine abdominal US with a dedicated ultrasound machine*. A microconvex curvilinear array transducer (3-9 MHz) and/or linear array transducer (4-13 MHz) were utilized for routine B-mode imaging. Probe selection and frequency, depth of

field, overall gain, time-gain compensation and focal zone were adjusted at the discretion of the sonographer to optimize image quality. The dedicated sonographer was either the primary resident or board-certified imaging faculty member responsible for the ultrasound service at the time of patient admission. Categorical variables were scored as presence or absence of specific lesions (pneumoperitoneum, hyperechoic mesentery, small intestinal plication, visible small intestinal foreign body); visible zone of transition if bowel plication/distension exist (not identified, proximal jejunum, mid jejunum, distal jejunum); location of small intestinal dilation if present (duodenum only, portion of jejunum, duodenum and portion of jejunum, all small bowel); and surgical vs. medical diagnosis (on the basis of imaging findings alone). Volume of peritoneal free fluid (none, focal, multifocal, generalized) was considered as an ordinal variable.

Routine B-mode US was immediately followed by CEUS of lesion(s) with questionable perfusion deficits using the same machine fitted with a variable band array linear transducer (3-11 MHz) utilizing specific contrast software†. Power and mechanical index were 5% and 0.03, respectively. Overall gain, depth of field and focal zone were adjusted at the discretion of the sonographer to maximize image quality. The region of interest was initially isolated in grey-scale. Split-screen technology was used in order to simultaneously visualize grey-scale and contrast enhanced images, respectively. One to two rapid bolus injections of microbubble contrast agent‡ were administered for each lesion in question. For patients weighing <20 kg, 0.1 cc of contrast was administered each time as a rapid IV bolus followed by a 2-3 cc 0.9% NaCl flush. For patients weighing >20 kg, 0.2 cc of contrast medium was administered each time as a rapid IV bolus, likewise followed by a 2-3 cc 0.9%

NaCl flush. An initial clip was obtained in all cases until subjective peak parenchymal enhancement. Additional clips and/or still images were collected as deemed necessary by the attending sonographer. Routine B-mode and CEUS images were evaluated prospectively at the time the scan was performed and again retrospectively by a single reviewer (MMS) for specific criteria: Presence of persistently non-enhancing pancreatic, gastric or small intestinal wall lesions; total number of hypoperfused lesions (liver, spleen); and estimated size of the largest hypoperfused lesion on pre- vs. post-contrast images (pancreas, liver) was also recorded.

All patients underwent awake or minimally sedated dual-phase contrast-enhanced abdominal CT using a 16-slice helical CT scanner§ as previously described[227] ,with the exception of one case where an arterial post-contrast phase was not attempted and a dual-phase protocol with two sequential venous phases was obtained. This same patient was scanned awake in sternal recumbency within the VetMouseTrap™|| using the following parameters: kV of 120, mA of 100, slice width (SW) of 2.5 mm (with 1.25 mm overlap), collimator pitch of 0.9 and rotation time of 0.8 seconds. Subsequent multiplanar reformatting was performed on the raw data in all patients to obtain reconstructed images in the dorsal and sagittal planes with a 0.625 mm SW. A dose of 2 ml/kg (600 mg I/kg) non-ionic iodinated contrast¶ was administered IV in all patients with the exception of two of the large breed dogs that received a maximum of 60 ml IV contrast (1.6 ml/kg and 1 ml/kg, respectively). The contrast agent was administered as a hand injected fast bolus in patients weighing ≤ 20 lbs. In patients ≥ 20 lbs, the contrast agent was administered via power injector at a rate of 3 ml/sec followed by a 10 ml 0.9% saline flush. While every

attempt was made to scan these patients awake, a proportion required intravenous (IV) sedation as previously described.[227] All scans were considered diagnostic using previously established criteria.[227]

The primary transverse CT images (pre-contrast, arterial and portal venous phases) in addition to dorsal and sagittal plane reformatted images were reviewed in a randomized blinded fashion by two board-certified radiologists (TS, RTO) and the primary author (MMS) on dedicated DICOM workstations with calibrated monitors. To prevent reviewer bias, eight additional CE-MDCT studies requiring a minimum of a dual phase protocol were incorporated randomly into the study population for interpretation but not statistical analysis. The reviewers were unaware of patient signalment, clinical history or final diagnosis. Window width and level could be adjusted at the discretion of the reviewer. Consensus was achieved for all variables evaluated. Categorical variables evaluated were scored as follows: presence/absence of specific lesions (pneumoperitoneum, fat stranding, small intestinal plication, visible small intestinal foreign material); presence of small bowel distension (duodenum only, portion of jejunum, duodenum and portion of jejunum, all small bowel); visible zone of transition if bowel plication/distension exist (duodenal, proximal jejunal, mid-jejunal, distal jejunal); and surgical vs. medical diagnosis (on the basis of imaging findings alone). Presence of peritoneal free fluid (none, focal, multifocal, generalized) was considered as an ordinal variable. On post-contrast venous images, the presence of persistently non-enhancing pancreatic, gastric or small intestinal wall lesions; total number of hypoperfused lesions (liver, spleen); and estimated size of the largest hypoperfused lesion if present (liver, pancreas) was also recorded.

Commercial software[#,**] was used for statistical analysis and a p-value < 0.05 was considered statistically significant. Continuous variables (age, duration of clinical signs, rectal temperature, heart rate, blood pressure, serum lactate, serum creatinine, urine specific gravity) were assessed for normality using a Shapiro-Wilk test.[218] For continuous data that met the assumption of normality, a Levene's test was performed to assess for homogeneity of variance.[219] For data that met the assumption of normality, mean, min-max and standard deviation (SD) were recorded. For non-normally distributed continuous data, median and 25th-75th percentiles were reported.

Agreement between modalities for categorical and ordinal variables was assessed with a Cohen's Kappa coefficient and weighted Kappa, respectively, given that many of the imaging features listed are not characterized by a strict reference or gold-standard. Interpretation of the Kappa coefficient was as follows: 0=chance agreement, <0.2=poor agreement, 0.21-0.40=fair agreement, 0.41-0.60=moderate agreement, 0.61-0.80=good agreement, >0.8=very good agreement and 1.0=perfect agreement.[233] To assess agreement between routine B-Mode and CEUS findings related to the size of a hypoechoic or hypoperfused pancreatic lesion respectively, a Bland-Altman plot was generated.

Sensitivity (true positive rate), specificity (true negative rate), positive predictive value (PPV), negative predictive value (NPV) and accuracy for differentiation of surgical from non-surgical conditions was also assessed for each modality. Exploratory laparotomy or necropsy with histopathology were considered the gold-standard for diagnosis of surgical

underlying conditions (small intestinal mechanical obstruction, GI perforation, traumatic diaphragmatic hernia or visceral abscess). Non-surgical conditions were confirmed at necropsy for cases that were humanely euthanized prior to discharge. For cases that survived to discharge, overall survival time (days) was recorded under the assumption that prolonged survival (greater than 30 days) suggested that the underlying condition in a given patient did not require immediate surgical intervention.

Results

Nineteen client-owned dogs were prospectively enrolled. Nine underwent awake diagnostic imaging while 10 received minimal sedation as previously described.[227] Breeds included one each of the following: Norwich Terrier, Tibetan Spaniel, Labrador Retriever, miniature Australian Shepherd, Bloodhound, Golden Retriever, Shetland Sheepdog, Scottish Terrrier, Basenji, Shih Tzu, Yorkshire Terrier, American Pit Bull Terrier, Boxer, Pug, Pomeranian, Dachshund, and 3 mix breed dogs. The mean age was 8.1 years (range 4-15.2, SD 3.2). Eight were female (all spayed) and 11 were male (4 intact, 7 neutered). Mean duration of clinical signs prior to presentation was 5 days (min-max 1-10, SD 2.9), with vomiting as the most commonly reported clinical sign (15/19, 79% of cases). Other reported clinical signs included anorexia/reduced appetite (12), lethargy (7), diarrhea (4) and respiratory distress (1). Mean rectal temperature at the time of presentation was 101.5^{0}C (min-max 99.2-104, SD 1.1), mean heart rate was 123.4 bpm (min-max 88-160, SD 19.1), mean systolic blood pressure (measured in 18/19 cases) was 150.3 mmHg (min-max 70-200, SD 32.2), median serum lactate (measured in 17/19 cases) was 2.3 mmol/l (25th-75th percentile=1.65-4), median serum creatinine (measured in 17/19 cases) was 0.8 mg/dl (25th-75th percentile=0.7-0.95), and mean urine specific gravity (measured in 13/19 cases) was 1.030 (min-max 1.01-1.05, SD 0.02). Sixteen patients (84%) were considered clinically dehydrated; 10/16 (63%) mildly dehydrated, 3/16 (19%) moderately dehydrated, and 3/16 (19%) severely dehydrated. Fifteen patients (79%) were considered to have a painful abdomen on presentation. No immediate contrast-related adverse reactions were noted at the time of CE-MDCT or CEUS.

Eight patients (42%) were considered to have an underlying condition that was non-surgical (7 acute pancreatitis, 1 gastric B-cell lymphoma). In cases with US findings consistent with acute pancreatitis (7/7, 100%),[38,68-71,216,217,232] a positive cPLI was identified in 5/7 (71%) cases and cytologic evidence of suppurative inflammation in 3/7 (43%) cases. The case of gastric B-cell lymphoma was diagnosed histologically following gross necropsy evaluation. Six of seven (86%) cases with acute pancreatitis survived to discharge with a mean survival of 427 days (range 103-634 days, SD 189). Five of these six cases remain alive to date. Prolonged duration of survival supports the assumption that these patients indeed suffered from a medical (rather than surgical) underlying condition.

Eleven patients (58%) were considered to have an underlying condition that would require surgical intervention. Ten of these cases had surgical and/or histologic confirmation of disease and all surgically excised lesions were submitted for histopathology: Hepatic abscess secondary to anaplastic carcinoma, widespread metastatic hemangiosarcoma with splenic abscessation (Fig. 5), gastric B-cell lymphoma with perforation, combined gastric and jejunal obstructive cloth foreign bodies, linear foreign body (4 cases; cloth, bandage material with sponge, multiple solid objects with fibrous connection, unknown material) (Fig. 6), proximal jejunal obstructive corn cob foreign body (Fig. 7) and traumatic diaphragmatic hernia. One case of multifocal hepatic abscessation was diagnosed with cytology alone as gross necropsy examination was not pursued. In the two cases of hepatic abscess formation, imaging alone was insufficient to make a definitive pre-operative surgical diagnosis with any modality given the absence of parenchymal or free peritoneal

gas. These cases required ultrasound-guided fine needle aspiration and cytology of cavitary hepatic lesions for confirmation of surgical disease.

The statistical agreement between all modalities for the identification of specific categorical and ordinal imaging features was assessed and is summarized in Table 13.

Survey radiography detected peritoneal free gas in 2/19 (11%) cases. In 3/4 (75%) linear foreign body cases, small bowel plication was detected radiographically. Small intestinal foreign material was considered opaque/visible in 5/6 (83%) cases with confirmed small intestinal obstruction secondary to foreign material and small bowel distension detected radiographically in 4/6 (67%) cases. Six of nineteen (32%) cases were considered to have loss of peritoneal serosal detail on survey radiographs. This was further characterized as generalized loss of serosal detail in 3/6 (50%) cases, focal loss of detail in 2/6 (33%) cases and multifocal loss of detail in 1/6 (17%) cases. Survey radiography correctly identified 8/9 (89%) cases as surgical for which a surgical diagnosis could be made with imaging findings alone. The single false negative radiographic diagnosis was a linear foreign body with extension from the pylorus to the distal duodenum.

In 10/19 (53%) cases, abdominal US evaluation was limited and considered only partially completed due to the inability to visualize specific organs that would normally be included in what is considered a thorough US examination. These omissions typically consisted of small parts (adrenal glands, sublumbar lymph nodes); although in the case of the traumatic diaphragmatic hernia, US evaluation was limited to a CEUS perfusion study of the herniated

spleen only given that the patient was in respiratory distress. Peritoneal free gas was not detected sonographically in any of the enrolled cases. Hyperechoic mesentery was identified sonographically in 9 cases: Splenic abscess formation with rupture, gastric perforation secondary to ulcerative B-cell lymphoma, gastric B-cell lymphoma without perforation, and acute pancreatitis (6 cases). Small bowel plication was noted in 4/4 (100%) cases with obstructive small intestinal linear foreign bodies. GI foreign material was considered sonographically visible in 4/6 (66%) cases. A distinct zone of transition was identified in 4/6 (67%) cases with evidence of small intestinal mechanical obstruction. The small bowel was considered distended in 5/6 (83%) cases. Peritoneal free fluid was detected sonographically in 5/19 (26%) cases. US correctly identified 8/9 (89%) cases as surgical for which a surgical diagnosis could be made with imaging findings alone. The false negative diagnosis was made in the case of gastric perforation due to an inability to identify pneumoperitoneum or parenchymal gas.

Pending the tentative diagnosis at the time of US evaluation, CEUS was performed in a targeted manner with a focus on the organ of interest: pancreas (7 cases), stomach wall (2), small intestine (6), liver (2), spleen (2). In both cases of gastric B-cell lymphoma, multifocal hypoperfused foci were noted within the gastric wall on CEUS. Mural perfusion deficits were noted in 2/6 (33%) cases for which CEUS was performed at the site of a small intestinal foreign body (Fig. 8). Both of these cases required jejunal resection and anastomosis at the time of surgery and both cases underwent spontaneous cardio-respiratory arrest (one during hospitalization and one shortly following discharge). In all 7 cases of acute pancreatitis, CEUS successfully identified a hypoperfused parenchymal

lesion. When the maximum dimension of a relatively hypoechoic pancreatic lesion on B-Mode US was compared with the maximal dimension of the same lesion on CEUS (hypoperfused portion only), there was poor agreement; with greatest discordance identified at larger lesion dimensions. Furthermore, there was a tendency for B-mode pancreatic lesion dimension to exceed the maximal dimension of the hypoperfused portion on CEUS (Fig. 9). In 2/3 (67%) cases for which a hypoperfused lesion was noted in the pancreas with both CEUS and CE-MDCT, maximum lesion dimension was relatively greater with CE-MDCT (255 vs. 96 mm^2 and 371 vs. 184 mm^2). In 2/2 cases for which a hypoperfused lesion was noted in the liver with both CEUS and CE-MDCT, maximum lesion dimension was consistently greater with CE-MDCT (1268 vs. 778 mm^2 and 441 vs. 276 mm^2). In one case with multifocal hypo-perfused hepatic lesions, CE-MDCT detected a greater number of total lesions than CEUS (12 vs. 4 respectively). In 2/3 (67%) cases for which number of splenic hypoperfused lesions were assessed with both CE-MDCT and CEUS, CE-MDCT detected a greater number of lesions (7 vs. 3 and 5 vs. 1).(stats?)

When combining data from multiple phases during CT acquisition, all routinely visualized organs could be evaluated with the exception of a single case in which pre-administered barium contrast material within the GI tract obscured portions of the cranial abdomen. CT detected peritoneal free gas in 2/19 (11%) cases. Overall, the CT imaging feature of mesenteric fat stranding was noted in a variety of disease processes including splenic abscess formation with rupture secondary to widespread hemangiosarcoma, gastric perforation secondary to ulcerative B-cell lymphoma (Fig. 10), linear foreign body (2) and acute pancreatitis (2). CE-MDCT correctly identified small bowel plication in 4/4 (100%)

linear foreign body cases. Gastrointestinal foreign material, small bowel distension, and a distinct zone of transition was consistently visualized on CT in all cases of small bowel obstruction (6/6, 100% of cases). Peritoneal free fluid was noted in 3/19 (16%) cases. If a surgical diagnosis could be achieved with imaging findings alone, the correct diagnosis was made with CT in 9/9 (100%) cases.

CE-MDCT identified persistently non-enhancing parenchymal lesions in 3/7 (43%) cases with acute pancreatitis (Fig. 9). In 2/3 (67%) cases for which a pancreatic perfusion deficit was noted on both CE-MDCT and CEUS, the maximal dimension of the lesion was greater on CT as described above. Given the small number of cases for which a pancreatic perfusion deficit was noted on both modalities, a statistical assessment of relative lesion size could not be performed. In both cases for which multifocal hypoperfused foci were noted within the gastric wall on CEUS, the same findings were reported on CE-MDCT. In 2/6 (33%) cases for which CEUS was performed at the site of a small intestinal foreign body, mural perfusion deficits were noted for which CE-MDCT failed to detect any deficits in small bowel perfusion (Fig. 8). When comparing the maximal dimension and total number of hypoperfused hepatic lesions on CE-MDCT vs. CEUS, CT consistently achieved a larger maximal dimension and showed a trend toward a relatively higher total number of lesions as described above. As a comparison of liver lesion size and number was performed on only two cases, this data could not be accurately assessed statistically. CE-MDCT and CEUS evaluation of discrete splenic lesions revealed similar results showing a greater number of lesions on CT as described above. Again, due to the small number of cases for which a comparison was possible, statistical analysis could not be performed.

Overall, the majority of imaging features showed at least moderate agreement (κ>0.41) between modalities (Table 13). Sensitivity, specificity, PPV, NPV and accuracy of each modality for the diagnosis of a surgical condition (excluding the two cases for which cytology was an absolute requirement) were as follows: CE-MDCT (100% in all cases), US and survey radiography (sensitivity 89%, specificity 100%, PPV 100%, NPV 89% and accuracy 94%).

Targeted helical CT of the abdomen is the current modality of choice for evaluation of the human acute abdominal patient.[145-147] This is largely due to the improved sensitivity and specificity of CE-MDCT relative to survey radiography. In a recent retrospective study, 72% of human patients whose abdominal radiography results were considered normal were found to have abnormal findings at follow-up imaging, including major abnormalities in 78% of cases.[18] A multicenter prospective trial evaluating human patients presenting to the emergency department with abdominal pain revealed similar limitations. A total of 1021 patients were included in the study. The diagnosis following radiographic evaluation was correct in only 50% of patients. Therefore, the authors concluded that plain radiography in human patients with acute abdominal pain was of limited value.[19]

Conversely, survey radiography and routine B-mode US are the current mainstay in the evaluation of veterinary clinical patients with acute abdominal signs. This is not surprising given the current expense of CT and frequent need for general anesthesia given the absence of MDCT technology in the majority of veterinary practices. Recently, awake and minimally

sedated CE-MDCT protocols using 16-slice technology have been used both safely and successfully in the evaluation of canine and feline patients with acute abdominal and respiratory conditions respectively.[213,227] Survey radiography and routine US are characterized by multiple limitations that may be overcome by the CE-MDCT protocol used in our study population. These limitations include, but are not limited to, the following: Duration of image acquisition, patient discomfort (especially with respect to abdominal US), superimposition/interference of organs of interest, inability/difficulty visualizing small parts, non-specific imaging findings (radiography), and poor sensitivity for critical surgical lesions such as pneumoperitoneum (US). In our study, a large number of US exams (53%) were considered only partially completed due to one or more of the reasons listed above. As a result, these modalities are often performed sequentially and therefore prolong the necessary time to make an accurate surgical diagnosis with the potential of having a negative impact on patient outcome. It is possible that by evaluating these modalities in combination with one another (parallel testing) that their complementary nature would improve overall diagnostic accuracy.

CE-MDCT and survey radiography detected pneumoperitoneum in 2 cases for which US findings were negative, accounted for by the poor statistical agreement found for this specific imaging feature. Gastric perforation secondary to B-cell lymphoma and splenic abscess (due to widespread hemangiosarcoma) were confirmed histologically in these two cases. In the case of gastric perforation, identification of peritoneal free gas was essential in establishing a surgical diagnosis, therefore, accounting for the single false negative result in the case of US. This single false negative resulted in the minimally decreased sensitivity,

negative predictive value, and ultimately the accuracy of US relative to CT for differentiating surgical from non-surgical disease with imaging findings alone. The case of splenic abscess formation with rupture was correctly classified as surgical with US findings alone due to the presence of gas-containing parenchymal cavitary splenic lesions (Fig. 5). CT and survey radiography are expected to have an increased sensitivity over US in the detection of pneumoperitoneum; however, the limited number of positive cases in our study can only suggest an impression rather than a proven statistical advantage.

The CT feature of fat stranding, defined as an abnormal increased attenuation in fat (mesenteric fat in the context of this study), is specifically addressed for the first time in the veterinary literature. The proposed underlying pathophysiologic process is increased edema and engorgement of local lymphatics.[228] This CT finding may manifest with multiple patterns including a subtle hazy/ground-glass like appearance in the presence of mild inflammation or a more reticular pattern with more well-defined linear areas of increased attenuation with more severe inflammatory conditions. A reticulonodular pattern may also be observed in association with neoplastic disease.[228] Not unexpectedly, this CT feature is identified across a broad spectrum of disease processes including, but not limited to, disease originating from the bowel, pancreas, gallbladder and upper urinary tract.[228] This lack of specificity is consistent with our study findings for which fat stranding was noted across a variety of pathological processes, including a case of solid organ abscess formation, small bowel obstructive disease, primary gastric neoplasia (with and without perforation), and acute pancreatitis. While the extent of fat stranding was not specifically quantified, this was subjectively most severe in the case of gastric perforation secondary to

B-cell lymphoma. The affected mesentery was evaluated histologically in this case revealing multifocal fat necrosis with infiltration by a large number of leukocytes, admixed with severe edema and fibrin deposition (Fig. 10). While statistical agreement was only fair between the CT feature of fat stranding and the sonographic detection of hyperechoic mesentery, these imaging findings did overlap in 4 cases, including splenic abscess formation secondary to hemangiosarcoma with rupture, gastric B-cell lymphoma with perforation, and two cases of acute pancreatitis. The lack of a statistical correlation between modalities is likely due to a combination of the small number of cases evaluated and frequently limited field of view in the case of abdominal US. We propose that the CT identification of fat stranding or the sonographic detection of hyperechoic mesentery, should prompt the radiologist to perform a more rigorous evaluation of the regional viscera as these imaging features were consistently identified adjacent to clinically significant lesions. While this technique is helpful in identifying an organ of interest, differential diagnoses remain numerous. Future studies that aim to specifically quantify the degree of fat stranding may be beneficial, as disproportionate fat stranding in human patients with acute abdominal pain have been found to help narrow the differential diagnoses for gastrointestinal disorders.[230]

In the characterization of small intestinal mechanical obstruction secondary to foreign material, plication associated with a linear foreign body was correctly identified in all 4 cases with CE-MDCT and US. Survey radiography failed to detect small bowel plication in a linear foreign body that extended from the pyloric antrum to the distal duodenum, resulting in a false negative diagnosis of a surgical abdomen and therefore minimally

reduced sensitivity, NPV and overall accuracy relative to CE-MDCT for the differentiation of surgical vs. medical underlying disease. Small intestinal foreign material, small bowel distension, and a distinct zone of transition were consistently visualized on CT. Small intestinal foreign material and luminal distension was noted in the majority of cases with survey radiography and US. Zone of transition was not specifically assessed radiographically due to visceral superimposition, however, was identified in 4/6 (67%) cases sonographically.

Overall, peritoneal free fluid was identified most frequently with abdominal US (5/19, 26%). Statistical agreement was moderate for the assessment of the sonographic or CT identification of peritoneal free fluid and loss of peritoneal serosal detail on survey radiographs. While there is not a perfect reference standard for the confirmation of the presence and degree of peritoneal effusion, our impression is that US is more sensitive in the detection of small volumes of peritoneal free fluid.

Targeted CEUS proved beneficial in the identification of multiple small bowel and pancreatic perfusion deficits that were not clearly identified with CE-MDCT. This can be explained with the improved spatial resolution of US relative to CT and the exquisite sensitivity of microbubble contrast material for assessment of perfusion deficiencies. In two such cases with small intestinal foreign bodies, jejunal resection and anastomosis was required and patient outcome was ultimately poor. In cases of acute pancreatitis, lesion size assessment with B-Mode US showed poor agreement with associated CEUS findings suggesting that CEUS may provide more accurate information when assessing patient

progress/prognosis and when guiding parenchymal sampling. There was a tendency, however, for CEUS to underestimate the total number and maximum surface area of parenchymal lesions that were also evaluated with both CEUS and CE-MDCT. This is not surprising given the limited field of view with US relative to CT. Given the exquisite sensitivity of CEUS in the characterization of visceral perfusion, it has recently emerged in human medicine as a modality of interest in the evaluation of acute abdominal conditions including ischemic bowel disease[101,102] and acute pancreatitis.[106,107] The veterinary literature thus far remains predominantly limited to characterization of normal visceral perfusion[114-121] and clinical conditions that are not typically associated with acute abdominal signs, including lymphomatous lymph nodes, porto-systemic shunt, and focal hepatic, splenic or renal lesions.[125-133,234] Given the data reported in our study, however, CEUS will likely provide similar promise as a method of enhancing the diagnostic potential of conventional B-mode US in veterinary clinical patients with acute abdominal signs.

When a surgical condition could be diagnosed with imaging findings alone, CT was successful in 100% of cases. No false positive diagnoses, however, were made with any of the modalities evaluated yielding a PPV of 100% in all cases. Sensitivity, NPV and accuracy for the diagnosis of a surgical condition were only minimally decreased in survey radiography and US when compared with MDCT for the reasons stated above. Overall, the data suggests that CT shows only slight improvement in accuracy when differentiating surgical from non-surgical conditions, however, the data may be skewed by a relative bias toward the diagnostic accuracy of US given that the majority of cases required the sonographic detection of a specified lesion for study inclusion.

Although the benefit of arterial phase imaging in CT was not specifically assessed in this study due to our small sample size and heterogeneity of underlying disease processes, arterial phase imaging warrants further investigation given the critical implications on overall prognosis in the human patient with acute abdominal pain. In a case series describing the contrast-enhanced CT diagnosis of acute bowel infarction in people, the following findings reportedly demonstrate a specificity of greater than 95%: superior mesenteric artery or vein thrombosis, intramural bowel gas, portal vein gas, focal lack of bowel enhancement, and ischemia of other organs.[174] In a separate study, arterial obstruction resulted in an 89% mortality rate while venous obstruction only resulted in 11%.[175] It is possible that arterial phase imaging may also provide indications of underlying malignancy as we observed both increased vessel number and tortuosity in an enrolled case of gastric B-cell lymphoma (Fig. 11). This is not unexpected given similar CEUS imaging features in malignant focal splenic and renal lesions in small animal clinical patients.[128,133]

Primary limitations of our study include small overall sample size and concurrent heterogeneity of specific underlying disease processes. Our primary goal, however, was not in the characterization of specific diseases but rather the assessment of agreement between multiple imaging modalities for specific imaging findings and in the ability to differentiate surgical vs. non-surgical conditions. Given the rigorous inclusion criteria, an additional limitation of this study is the relatively narrow spectrum in severity of acute abdominal disease as milder forms of acute abdominal pain (namely self-limiting

gastroenteritis) were not included. This may have resulted in overestimation of diagnostic accuracy in all modalities evaluated as it relates to the differentiation of surgical vs. medical conditions. As the majority of cases required sonographic detection of a specified lesion for study inclusion, a relative bias contributing to the overall accuracy of US in differentiating surgical from medical conditions must be considered. Further studies evaluating a spectrum of specific disease entities (e.g., small intestinal obstruction due to foreign body, GI or visceral neoplasms, acute pancreatitis) are necessary in an attempt to determine if a correlation exists between the identification of specific lesions and patient outcome/prognosis.

We propose that CE-MDCT may be used safely and effectively as a preliminary imaging screening modality for canine patients with acute abdominal signs as this will provide both a rapid and accurate diagnosis with minimal patient discomfort. Furthermore, given the improved sensitivity in the evaluation of bowel and pancreatic perfusion relative to CT, targeted CEUS of lesions identified on preliminary CE-MDCT provides great promise in the diagnostic assessment of critically ill canine patients.

Footnotes

* MyLab70 XVG, Esaote, Indianapolis, IN
† CnTI™, Esaote, Indianapolis, IN
‡ Definity, Lantheus Medical Imaging, North Billerica, MA
§ GE Lightspeed 16 Slice CT Milwaukee, WI, USA
|| VetMouseTrap™ University of Illinois, Urbana, IL
¶ Omnipaque 300™ Iohexol injection, GE Healthcare, Princeton, NJ
# SPSS IBM Company, Chicago, IL
** MedCalc Version 12.3.0, Mariakerke, Belgium

CHAPTER 4

FIGURES AND TABLES

Figure 1:

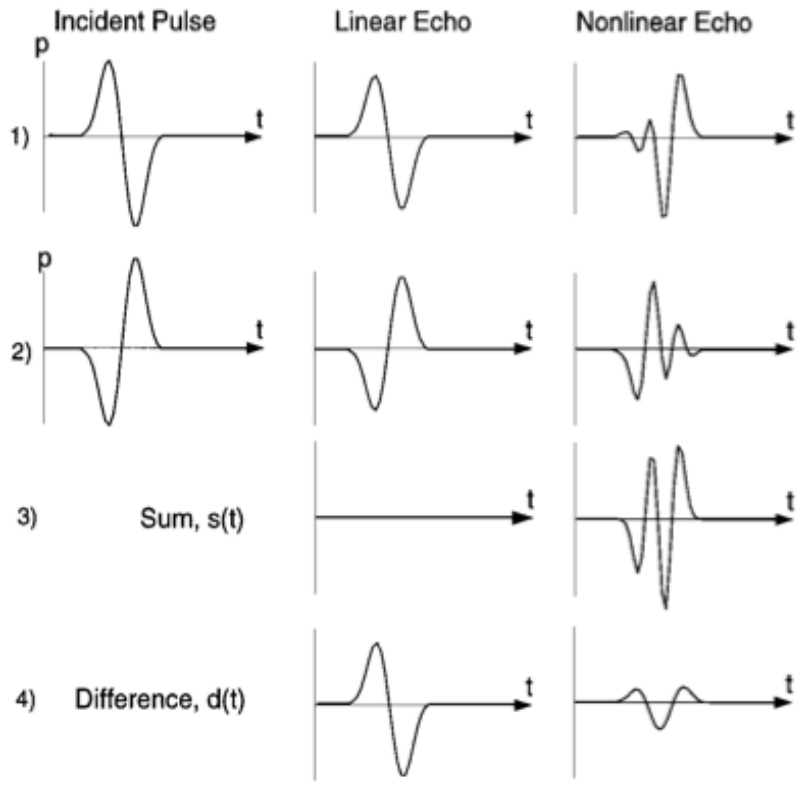

Principles of inversion detection: (1) a pulse of sound is transmitted and echoes are detected from linear and nonlinear scatterers; (2) an inverted copy of the same pulse is transmitted, and the echoes are detected; (3) the two echoes are summed; (4) the two echoes can also be subtracted. The sum, s(t) is nonzero for nonlinear scattering [93].

Figure 2:

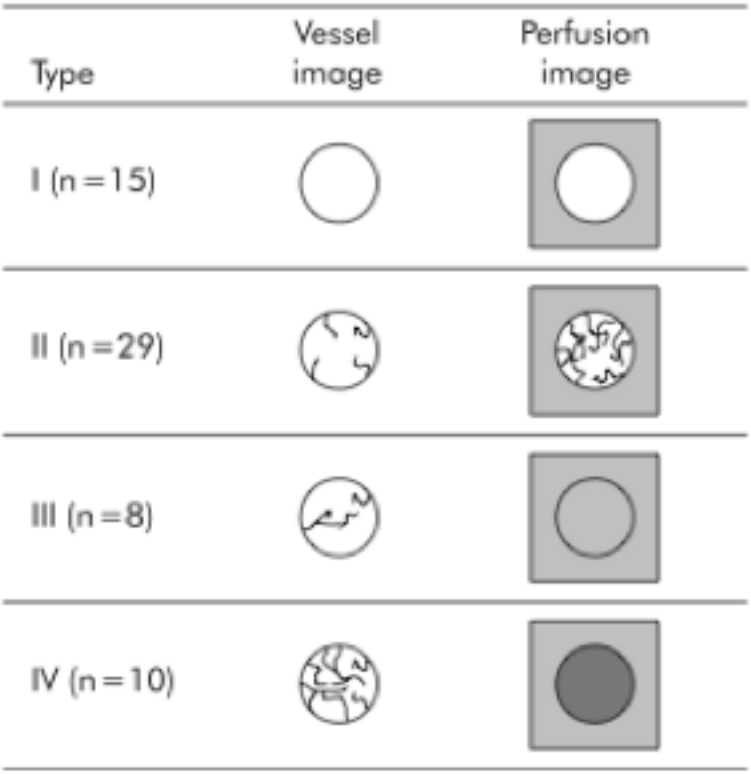

Classification of vascular patterns of pancreatic tumors. Type I: no vessels on the vessel image and no enhancement on the perfusion image. Type II: few vessels on the vessel image and heterogeneous enhancement in the hypovascular area on the perfusion image. Vascularity is less than in the surrounding pancreatic tissue. Type III: similar vascularity to the surrounding pancreatic tissue on the vessel image and homogenous isovascular enhancement on the perfusion image. Type IV: abundant vessels on the vessel image and hypervascular enhancement on the perfusion image[103].

Figure 3:

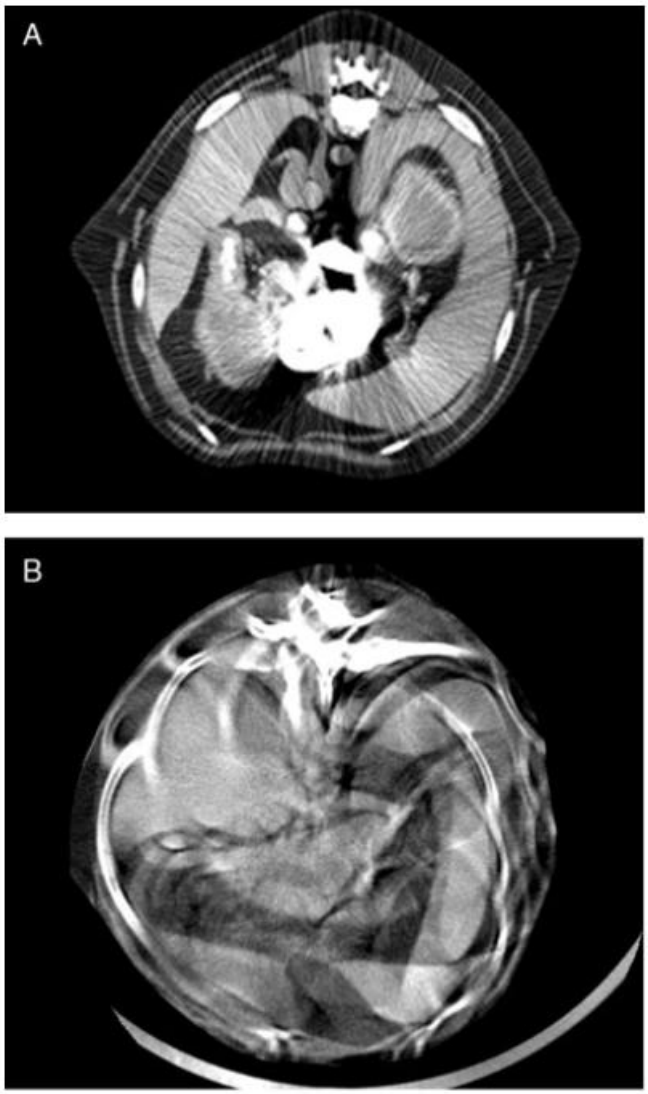

Transverse contrast-enhanced MDCT image examples of diagnostic studies of poor quality in awake dogs with acute abdominal pain

a) 7 year old male castrated Boxer who underwent awake CT evaluation. Note severe beam hardening artifact due to barium within the transverse colon.
b) 10.8 year old male intact Shetland Sheepdog who was recently discontinued from a continuous rate infusion of fentanyl, lidocaine, and ketamine prior to CT evaluation. Note severe motion artifact with complete distortion of regional visceral anatomy.

Figure 4:

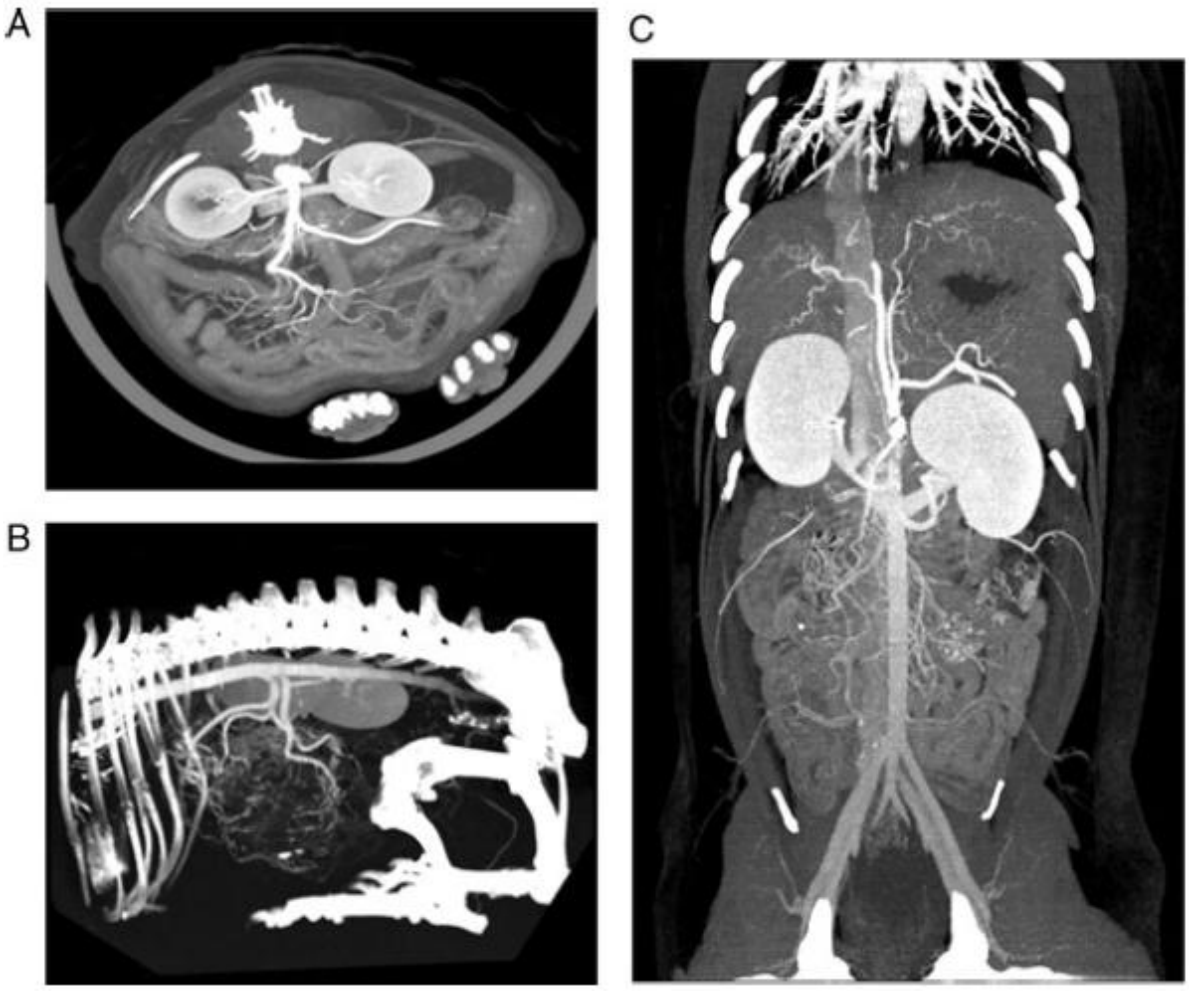

Maximum Intensity Projection (MIP) and 3D Volume Rendering (VR) reconstructions from contrast-enhanced MDCT scans of excellent diagnostic quality obtained in the arterial phase for dogs with acute abdominal pain. A) 7 year old male neutered Scottish Terrier who underwent awake CT. Transverse plane MIP displayed with window width of 800, window level of 70, individual slice thickness of 0.625 mm and slab thickness of 29.8 mm. The patient's right is to the reader's left. The patient was positioned in sternal recumbency within the Vetmousetrap™ device. B) 3D VR reconstruction displayed with window width of 600 and window level of 374 of same patient as in part (a). The patient's head is oriented to the reader's left. C) 8 year old female spayed mix breed dog who underwent CT with intravenous sedation (single 5 microgram/kg fentanyl bolus). Dorsal plane MIP displayed with window width of 328, window level of 140, individual slice thickness of 0.625 mm and slab thickness of 37.5 mm. The patient's right is to the reader's left.

Figure 5:

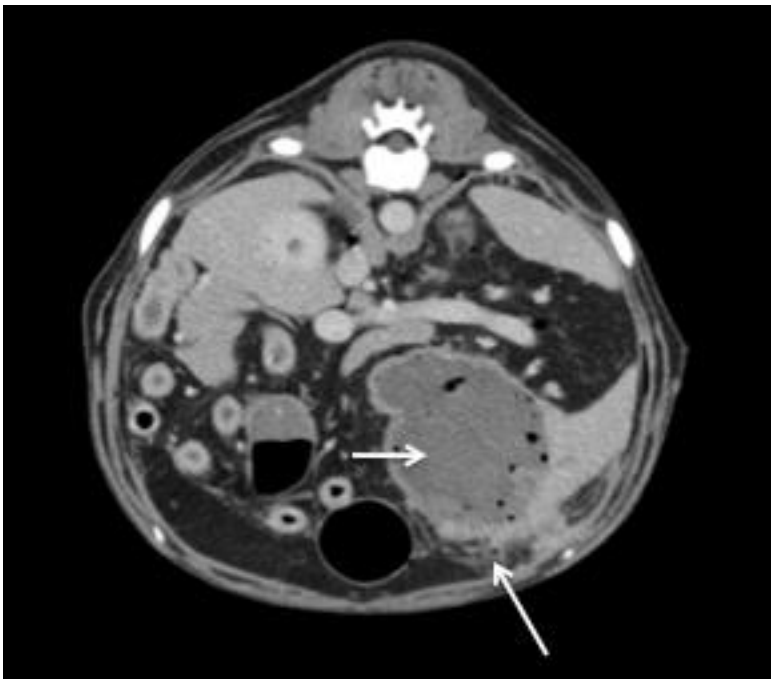

9.5 year old male neutered mix breed dog with a splenic abscess secondary to widespread hemangiosarcoma metastasis. Transverse CT image acquired in the portal venous phase displayed and in a soft tissue window. The patient's right is to the reader's left. Note the rim-enhancing mixed gas and fluid attenuating mass lesion within the splenic tail (short arrow). Along the ventral margin of this mass lesion noted the mesenteric fat stranding (long arrow). Multiple gas attenuating foci are additionally noted within the peritoneal cavity.

Figure 6 A (top), B (middle), C (next page):

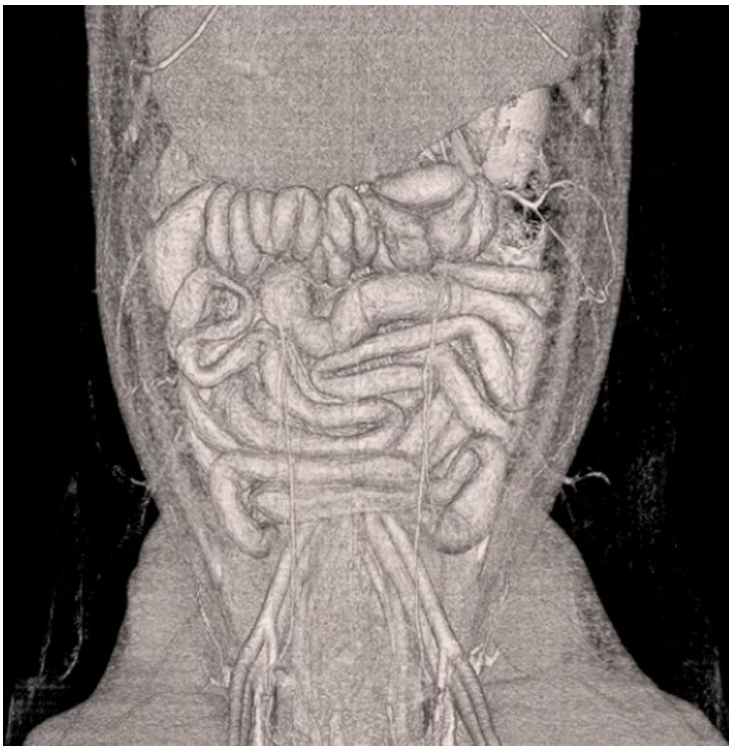

Figure 6 C

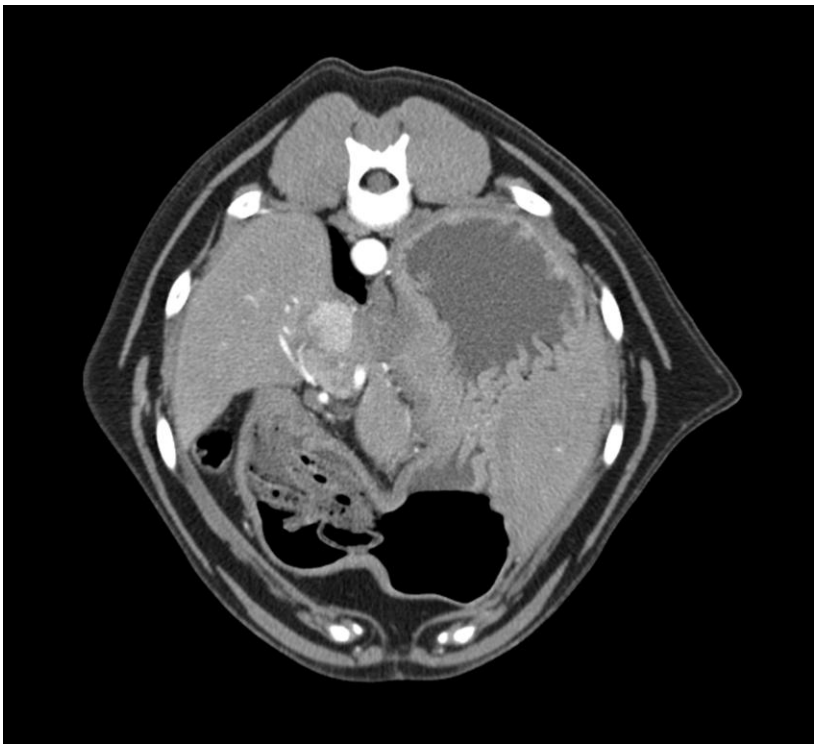

5.1 year old female spayed mix breed dog with a linear foreign body where plication was detected using all imaging modalities. The patient's right is to the reader's left. A) 3D volume rendering reconstruction acquired in the arterial phase displayed with visible voxel values ranging from 40-203 HU in a dorsal plane. Note the clearly demonstrated marked jejunal plication in the mid abdomen. B) Transverse plane CT image acquired in the arterial phase at the level of the jejunal plication noted in (A). C) Transverse plane CT image acquired in the arterial phase at the level of the pylorus where the proximal extension of the linear foreign body is clearly visualized.

Figure 7 A (top), B (bottom):

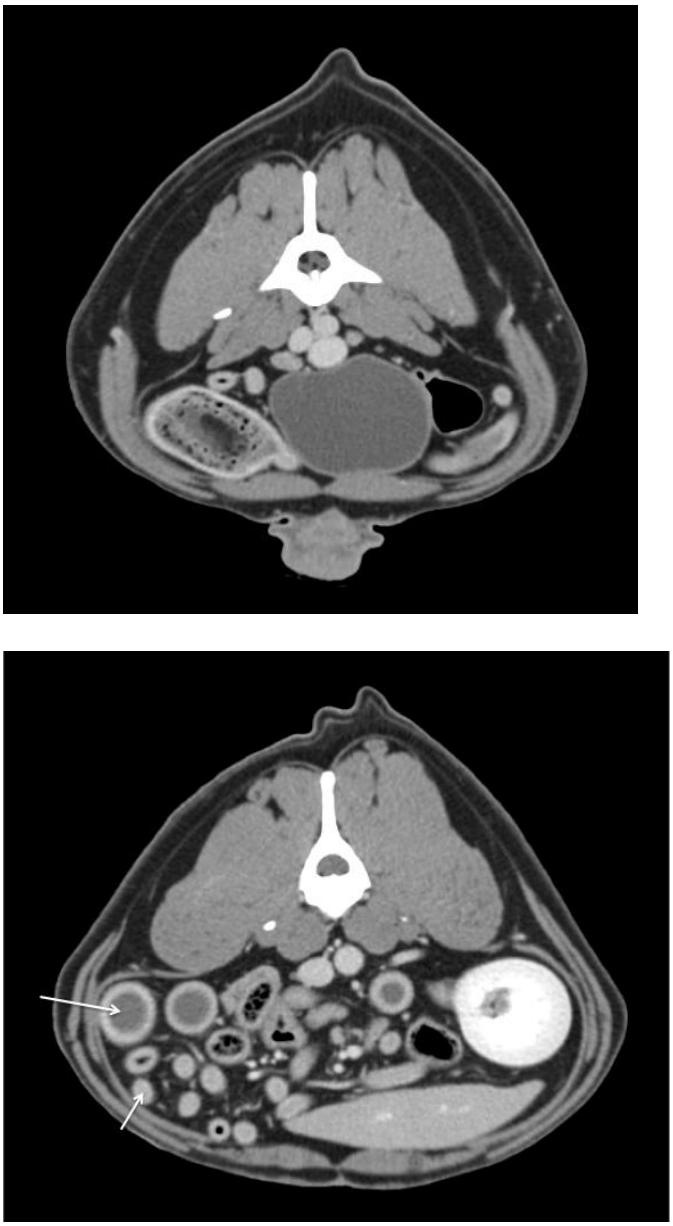

7.1 year old male intact American Pit Bull Terrier with a corn cob jejunal foreign body. Transverse CT image acquired in the portal venous phase and displayed in a soft tissue window. The patient's right is to the reader's left. A) Note the clearly visible luminal jejunal foreign body with uniform surrounding bowel wall enhancement. The foreign body was removed via enterotomy. B) Note the two populations of small bowel; empty segment (short arrow) and fluid distended segment (long arrow).

Figure 8 A (top), B (bottom):

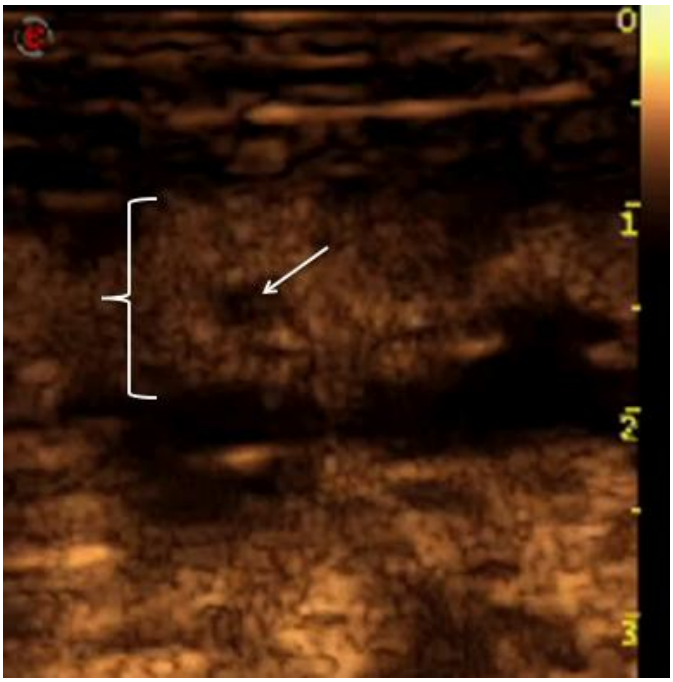

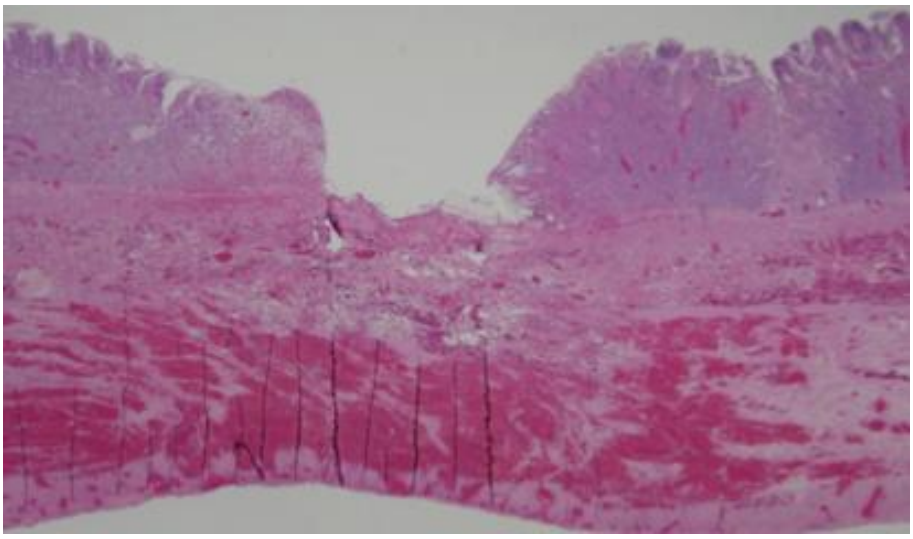

8 year old female spayed Golden Retriever with a cloth linear foreign body. A) CEUS image of a segment of affected jejunum with a rounded focal perfusion deficit (arrow) noted in the near wall (bracket) at peak enhancement. Jejunal resection and anastomosis was performed. B) Corresponding histologic section. H&E stain, original magnification 1.25x. The jejunal mucosa is focally severely ulcerated. The submucosa is severely edematous and the muscle layers contain marked, multifocal hemorrhage.

Figure 9 A (top), B (middle), C (next page):

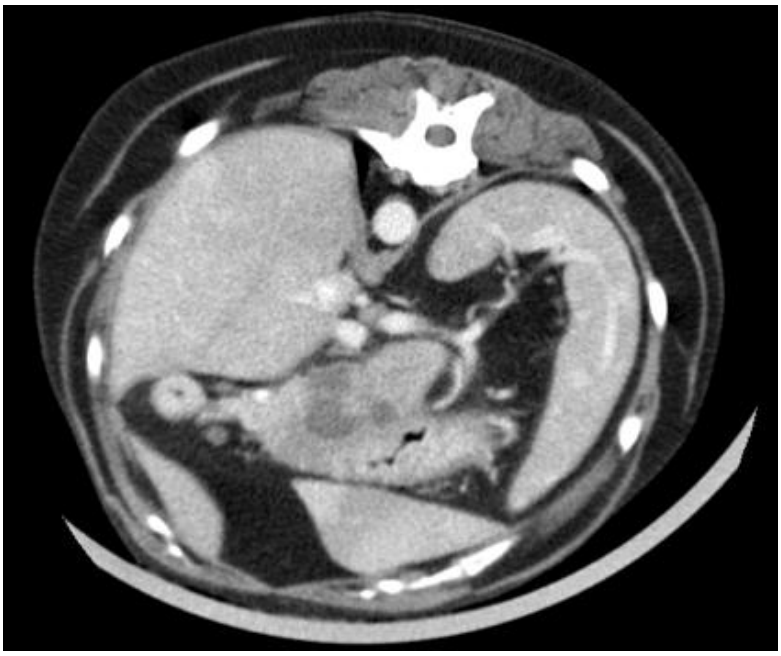

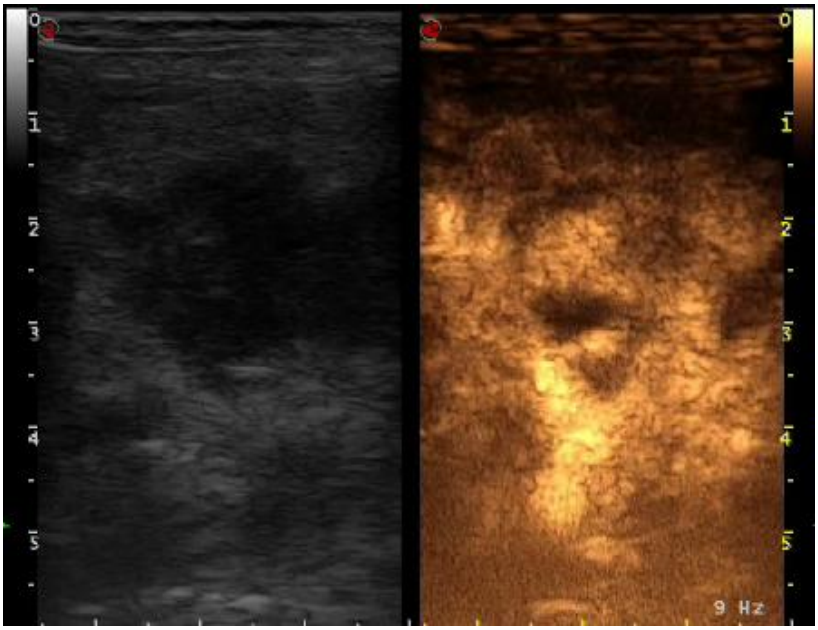

Figure 9 C

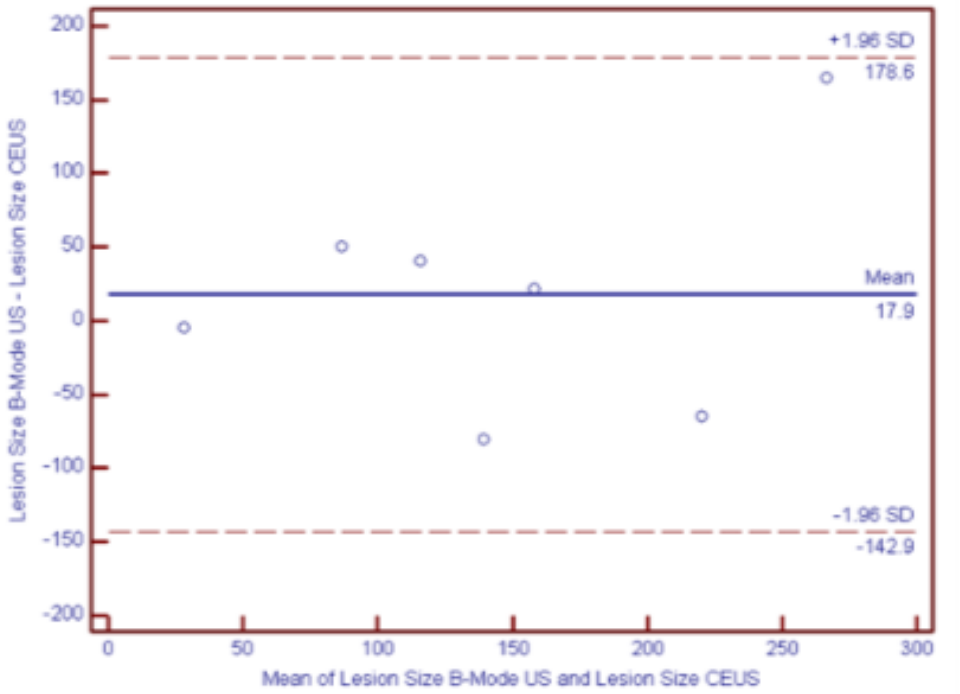

10.8 year old male intact Shetland Sheepdog with acute pancreatitis. A) Transverse CT image acquired in the portal venous phase and displayed in a soft tissue window. The patient's right is to the reader's left. Note that there are multiple ill-marginated relatively hypoperfused foci within the body of the pancreas. B) B-mode (left) and CEUS (right) image of the same region of the pancreas at peak perfusion. Note the poor agreement in the overall size of the hypoechoic lesion noted on B-mode US when compared with the relatively small foci of hypoperfusion detected with CEUS. C) Bland-Altman plot. Note poor agreement of pancreatic lesion dimension when measured with B-Mode US versus CEUS with greater discordance noted at larger lesion dimensions. Overall, there is a tendency for lesion dimension on B-mode images to exceed lesion dimension on CEUS..

Figure 10 A (top), B (bottom):

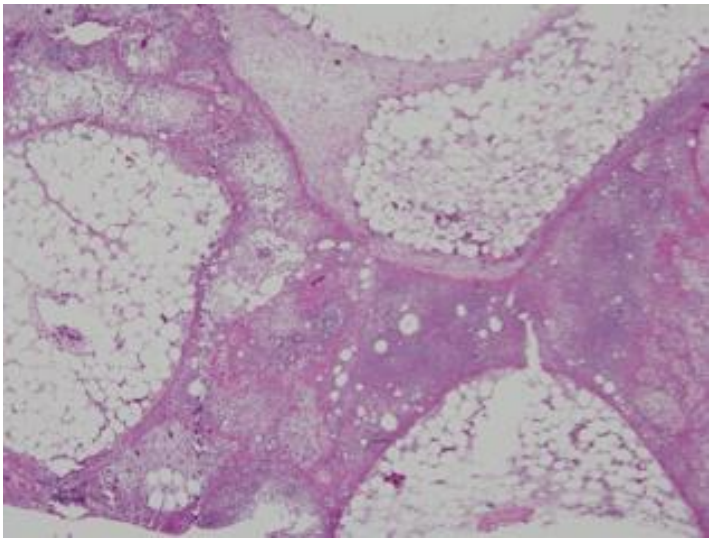

6 year old male intact Labrador Retriever with a gastric perforation secondary to ulcerative B-cell lymphoma. Transverse CT image acquired in the portal venous phase and displayed in a soft tissue window. The patient's right is to the reader's left. A) Note the soft tissue attenuating streaky appearance throughout the mesentery in the left cranio-dorsal abdomen adjacent to the stomach; multiple gas attenuating foci are noted free within the peritoneal cavity at this level. Note the non-uniform gastric wall contrast enhancement consistent with ulceration. B) Histologic section obtained from the peri-gastric adipose tissue described in (A). H&E stain, original magnification 4x. Multifocal fat necrosis with infiltration by a large number of leukocytes, admixed with severe edema and fibrin deposition.

Figure 11:

7 year old female spayed Scottish Terrier with gastric B-cell lymphoma. Dorsal plane maximum intensity projection (MIP) reconstruction with 43.5 mm slab thickness, window width of 385 and window level of 152 acquired in the arterial phase. The patient's right is to the reader's left. Not the large number of anomalous tortuous arterial vessels supplying the gastric wall.

Table 1[146]:

Suggested Routine Helical CT Protocol for Nonlocalized Acute Abdominal Pain

Parameter	Suggested Protocol
Contrast agent	
Oral administration	750–1,000 mL 3% diatrizoate meglumine*
Intravenous administration	110–120 mL nonionic contrast material (iohexol);† injection rate, 2 mL/sec
Acquisition	Single phase
Scan delay	70–90 sec (portal venous phase)
Scan area	Diaphragm to symphysis pubis
Section thickness	
Abdominal imaging	5 mm
Pelvic imaging	5–8 mm
Pitch	1.6 (table speed, 8 mm/rotation)
Reconstruction interval	
Abdominal imaging	5 mm
Pelvic imaging	5–8 mm

*Hypaque; Nycomed Amersham, Princeton, NJ.
†Omnipaque-350, Nycomed Amersham.

Table 2[146]:

Variations in Helical CT Protocol for Acute Abdomen Based on Working Clinical Diagnosis

Variation	Working Diagnosis
No intravenous contrast agent	Ureteral stone
No oral contrast agent	Ureteral stone, high-grade small bowel obstruction*
Negative oral contrast agent (water)	Peptic ulcer disease,† vascular disease†
Rectal contrast agent	Appendicitis,† diverticulitis†
Increased rate of administration of intravenous contrast agent (3–4 mL/sec)	Vascular disease,‡ hemorrhage,‡ bowel ischemia,‡ pancreatitis,‡ renal infarct‡
Dual-phase acquisition§	Pancreatitis,† pyelonephritis†
Delayed acquisition (5-min delay)	Pelvic disease,† pyelonephritis†
Narrow collimation (3 mm)	Ureteral stone, choledocholithiasis, pancreatitis, vascular disease‖
Small reconstruction intervals (3 mm)	Ureteral stone, choledocholithiasis, pancreatitis,† vascular disease‖

*Evaluated with intravenous bolus administration of contrast agent.
†Variation in protocol optional.
‡Evaluated with arterial-phase acquisition beginning 30 sec after intravenous injection.
§Arterial-phase acquisition (30 sec after contrast agent administration) combined with portal venous phase acquisition (70–90 sec).
‖Three-dimensional (3D) imaging (variation in protocol optional).

Table 3[156]:

Parameter	Value
At admission	
Age	>55 y
WBC count	>16,000/μL (16 × 10^9/L)
Serum glucose level	>11.1 mmol/L
SLDH/ALT	>350 IU/L
AST level	>250 IU/L
During initial 48 h	
Hematocrit	Decrease of more than 0.10
BUN level	Increase of more than 5 mg/dL (1.8 mmol/L)
Calcium	<2 mmol/L
Pao_2	<60 mm Hg
Base deficit	>4 mmol/L
Fluid sequestration	>6 L

Note.—AST = asparate aminotransferase, BUN = blood urea nitrogen, SLDH/ALT = serum lactate dehydrogenase to alanine aminotransferase ratio, WBC = white blood cell.

Table 4[155]:

Acute Pancreatitis Graded with CT

Grade	CT Finding
A	Normal pancreas
B	Pancreatic enlargement
C	Pancreatic inflammation and/or peripancreatic fat
D	Single peripancreatic fluid collection
E	Two or more fluid collections and/or retroperitoneal air

Table 5[155]:

CT Severity Index

CT Grade	Points	Necrosis		Severity Index*
		Percentage	Additional Points	
A	0	0	0	0
B	1	0	0	1
C	2	<30	2	4
D	3	30–50	4	7
E	4	>50	6	10

* CT grade points are added to points assigned for percentage of necrosis.

Table 6[158]:

Prognostic Indicator	Points
Pancreatic inflammation	
Normal pancreas	0
Intrinsic pancreatic abnormalities with or without inflammatory changes in peripancreatic fat	2
Pancreatic or peripancreatic fluid collection or peripancreatic fat necrosis	4
Pancreatic necrosis	
None	0
≤ 30%	2
> 30%	4
Extrapancreatic complications (one or more of pleural effusion, ascites, vascular complications, parenchymal complications, or gastrointestinal tract involvement)	2

Table 7[165]:

Point values for CT scoring system	
Initial CT findings	
Free air	5
Transition point	3
Complete obstruction	3
Closed loop	3
Free fluid	3
Partial obstruction	2
Repeat CT findings	
Resolution	−5
Improved obstruction	−2
Persistent SBO	+2
Worsening obstruction	+3
Free air	+5

Table 8 [178]:

Correlation between pathologic damage and CT findings	
Pathologic damage	CT findings
Vasodilation	Wall hyperdensity
Vasoconstriction	Absence of wall enhancement
Increased capillary permeability	Wall thickening
	Bowel dilation
Mucosal cellular necrosis	Pneumatosis
	Gas in mesenteric vein branches
	Gas in the portal vein branches
Transmural bowel necrosis	Pneumoperitoneum
	Retropneumoperitoneum
	Ascitis

Table 9:

Breed	Age (years)	Weight (kg)	Mentation	Positioning	Sedation
Norwich Terrier	13.5	6.2	BAR	Sternal	Fentanyl, lidocaine, ketamine CRI 3 mcg/kg/h, 25 mcg/kg/min, 3 mcg/kg/min
Tibetan Spaniel	15.2	6.3	QAR	Dorsal	Butorphanol 0.4 mg/kg
Mix Breed	9.5	29.3	QAR	Dorsal	Butorphanol 0.4 mg/kg, Midazolam 0.2 mg/kg
Labrador Retriever	6	55.5	QAR	Dorsal	Fentanyl 5 mcg/kg, Diazepam 0.2 mg/kg
Mix Breed	7	12.1	QAR	Dorsal	Fentanyl 10 mcg/kg, Midazolam 0.4 mg/kg
Miniature Australian Shepherd	7.7	11	QAR-BAR	Dorsal	Fentanyl 10 mcg/kg, Diazepam 0.2 mg/kg
Bloodhound	4	58	QAR	Sternal	Fentanyl 3 mcg/kg/h
Mix Breed	5.1	28.5	QAR	Dorsal	Fentanyl 5 mcg/kg
Golden Retriever	8	33.9	BAR	Dorsal	Hydromorphone 0.05 mg/kg, Midazolam 0.1 mg/kg
Shetland Sheepdog	10.8	13	QAR	Sternal	Fentanyl CRI 4 mcg/kg/h

CE-MDCT, contrast-enhanced multi-detector computed tomography; CRI, continuous rate infusion; QAR, quiet, alert and responsive; BAR, bright, alert, and responsive.

Table 10:

CT characteristic	Evaluation criteria
Motion artifact	Absent = 0 vs. present (mild = 1: barely noticeable; moderate = 2: noticeable without significant anatomic distortion; severe = 3: easily noticeable, peritoneal organs cannot be evaluated)
Anatomic exclusion	Absent = 0 vs. present (1 = <20% peritoneal cavity; 2 = 20–50% peritoneal cavity; 3 = >50% peritoneal cavity)
Beam hardening	Absent = 0 vs. present (mild = 1: focal to origin however immediately surrounding structures maintain anatomic detail; moderate = 2: signal loss in plane of origin affecting <20% peritoneal cavity; severe = 3: signal loss >20% of surrounding peritoneal contents)
Achievement of arterial phase	0 = No, 1 = Yes
Renal excretion of contrast agent	0 = No, 1 = Yes

Table 11:

Diagnostic Quality	Criteria
Excellent = 3	Respiratory/patient motion, beam hardening: Absent or mild (moderate on precontrast only) Anatomic exclusion: Not present Vascular phase achieved: All
Good = 2	Respiratory/patient motion, beam hardening: Moderate-severe/sufficient to hamper regional organ interpretation (in only one phase) or moderate motion in multiple phases. Anatomic exclusion: Graded as 1 on precontrast and/or no more than one postcontrast phase Vascular phase achieved: No more than one (arterial or portal venous) is absent
Fair = 1	Respiratory/patient motion, beam hardening: Moderate-severe/sufficient to hamper regional organ interpretation (affecting two phases; no more than one postcontrast phase) Anatomic exclusion: Graded as 1 on both postcontrast phases Vascular phase achieved: Precontrast and one postcontrast series absent
Poor = 0	Respiratory/patient motion, beam hardening: Moderate-severe/sufficient to hamper regional organ interpretation (in all phases) Anatomic exclusion: Grade of 2 or greater on both postcontrast phases Vascular phase achieved: None of postcontrast series achieved

Table 12:

Scan field	Arterial phase	Portal venous phase	Delayed phase (optional)
All phases scanned cranial to caudal. Cardiac apex to coxofemoral joints.	Initiate immediately at termination of contrast injection	Initiate at 40 s post start of contrast injection. If arterial scan time + initial scan delay exceeds 40 s, then initiate this phase immediately following arterial phase.	Initiate scan at 120 s following termination of the portal venous phase to confirm renal excretion of contrast.

Patient weight < 20 lbs → 600 mgI/kg rapid hand-injected bolus.
Patient weight > 20 lbs → 600 mgI/kg via power injector at a rate of 3 ml/s
Scan parameters: kV 120; mA 200–325; slice width 2.5 mm with 1.25 mm overlap; pitch 0.9–1.3:1; rotation time 0.5 s

Table 13:

Assessment of Agreement (κ) Between Modalities for Specific Imaging Findings

Imaging Finding	**κ (Rad vs. US)**	**κ (Rad vs. CT)**	**κ (CT vs. US)**
Categorical data			
Peritoneal free gas	0.00	1.00	0.00
Small intestinal plication	0.82	0.82	1.00
Small intestinal distension	0.48	0.50	0.54
Visible GI foreign material	0.56	0.73	0.87
Zone of transition (if small intestinal plication/distension)			0.20
Peritonitis (fat stranding on CT, hyperechoic mesentery on US)			0.22
Medical vs. surgical diagnosis	0.78	0.89	0.89
Ordinal data (weighted κ)			
Free peritoneal fluid (CT, US) vs. loss of serosal detail (Rad)	0.60	0.47	0.60

Rad=Survey Radiography, US=Ultrasound, CT=Computed Tomography, GI=Gastrointestinal

CHAPTER 5

REFERENCES

1. Bushberg JT, Seibert JA, Leidholdt EM, Boone JM. The Essential Physics of Medical Imaging 2nd Edition. Lippincott Williams & Wilkins. 2002.

2. Thrall DE. Textbook of Veterinary Diagnostic Radiology Fifth Edition. Saunders. 2007.

3. Widmer WR. Acquisition hardware for digital imaging. *Vet Radiol Ultrasound.* 2008;49:S2-S8.

4. Armbrust LJ. Comparing types of digital capture. *Veterinary Clinics of North America: Small Animal Practice.* 2009;39(4):677-688.

5. Popper H. Die diagnose der darmperforation mit hilfe der roentgendurchleuchtung. . *Dtsch Med Wochenschr.* 1915;35:1034-1306.

6. Miller RE, Nelson SW. The roentgenologic demonstration of tiny amounts of free intraperitoneal gas: experimental and clinical studies. *AJR.* 1971;112:574-585.

7. Mirvis SE, Young JWR, Keramati B, et al. Plain film evaluation of patients with abdominal pain: Are three radiographs necessary? *AJR.* 1986;147:501-503.

8. Chiu Y-H, Chen J-D, Tiu C-M, et al. Reappraisal of radiographic signs of pneumoperitoneum at emergency department. *The American Journal of Emergency Medicine.* 2009;27(3):320-327.

9. Lacey GJ, Wignall BK, Bradbrooke S, et al. Rationalising abdominal radiography in the accident and emergency department. *Clinical Radiology.* 1980;31:453-455.

10. Eisenberg RL, Heineken P, Hedgcock MW, et al. Evaluation of plain abdominal radiographs in the diagnosis of abdominal pain. *Annals of Internal Medicine.* 1982;97:257-261.

11. Hayward MWJ, Hayward C, Ennis WP, Roberts CJ. A pilot evaluation of radiography of the acute abdomen. *Clinical Radiology.* 1984;35:289-291.

12. Balthazar EJ, Lutzker S. Radiological signs of acute pancreatitis. *CRC Critical Reviews in Clinical Radiology and Nuclear Medicine.* 1976;7:199-242.

13. Millward SF, Breatnach E, Simpkins KC, McMahon MJ. Do plain films of the chest and abdomen have a role in the diagnosis of acute pancreatitis? *Clinical Radiology.* 1983;34(133-137).

14. Ashindoitiang JA, Atoyebi AO, Arogundade RA. The value of plain abdominal radiographs in management of abdominal emergencies in Luth. *Nig Q J Hosp Med.* 2008;18(3):170-174.

15. Prasannan S, Zhueng TJ, Gul YA. Diagnostic value of plain abdominal radiographs in patients with acute abdominal pain. *Asian J Surg.* 2005;28(4):246-251.

16. Boleslawski E, Panis Y, Benoist S, et al. Plain abdominal radiography as a routine procedure for acute abdominal pain of the right lower quadrant: Prospective evaluation. *Wold J. Surg.* 1999;23:262-264.

17. Rao PM, Rhea JT, Rao JA, Conn AKT. Plain abdominal radiography in clinically suspected appendicitis: Diagnostic yield, resource use, and comparison With CT. *American Journal of Emergency Medicine.* 1999;17(4):325-328.

18. Kellow ZS, MacInnes M, Kurzencwyg D. et al. The role of abdominal radiography in the evaluation of the nontrauma emergency patient. *Radiology.* 2008;248(3):887-893.

19. van Randen A, Laméris W, Luitse JSK, et al. The role of plain radiographs in patients with acute abdominal pain at the ED. *The American Journal of Emergency Medicine.* 2011;29(6):582-589.e582.

20. Thompson WM, Kilani RK, Smith BB, et al. Accuracy of abdominal radiography in acute small-bowel obstruction: Does reviewer experience matter? *American Journal of Roentgenology.* 2007;188(3):W233-W238.

21. Lim CBB, Chen V, Barsam A, Berger J, Harrison RA. Plain abdominal radiographs: can we interpret them? *Annals of The Royal College of Surgeons of England.* 2006;88(1):23-26.

22. Schnelle GB. The history of veterinary radiology. *The First International Conference of Veterinary Radiologists.* 1968;9:5-10.

23. Bischoff MG. Radiographic techniques and interpretation of the acute abdomen. *Clinical Techniques in Small Animal Practice.* 2003;18(1):7-19.

24. Ljunggren G, Olsson SE. The early radiographic diagnosis of peritonitis in the dog and cat. *Acta radiologica. Supplementum.* 1972;319:191-194.

25. Guffy MM. A radiological study of hydroperitoneum and pneumoperitoneum in the dog. Thesis. Colorado State University. 1966.

26. Rendano VT. Radiology of the gastrointestinal tract of small animals. *Can Vet J.* 1981;22:331-334.

27. Shealy PM, Henderson RA. Canine intestinal volvulus a report of nine new cases. *Veterinary Surgery.* 1992;21(1):15-19.

28. Carberry CA, Flanders JA. Cecal-colic volvulus in two dogs. *Veterinary Surgery.* 1993;22(3):225-228.

29. Cairo J, Font J, Gorraiz J, et al. Intestinal volvulus in dogs: a study of four clinical cases. *Journal of Small Animal Practice.* 1999;40:136-140.

30. Root CR, Lord PF. Linear radiolucent gastrointestinal foreign bodies in cats and dogs: their radiologic appearance. *J Am Vet Radiol Soc.* 1971;12:45-53.

31. Lamb CR. Radiology corner: Radiological identification of nonopaque intestinal foreign bodies. *Vet Radiol Ultrasound.* 1994;35:87-88.

32. Graham JP, Lord PF, Harrison JM. Quantitative estimation of intestinal dilation as a predictor of obstruction in the dog. *Journal of Small Animal Practice.* 1998;39:521-524.

33. Farrow CS. The obstructive bowel pattern: An inconsistent radiographic sign of obstruction. *Can Vet J.* 1997;38:309-310.

34. O'Brien TR. Radiographic Diagnosis of Abdominal Disorders in the Dog and Cat. 1978:279-351.

35. Armbrust LJ, Biller DS, Hoskinson JJ. Case examples demonstrating the clinical utility of obtaining both right and left lateral abdominal radiographs in small animals. *J Am Anim Hosp Assoc.* 2000;36:531-536.

36. Kleine LJ, Hornbuckle WE. Acute pancreatitis: The radiographic findings in 182 dogs. *J Am Vet Radiol Soc.* 1978;19:102-106.

37. Steyn PE, Wittum TE. Radiographic, epidemiologic, and clinical aspects of simultaneous pleural and peritoneal effusions in dogs and cats: 48 cases (1982-1991). *J Am Vet Med Assoc.* 1993;202:307-312.

38. Hess RS, Saunders HM, Van Winkle TJ, et al. Clinical, clinicopathologic, radiographic, and ultrasonographic abnormalities in dogs with fatal acute pancreatitis: 70 cases (1986-1995). *JAVMA.* 1998;213(5):665-670.

39. Ruaux CG. Diagnostic approaches to acute pancreatitis. *Clinical Techniques in Small Animal Practice.* 2003;18(4):245-249.

40. Stickle RL. Radiographic signs of isolated splenic torsion in dogs: Eight cases (1980-1987). *JAVMA.* 1989;194:103-106.

41. Neath PJ, Brockman DJ, Saunders HM. Retrospective analysis of 19 cases of isolated torsion of the splenic pedicle in dogs. *Journal of Small Animal Practice.* 1997;38:387-392.

42. Filly RA, Freimanis AL. Echographic diagnosis of pancreatic lesions. . *Radiology.* 1970;96.

43. Madrazo BL, Hricak H, Sandler MA, Eyler WR. Sonographic findings in complicated peptic ulcer. *Radiology.* 1981;140:457-461.

44. Laing FC, Federle MP, Jeffrey RB, Brown TW. Ultrasonic evaluation of patients with acute right upper quadrant pain. *Radiology.* 1981;140:449-455.

45. Simeone JF, Novelline RA, Ferucci JT, et al. Comparison of sonography and plain films in evaluation of the acute abdomen. *AJR.* 1985;144:49-52.

46. Puylaert JBCM. Ultrasound of acute GI tract conditions. *Eur Radiol.* 2001;11:1867-1877.

47. Grassi R, Romano S, Pinto A, Romano L. Gastro-duodenal perforations: Conventional plain film, US and CT findings in 166 consecutive patients. *European Journal of Radiology.* 2004;50(1):30-36.

48. Grassi R, Romano S, D'Amario F, et al. The relevance of free fluid between intestinal loops detected by sonography in the clinical assessment of small bowel obstruction in adults. *European Journal of Radiology.* 2004;50(1):5-14.

49. Austin H. Acute right upper quadrant abdominal pain: Ultrasound approach. *J Clin Ultrasound.* 1983;11:187-192.

50. Gai H. Acute abdominal pain actual surgical aspects of sonography. *Surg Endosc.* 1988;2:28-35.

51. Chang-Chien C-S, Lin H-H, Yen C-L, et al. Sonographic demonstration of free air in perforated peptic ulcers: Comparison of sonography with radiography. *J Clin Ultrasound.* 1989;17:95-100.

52. Quillin SP, Siegel MJ. Color Doppler US of children with acute lower abdominal pain. *Radiographics.* 1993;13:1281-1293.

53. Barr LL. Sonography in the infant with acute abdominal symptoms. *Seminars in Ultrasound, CT, and MRI.* 1994;15(4):275-289.

54. Carrico CW, Fenton LZ, Taylor GA, et al. Impact of sonography on the diagnosis and treatment of acute lower abdominal pain in children and young adults. *AJR.* 1998;172:513-516.

55. Silva CT, Daneman A, Navarro OM, et al. Correlation of sonographic findings and outcome in necrotizing enterocolitis. *Pediatric Radiology.* 2007;37(3):274-282.

56. Williams RJL, Windsor ACJ, Rosin RD, et al. Ultrasound scanning of the acute abdomen by surgeons in training. *Ann R Coll Surg Engl.* 1994;76:228-233.
57. Bode PJ, Edwards MJR, Kruit MC, van Vugt AB. Sonography in a clinical algorithm for early evaluation of 1671 patients with blunt abdominal trauma. *AJR.* 1999;172:905-911.
58. Richards JR, Schleper NH, Woo BD, et al. Sonographic assessment of blunt abdominal trauma: A 4-year prospective study. *Journal of Clinical Ultrasound.* 2001;30(2):59-67.
59. Sirlin CB, Brown MA, Andrade-Barreto OA, et al. Blunt abdominal trauma: Clinical value of negative screening US scans. *Radiology.* 2004;230:661-668.
60. Lee BC, Ormsby EL, McGahan JP, et al. The utility of sonography for the triage of blunt abdominal trauma patients to exploratory laparotomy. *American Journal of Roentgenology.* 2007;188(2):415-421.
61. Blaivas M, Brannam L, Hawkins M, et al. Bedside emergency ultrasonographic diagnosis of diaphragmatic rupture in blunt abdominal trauma. *The American Journal of Emergency Medicine.* 2004;22(7):601-604.
62. Udobi KF, Rodriguez A, Chiu WC, Scalea TM. Role of ultrasonography in penetrating abdominal trauma: A prospective clinical study. *J Trauma.* 2001;50:475-479.
63. Puylaert JBCM. Ultrasonography of the acute abdomen: lost art or future stethoscope? *Eur Radiol.* 2003;13:1203-1206.
64. James AE, Osterman FO, Bush RM, et al. The use of compound B-mode ultrasound in abdominal disease of animals. Department of Radiology Vanderbilt University Hospital, Nashville, TN. 1976.
65. Nyland TG, Park RD, Lattimer JC, et al. Gray-scale ultrasonography of the canine abdomen. *Veterinary Radiology.* 1981;22(5):220-227.
66. Park RD, Nyland TG, Lattimer JC, et al. B-mode gray-scale ultrasound: Imaging artifacts and interpretation principles. *Veterinary Radiology.* 1981;22(5):204-210.
67. Rantanen NW, Ewing RL. Principles of ultrasound application in animals. *Veterinary Radiology.* 1981;22(5):196-203.
68. Hecht S, Henry G. Sonographic evaluation of the normal and abnormal pancreas. *Clinical Techniques in Small Animal Practice.* 2007;22(3):115-121.
69. Murtaugh RJ, Herring DS, Jacobs RM, DeHoff WD. Pancreatic ultrasonography in dogs with experimentally induced acute pancreatitis. *Veterinary Radiology.* 1985;26(1):27-32.
70. Saunders HM. Ultrasonography of the pancreas. *Problems in Veterinary Medicine.* 1991;3(4).
71. Jaeger JQ, Mattoon JS, Bateman SW, Morandi F. Combined use of ultrasonography and contrast enhanced computed tomography to evaluate acute necrotizing pancreatitis in two dogs. *Vet Radiol Ultrasound.* 2003;44(1):72-79.
72. Penninck DG, Nyland TG, Kerr LY, et al. Ultrasonography of the normal canine gastrointestinal tract. *Veterinary Radiology.* 1989;30(6):272-276.
73. Penninck DG, Nyland TG, Kerr LY, Fisher PE. Ultrasonographic evaluation of gastrointestinal diseases in small animals. *Veterinary Radiology.* 1990;31(3):134-141.
74. Tidwell AS, Penninck DG. Ultrasonography of gastrointestinal foreign bodies. *Vet Radiol Ultrasound.* 1992;33(3):160-169.

75. Hoffman KL. Sonographic signs of gastroduodenal linear foreign bodies in 3 dogs. *Vet Radiol Ultrasound.* 2003;44(4):466-469.
76. Penninck D, Mitchell SL. Ultrasonographic detection of ingested and perforating wooden foreign bodies in four dogs. *JAVMA.* 2003;223(2):206-209.
77. Tyrrell D, Beck C. Survey of the use of radiography vs. ultrasonography in the investigation of gastrointestinal foreign bodies in small animals. *Vet Radiol Ultrasound.* 2006;47(4):404-408.
78. Sharma A, Thompson MS, Scrivani PV, et al. Comparison of radiography and ultrasonography for diagnosing small-intestinal mechanical obstruction in vomiting dogs. *Vet Radiol Ultrasound.* 2011;52(3):248-255.
79. Lamb CR, Mantis P. Ultrasonographic features of intestinal intussusception in 10 dogs. *Journal of Small Animal Practice.* 1998;39:437-441.
80. Kaser-Hotz B, Hauser B, Arnold P. Ultrasonographic findings in canine gastric neoplasia in 13 patients. *Vet Radiol Ultrasound.* 1996;37(1):51-56.
81. Rivers BJ, Walter PA, Johnston GR, et al. Canine gastric neoplasia: Utility of ultrasonography in diagnosis. *J Am Anim Hosp Assoc.* 1997;33:144-155.
82. Penninck DG, Moore AS, Gliatto J. Ultrasonography of canine gastric epithelial neoplasia. *Vet Radiol Ultrasound.* 1998;39(4):342-348.
83. Lamb CR, Grierson J. Ultrasonographic appearance of primary gastric neoplasia in 21 dogs. *Journal of Small Animal Practice.* 1999;40:211-215.
84. Penninck D, Tidwell A. Ultrasonography of gastric ulceration in the dog. *Vet Radiol Ultrasound.* 1997;38(4):308-312.
85. Schelling CG, Wortman JA, Saunders HM. Ultrasonic detection of splenic necrosis in the dog three case reports of splenic necrosis secondary to infarction. *Veterinary Radiology.* 1988;29(4):227-233.
86. Henley RK, Hager DA, Ackerman N. A comparison of two-dimensional ultrasonography and radiography for the detection of small amounts of free peritoneal fluid in the dog. *Veterinary Radiology.* 1989;30(3):121-124.
87. Lisciandro GR, Lagutchik MS, Mann KA, et al. Evaluation of an abdominal fluid scoring system determined using abdominal focused assessment with sonography for trauma in 101 dogs with motor vehicle trauma. *Journal of Veterinary Emergency and Critical Care.* 2009;19(5):426-437.
88. Lisciandro GR. Abdominal and thoracic focused assessment with sonography for trauma, triage, and monitoring in small animals. *Journal of Veterinary Emergency and Critical Care.* 2011;21(2):104-122.
89. Boysen SR, Tidwell AS, Penninck DG. Ultrasonographic findings in dogs and cats with gastrointestinal perforation. *Vet Radiol Ultrasound.* 2003;44(5):556-564.
90. Ferrell EA, Graham JP. Ultrasound corner diagnosis of pneumoperitoneum. *Vet Radiol Ultrasound.* 2003;44(3):307-308.
91. Spattini G, Rossi F, Vignoli M, Lamb CR. Use of ultrasound to diagnose diaphragmatic rupture in dogs and cats. *Vet Radiol Ultrasound.* 2003;44(2):226-230.
92. Wilson SR, Burns PN. Microbubble-enhanced US in body imaging: What role? *Radiology.* 2010;257:24-39.
93. Simpson DH, Chin CT, Burns PN. Pulse inversion doppler: A new method for detecting nonlinear echoes from microbubble contrast agents. *Transactions on Ultrasonics, Ferroelectrics, and Frequency Control.* 1999;46(2):372-382.

94. Kitzman DW, Goldman ME, Gillam LD, et al. Efficacy and safety of the novel ultrasound contrast agent perflutren (Definity) in patients with suboptimal baseline left ventricular echocardiographic images. *Am J Cardiol.* 2000;86:669-674.

95. Jakobsen J, Oyen R, Thomsen HS, Morcos SK. Safety of ultrasound contrast agents. *European Radiology.* 2005;15(5):941-945.

96. Yamaya Y, Niizeki K, Kim J, et al. Anaphylactoid response to Optison\ and its effects on pulmonary function in two dogs. *J Vet Med Sci.* 2004;66(11):1429-1432.

97. Yamaya Y, Niizeki K, Kim J, et al. Effects of Optison\ on pulmonary gas exchange and hemodynamics. *Ultrasound in Medicine & Biology.* 2002;28(8):1005-1013.

98. Piscaglia F, Bolondi L. The safety of Sonovue® in abdominal applications: Retrospective analysis of 23188 investigations. *Ultrasound in Medicine & Biology.* 2006;32(9):1369-1375.

99. Kusnetzky LL, Khalid A, Khumri TM, et al. Acute mortality in hospitalized patients undergoing echocardiography with and without an ultrasound contrast agent. *Journal of the American College of Cardiology.* 2008;51(17):1704-1706.

100. Gore RM, Yaghmai V, Thakrar KH, et al. Imaging in intestinal ischemic disorders. *Radiologic Clinics of North America.* 2008;46(5):845-875.

101. Hata J, Kamada T, Haruma K, Kusunoki H. Evaluation of bowel ischemia with contrast-enhanced US: Initial experience. *Radiology.* 2005;236:712-715.

102. Hamada T, Yamauchi M, Tanaka M, et al. Prospective evaluation of contrast-enhanced ultrasonography with advanced dynamic flow for the diagnosis of intestinal ischaemia. *Br J Radiol.* 2007;80:603-608.

103. Kitano M, Kudo M, Maekawa K, et al. Dynamic imaging of pancreatic diseases by contrast enhanced coded phase inversion harmonic ultrasonography. *Gut.* 2004;53(6):854-859.

104. Kersting S, Konopke R, Kersting F, et al. Quantitative perfusion analysis of transabdominal contrast-enhanced ultrasonography of pancreatic masses and carcinomas. *Gastroenterology.* 2009;137(6):1903-1911.

105. Beyer-Enke SA, Hocke M, Ignee A, et al. Contrast enhanced transabdominal ultrasound in the characterisation of pancreatic lesions with cystic appearance. *J Pancreas (Online).* 2010;11(5):427-433.

106. Ripollés T, Martínez MJ, López E, et al. Contrast-enhanced ultrasound in the staging of acute pancreatitis. *European Radiology.* 2010;20(10):2518-2523.

107. Golea A, Badea R, Socaciu M, et al. Quantitative analysis of tissue perfusion using contrast-enhanced transabdominal ultrasound (CEUS) in the evaluation of the severity of acute pancreatitis. *Medical Ultrasonography.* 2010;12(3):198-204.

108. Poletti P, Platon A, Becker CD, et al. Blunt abdominal trauma: Does the use of a second-generation sonographic contrast agent help to detect solid organ injuries? *AJR.* 2004;183:1293-1301.

109. Valentino M, Serra C, Zironi G, et al. Blunt abdominal trauma: Emergency contrast-enhanced sonography for detection of solid organ injuries. *American Journal of Roentgenology.* 2006;186(5):1361-1367.

110. Catalano O, Aiani L, Barozzi L, et al. CEUS in abdominal trauma: multi-center study. *Abdominal Imaging.* 2008;34(2):225-234.

111. Valentino M, Serra C, Pavlica P, Labate AMM, et al. Blunt abdominal trauma: Diagnostic performance of contrast-enhanced US in children—Initial experience. *Radiology.* 2008;245(3).
112. Catalano O, Cusati B, Nunziata A, Siani A. Active abdominal bleeding: Contrast-enhanced sonography. *Abdominal Imaging.* 2005;31(1):9-16.
113. Catalano O, Sandomenico F, Raso MM, Siani A. Real-time, contrast-enhanced sonography: A new tool for detecting active bleeding. *The Journal of Trauma: Injury, Infection, and Critical Care.* 2005;59(4):933-939.
114. Bahr A, Wrigley R, Salman M. Quantitative evaluation of Imagent as an abdominal ultrasound contrast medium in dogs. *Vet Radiol Ultrasound.* 2000;41(1):50-55.
115. Bigliardi E, Ferrari L. Contrast-enhanced ultrasound of the normal canine prostate gland. *Vet Radiol Ultrasound.* 2011; 52(1): 107-110.
116. Gaschen L, Angelette NIK, Stout R. Contrast-enhanced harmonic ultrasonography of medial iliac lymph nodes in healthy dogs. *Vet Radiol Ultrasound.* 2010;51(6):634-637.
117. Jimenez DA, O'Brien RT, Wallace JD, Klocke E. Intraoperative contrast-enhanced ultrasonography of normal canine jejunum. *Vet Radiol Ultrasound.* 2011;52(2):196-200.
118. Johnson-Neitman JL, O'Brien RT, Wallace JD. Quantitative perfusion analysis of the pancreas and duodenum in healthy dogs by use of contrast-enhanced ultrasonography. *Am J Vet Res.* 2012; 73(3): 385-92.
119. Pey P, Vignoli M, Haers H, et al. Contrast-enhanced ultrasonography of the normal canine adrenal gland. *Vet Radiol Ultrasound.* 2011; 52(5): 560-7.
120. Waller KR, O'Brien RT, Zagzebski JA. Quantitative contrast ultrasound analysis of renal perfusion in normal dogs. *Vet Radiol Ultrasound.* 2007;48(4):373-377.
121. Nyman HT, Kristensen AT, Kjelgaard-Hansen M, McEvoy FJ. Contrast-enhanced ultrasonography in normal canine liver. Evaluation of imaging and safety parameters. *Vet Radiol Ultrasound.* 2005;46(3):243-250.
122. Ziegler LE, O'Brien RT, Waller KR, Zagzebski JA. Quantitative conrast harmonic ultrasound imaging of normal canine liver. *Vet Radiol Ultrasound.* 2003;44(4):451-454.
123. Nakamura K, Sasaki N, Yoshikawa M, et al. Quantitative contrast-enhanced ultrasonography of canine spleen. *Vet Radiol Ultrasound.* 2009;50(1):104-108.
124. Rossi F, Rabba S, Vignoli M, et al. B-mode and contrast-enhanced sonographic assessment of accessory spleen in the dog. *Vet Radiol Ultrasound.* 2010;51(2):173-177.
125. Nakamura K, Sasaki N, Murakami M, et al. Contrast-enhanced ultrasonography for characterization of focal splenic lesions in dogs. *J Vet Intern Med.* 2010;24:1290-1297.
126. O'Brien RT, Iani M, Matheson J, et al. Contrast harmonic ultrasound of spontaneous liver nodules in 32 dogs. *Vet Radiol Ultrasound.* 2004;45(6):547-553.
127. Ohlerth S, Dennler M, Ruefli E, et al. Contrast harmonic imaging characterization of canine splenic lesions. *J Vet Intern Med.* 2008;22:1095-1102.
128. Rossi F, Leone VF, Vignoli M, et al. Use of contrast-enhanced ultrasound for characterization of focal splenic lesions. *Vet Radiol Ultrasound.* 2008;49(2):154-164.

129. Kanemoto H, Ohno K, Nakashima K, et al. Characterization of canine focal liver lesions with contrast-enhanced ultrasound using a novel contrast agent—Sonazoid. *Vet Radiol Ultrasound.* 2009;50(2):188-194.
130. O'Brien RT. Improved detection of metastatic hepatic hemangiosarcoma nodules with contrast ultrasound in three dogs. *Vet Radiol Ultrasound.* 2007;48(2):146-148.
131. Salwei RM, O'Brien RT, Matheson JS. Use of contrast harmonic ultrasound for the diagnosis of congenital portosystemic shunts in three dogs. *Vet Radiol Ultrasound.* 2003;44(3):301-305.
132. Salwei RM, O'Brien RT, Matheson JS. Characterization of lymphomatous lymph nodes in dogs using contrast harmonic and power doppler ultrasound. *Vet Radiol Ultrasound.* 2005;46(5):411-416.
133. Haers H, Vignoli M VM, Paes G, et al. Contrast harmonic ultrasonographic appearance of focal space-occupying renal lesions. *Vet Radiol Ultrasound.* 2010;51(5):516-522.
134. Seeram E. Computed Tomography: Physical Principles, Clinical Applications, and Quality Control Third Edition. Saunders. 2009.
135. Bertolini G, Prokop M. Multidetector-row computed tomography: Technical basics and preliminary clinical applications in small animals. *The Veterinary Journal.* 2011;189(1):15-26.
136. Omnipaque Package Insert. 2007.
137. Rundback JH, Nahl D, Yoo V. Contrast-induced nephropathy. *Journal of Vascular Surgery.* 2011;54(2):575-579.
138. Laville M, Juillard L. Contrast-induced acute kidney injury: How should at-risk patients be identified and managed? *jnephrol.* 2010;23(4):387-398.
139. Kim KS, Kim K, Hwang SS, et al. Risk stratification nomogram for nephropathy after abdominal contrast-enhanced computed tomography. *The American Journal of Emergency Medicine.* 2011;29(4):412-417.
140. Fishman EK, Reddan D. What are radiologists doing to prevent contrast-induced nephropathy (CIN) compared with measures supported by current evidence? A survey of european radiologists on CIN associated with computed tomography. *Acta Radiologica.* 2008;49(3):310-320.
141. Taourel P, Pradel J, Fabre JM, et al. Role of CT in the acute nontraumatic abdomen. *Seminars in Ultrasound, CT, and MRI.* 1995;16(2):151-164.
142. Siewert B, Raptopoulos V, Mueller MF, et al. Impact of CT on diagnosis and management of acute abdomen in patients initially treated without surgery. *AJR.* 1997;168:173-178.
143. Taourel P, Baron MP, Pradel J, et al. Acute abdomen of unknown origin- Impact of CT on diagnosis and management. *Gastroinest Radiol.* 1992;17:287-291.
144. Mindelzun RE, Jeffrey RB. The acute abdomen: Current CT imaging techniques. *Seminars in Ultrasound, CT, and MRI.* 1999;20(2):63-67.
145. Gore RM, Miller FH, Pereles FS, et al. Helical CT in the evaluation of the acute abdomen. *AJR.* 2000;174:901-913.
146. Urban BA, Fishman EK. Tailored helical CT evaluation of acute abdomen. *Radiographics.* 2000;20:725-749.

147. Urban BA, Fishman EK. Targeted helical CT of the acute abdomen: Appendicitis, diverticulitis, and small bowel obstruction. *Seminars in Ultrasound, CT, and MRI.* 2000;21(1):20-39.
148. Federle MP. CT of the acute (emergency) abdomen. *European Radiology Supplements.* 2005;15(S4):d100-d104.
149. Leschka S, Alkadhi H, Wildermuth S, Marincek B. Multi-detector computed tomography of acute abdomen. *European Radiology.* 2005;15(12):2435-2447.
150. Strömberg C, Johansson G, Adolfsson A. Acute abdominal pain: Diagnostic impact of immediate CT scanning. *World Journal of Surgery.* 2007;31(12):2347-2354.
151. MacKersie AB, Lane MJ, Gerhardt RT, et al. Nontraumatic acute abdominal pain: Unenhanced helical CT compared with three-view acute abdominal series. *Radiology.* 2005;237:114-122.
152. Udayasankar UK, Li J, Baumgarten DA, et al. Acute abdominal pain: Value of non-contrast enhanced ultra-low-dose multi-detector row CT as a substitute for abdominal radiographs. *Emergency Radiology.* 2008;16(1):61-70.
153. Hill BC, Johnson SC, Owens EK, et al. CT scan for suspected acute abdominal process: Impact of combinations of IV, oral, and rectal contrast. *World Journal of Surgery.* 2010;34(4):699-703.
154. Haller O, Karlsson L, Nyman R. Can low-dose abdominal CT replace abdominal plain film in evaluation of acute abdominal pain? *Upsala Journal of Medical Sciences.* 2010;115(2):113-120.
155. Balthazar EJ. Acute pancreatitis: Assessment of severity with clinical and CT evaluation. *Radiology.* 2002;223:603-613.
156. Ranson JHC ,Rifkind KM, Roses DF, et al. Objective early identification of severe acute pancreatitis. *Am J Gastroenterol.* 1974;61:443-451.
157. Casas JD, Diaz R, Valderas G, et al. Prognostic value of CT in the early assessment of patients with acute pancreatitis. *AJR.* 2004;182:569-574.
158. Mortele KJ, Wiesner W, Intriere L, et al. A modified CT severity index for evaluating acute pancreatitis: Improved correlation with patient outcome. *AJR.* 2004;183:1261-1265.
159. Bharwani N, Patel S, Prabhudesai S, et al. Acute pancreatitis: The role of imaging in diagnosis and management. *Clinical Radiology.* 2011;66(2):164-175.
160. Caoili EM, Paulson EK. CT of small-bowel obstruction: Another perspective using multiplanar reformations. *AJR.* 2000;174:993-998.
161. Frager D, Medwid SW, Baer JW, et al. CT of small-bowel obstruction: Value in establishing the diagnosis and determining the degree and cause. *AJR.* 1994;162:37-41.
162. Frager D, Baer JW, Rothpearl A, Bossart PA. Distinction between postoperative ileus and mechanical small-bowel obstruction: Value of CT compared with clinical and other radiographic findings. *AJR.* 1995;164:891-894.
163. Taourel PG, Fabre J-M, Pradel JA, et al. Value of CT in the diagnosis and management of patients with suspected acute small-bowel obstruction. *AJR.* 1995;165:1187-1192.
164. Nicolaou S, Kai B, Ho S, et al. Imaging of acute small-bowel obstruction. *American Journal of Roentgenology.* 2005;185(4):1036-1044.

165. Jones K, Mangram AJ, Lebron RA, et al. Can a computed tomography scoring system predict the need for surgery in small-bowel obstruction? *The American Journal of Surgery.* 2007;194(6):780-784.
166. Sherck J, Shatney C, Sensaki K, Selivanov V. The accuracy of computed tomography in the diagnosis of blunt small-bowel perforation. *The Americal Journal of Surgery.* 1994;168:670-675.
167. Maniatis V, Chryssikopoulos AH, Kalamara C, et al. Perforation of the alimentary tract: Evaluation with computed tomography. *Abdominal Imaging.* 2000;25(4):373-379.
168. Yeung K-W, Chang M-S, Hsiao C-P, Huang J-F. CT evaluation of gastrointestinal tract perforation. *Clinical Imaging.* 2004;28(5):329-333.
169. Hainaux B, Agneessens E, Bertinotti R, et al. Accuracy of MDCT in predicting site of gastrointestinal tract perforation. *American Journal of Roentgenology.* 2006;187(5):1179-1183.
170. Ghekiere O, Lesnik A, Hoa D, et al. Value of computed tomography in the diagnosis of the cause of nontraumatic gastrointestinal tract perforation. *J Comput Assist Tomogr.* 2007;31:169-176.
171. Imuta M, Awai K, Nakayama Y, et al. Multidetector CT findings suggesting a perforation site in the gastrointestinal tract: analysis in surgically confirmed 155 patients. *Radiation Medicine.* 2007;25(3):113-118.
172. Cho HS, Yoon SE, Park SH, et al. Distinction between upper and lower gastrointestinal perforation: Usefulness of the periportal free air sign on computed tomography. *European Journal of Radiology.* 2009;69(1):108-113.
173. Frager D, Baer JW, Medwid SW, et al. Detection of intestinal ischemia in patients with acute small-bowel obstruction due to adhesions or hernia: Efficacy of CT. *AJR.* 1996;166:67-71.
174. Gellett LR, Harries SR, Roobottom CA. Urgent contrast enhanced computed tomography in the diagnosis of acute bowel infarction. *Emerg Med J.* 2002;19:480-481.
175. Moschetta M, Stabile Ianora AA, Pedote P, et al. Prognostic value of multidetector computed tomography in bowel infarction. *La radiologia medica.* 2009;114(5):780-791.
176. Kirkpatrick IDC, Kroeker MA, Greenberg HM. Biphasic CT with mesenteric CT angiography in the evaluation of acute mesenteric ischemia: Initial experience. *Radiology.* 2003;229:91-98.
177. Aschoff AJ, Stuber G, Becker BW, et al. Evaluation of acute mesenteric ischemia: accuracy of biphasic mesenteric multi-detector CT angiography. *Abdominal Imaging.* 2008;34(3):345-357.
178. Angelelli G, Scardapane A, Memeo M, et al. Acute bowel ischemia: CT findings. *European Journal of Radiology.* 2004;50(1):37-47.
179. Wiesner W, Hauser A, Steinbrich W. Accuracy of multidetector row computed tomography for the diagnosis of acute bowel ischemia in a non-selected study population. *European Radiology.* 2004;14(12):2347-2356.
180. Mallo R, Salem L, Lalani T, Flum D. Computed Tomography Diagnosis of Ischemia and Complete Obstruction in Small Bowel Obstruction: A Systematic Review. *Journal of Gastrointestinal Surgery.* 2005;9(5):690-694.

181. Yamazoe K, Ohashi F, Kadosawa T, et al. Computed tomography on renal masses in dogs and cats. *J Vet Med Sci.* 1994;56(4):813-816.
182. Moe L, Lium B. Computed tomography of hereditary multifocal renal cystadenocarcinomas in german shepherd dogs. *Vet Radiol Ultrasound.* 1997;38(5):335-343.
183. Barthez PY, Begon D, Delisle F. Effect of contrast medium dose and image acquisition timing on ureteral opacification in the normal dog as assessed by computed tomography. *Vet Radiol Ultrasound.* 1998;39(6):524-527.
184. Samii VF, Mcloughlin MA, Mattoon JS, et al. Digital fluoroscopic excretory urography, digital fluoroscopic urethrography, helical computed tomography, and cystoscopy in 24 dogs with suspected ureteral ectopia. *J Vet Intern Med.* 2004;18:271-281.
185. Samii VF. Inverted contrast medium-urine layering in the canine urinary bladder on computed tomography. *Vet Radiol Ultrasound.* 2005;46(6):502-505.
186. Secrest S, Britt L, Cook C. Imaging diagnosis-bilateral orthotopic ureteroceles in a dog. *Vet Radiol Ultrasound.* 2011;52(4):448-450.
187. Lee S, Jung J, Chang J, et al. Evaluation of triphasic helical computed tomography of the kidneys in clinically normal dogs. *J Vet Res.* 2011;72:345-349.
188. Patsikas MN, Rallis T, Kladakis S, Dessiris AK. Computed tomography diagnosis of isolated splenic torsion in a dog. *Vet Radiol Ultrasound.* 2001;42(3):235-237.
189. Ohta H, Takagi S, Murakami M, et al. Primary splenic torsion in a boston terrier. *J Vet Med Sci.* 2009;71(11):1533-1535.
190. Frank P, Mahaffey M, Egger C, Cornell KK. Helical computed tomographic portography in ten normal dogs and ten dogs with a portosystemic shunt. *Vet Radiol Ultrasound.* 2003;44(4):392-400.
191. Zwingenberger AL, Schwarz T. Dual-phase CT angiography of the normal canine portal and hepatic vasculature. *Vet Radiol Ultrasound.* 2004;45(2):117-124.
192. Winter MD, Kinney LM, Kleine LJ. Three-dimensional helical computed Tomographic angiography of the liver in five dogs. *Vet Radiol Ultrasound.* 2005;46(6):494-499.
193. Zwingenberger AL, McLear RC, Weisse C. Diagnosis of arterioportal fistulae in four dogs using computed tomographic angiography. *Vet Radiol Ultrasound.* 2005;46(6):472-477.
194. Zwingenberger AL, Schwarz T, Saunders HM. Helical computed tomographic angiography of canine portosystemic shunts. *Vet Radiol Ultrasound.* 2005;46(1):27-32.
195. Bertolini G, Rolla EC, Zotti A, Caldin M. Three-dimensional multislice helical computed tomography techniques for canine extra-hepatic portosystemic shunt assessment. *Vet Radiol Ultrasound.* 2006;47(5):439-443.
196. Echandi RL, Morandi F, Daniel WT, et al. Comparison of transplenic multidetector CT portography to multidetector CT-angiography in normal dogs. *Vet Radiol Ultrasound.* 2007;48(1):38-44.
197. Stieger SM, Zwingenberger A, Pollard RE, et al. Hepatic volume estimation using quantitative computed tomography in dogs with portosystemic shunts. *Vet Radiol Ultrasound.* 2007;48(5):409-413.
198. Zwingenberger AL, Shofer FS. Dynamic computed tomographic quantitation of hepatic perfusion in dogs with and without portal vascular anomalies. *Am J Vet Res.* 2007;68:970-974.

199. Irausquin RA, Scavelli TD, Corti L, et al. Comparative evaluation of the liver in dogs with a splenic mass by using ultrasonography and contrast-enhanced computed tomography. *Can Vet J.* 2008;49:46-52.
200. Kummeling A, Vrakking DJE, Roghuizen J, et al. Hepatic volume measurements in dogs with extrahepatic congenital portosystemic shunts before and after surgical attenuation. *J Vet Intern Med.* 2010;24:114-119.
201. Nelson NC, Nelson LL. Anatomy of extrahepatic portosystemic shunts in dogs as determined by computed tomography angiography. *Vet Radiol Ultrasound.* 2011;52(5):498-506.
202. Zwingenberger AL, Spriet M, Hunt GB. Imaging diagnosis-portal vein aplasia and interruption of the caudal vena cava in three dogs. *Vet Radiol Ultrasound.* 2011;52(4):444-447.
203. Robben JH, Pollak YWEA, Kirpensteijn J, et al. Comparison of ultrasonography, computed tomography, and single-photon emission computed tomography for the detection and localization of canine insulinoma. *J Vet Intern Med.* 2005;19:15-22.
204. Cáceres AV, Zwingenberger AL, Hardam E, et al. Helical computed tomographic angiography of the normal canine pancreas. *Vet Radiol Ultrasound.* 2006;47(3):270-278.
205. Yasuda D, Fujita M, Yasuda S, et al. Usefulness of MRI compared with CT for diagnosis of mesenteric lymphoma in a dog. *J Vet Med Sci.* 2004;66(11):1447-1451.
206. Spector DI, Fischetti AJ, Kovak-McClaran JR. Computed tomographic characteristics of intrapelvic masses in dogs. *Vet Radiol Ultrasound.* 2011;52(1):71-74.
207. Bertolini G, Furlanello T, De Lorenzi D, Caldin M. Computed tomographic quantification of canine adrenal gland volume and attenuation. *Vet Radiol Ultrasound.* 2006;47(5):444-448.
208. Bertolini G, Furlanello T, Drigo M, Caldin M. Computed tomographic adrenal gland quantification in canine adrenocorticotroph hormone-dependent hyperadrenocorticism. *Vet Radiol Ultrasound.* 2008;49(5):449-453.
209. Schultz RM, Wisner ER, Johnson EG, Macleod JS. Contrast-enhanced computed tomography as a preoperative indicator of vascular invasion from adrenal masses in dogs. *Vet Radiol Ultrasound.* 2009;50(6):625-629.
210. Yamada K, Morimoto M, Kishimoto M, Wisner ER. Virtual endoscopy of dogs using multi-detector row CT. *Vet Radiol Ultrasound.* 2007;48(4):318-322.
211. Beal M. Approach to the acute abdomen. *Veterinary Clinics of North America: Small Animal Practice.* 2005;35(2):375-396.
212. Terragni R, Vignoli M, Rossi F, et al. Stomach wall evaluation using helical hydro-computed tomography. *Vet Radiol Ultrasound.* 2012; 53(4): 402-5.
213. Oliveira CR, Mitchell MA, O'Brien RT. Thoracic computed tomography in feline patients without use of chemical restraint. *Vet Radiol Ultrasound.* 2011;52(4):368-376.
214. Oliveira CR, Ranallo FN, Pijanowski GJ, et al. The Vetmousetrap™: A device for computed tomographic imaging of the thorax of awake cats. *Vet Radiol Ultrasound.* 2010; 52(1): 41-52.
215. Stadler K, Hartman S, Matheson J, O'Brien R. Computed tomographic imaging of dogs with primary laryngeal or tracheal airway obstruction. *Vet Radiol Ultrasound.* 2011;52(4):377-384.

216. Lamb CR, Simpson KW. Ultrasonographic findings in cholecystokinin induced pancreatitis in dogs. *Vet Radiol Ultrasound.* 1995;36:139-145.
217. Nyland TG, Mulvany MH, Strombeck DR. Ultrasonic features of experimentally induced, acute pancreatitis in the dog. *Veterinary Radiology.* 1983;24:260-266.
218. Shapiro SS, Wilk MB. An analysis of variance test for normality (complete samples). *Biometrika.* 1965;52:591-611.
219. Levene H. Robust tests for equality of variances. *Ingram Olkin, Harold Hotelling, et alia. Stanford University Press.* 1960:278-292.
220. Mann HB, Whitney DR. On a test of whether one of two random variables is ttochastically larger than the other. *Annals of Mathematical Statistics.* 1947;18:50-60.
221. Fisher RA. Statistical methods for research workers. *Edinburgh: Oliver and Boyd.* 1934;5th ed.
222. Ihle SL, Kostolich M. Acute renal failure associated with contrast medium administration in a dog. *J Am Vet Med Assoc.* 1991;199:899-901.
223. Pollard RE, Pascoe PJ. Severe reaction to intravenous administration of an ionic iodinated contrast agent in two anesthetized dogs. *J Am Vet Med Assoc.* 2008;233:274-278.
224. Pollard RE, Puchalski SM, Pascoe PJ. Hemodynamic and serum biochemical alterations associated with intravenous administration of three types of contrast media in anesthetized dogs. *Am J Vet Res.* 2008;69:1268-1273.
225. Fields EL, Robertson ID, Brown JC. Optimization of contrast-enhanced multidetector abdominal computed tomography in sedated canine patients. *Vet Radiol Ultrasound.* 2012;53(5):507-512.
226. Fields EL, Robertson ID, Osborne JA, Brown JC. Comparison of abdominal computed tomography and abdominal ultrasound in sedated dogs. *Vet Radiol Ultrasound.* 2012;53(5):513-517.
227. Shanaman MM, Hartman SK, O'Brien RT. Feasibility for using dual-phase contrast-enhanced multi-detector helical computed tomography to evaluate awake and sedated dogs with acute abdominal signs. *Vet Radiol Ultrasound.* 2012; 53(6): 605-612.
228. Thornton E, Mendiratta-Lala M, Siewert B, Eisenberg RL. Patterns of fat stranding. *AJR.* 2011;197:W1-W14.
229. Sahani DV, Sainani NI, Deshpande V, et al. Autoimmune pancreatitis: disease evolution, staging, response assessment, and CT features that predict response to corticosteroid therapy. *Radiology.* 2008;250(1):118-129.
230. Pereira JM, Sirlin CB, Pinto PS, et al. Disproportionate fat stranding- a helpful CT sign in patients with acute abdominal pain. *Radiographics.* 2004;24(3):703-715.
231. Horton KM, Fishman EK. CT angiography of the mesenteric circulation. *Radiologic Clinics of North America.* 2010;48(2):331-345.
232. Nyland TG, Mattoon JS. Small animal diagnostic ultrasound second edition. *Saunders*. Philadelphia, PA. 2002.
233. Jakobssen U, Westergren A. Statistical methods for assessing agreement for ordinal data. *Scand J Caring Sci.* 2005;19:427-431.
234. Ivančić M, Long F, Seiler GS. Contrast harmonic ultrasonography of splenic masses and associated liver nodules in dogs. *J Am Vet Med Assoc.* 2009;234:88-94.